Universität für Bodenkultur Wien

Department für Wasser-Atmosphäre-Umwelt

Institut für Siedlungswasserbau, Industriewasserwirtschaft und Gewässerschutz

Vorstand: Thomas Ertl

Betreuer: Thomas Ertl

WASTEWATER TREATMENT WITH SMALL SCALE PARTIAL NITRATION ANAMMOX –

KOMPAKTE BEHANDLUNG VON ABWASSERSTRÖMEN MITTELS DEAMMONIFKATION

Dissertation
zur Erlangung des Doktorgrades
an der Universität für Bodenkultur Wien - Institut für Siedlungswasserbau, Industriewasserwirtschaft und Gewässerschutz

Eingereicht von
Thomas Schoepp

Vienna, November 2020- Institut für Siedlungswasserbau, Industriewasserwirtschaft und Gewässerschutz

Acknowledgements

I would like to thank all those who contributed to this thesis, those who supported me during my work at the BOKU Institute of Sanitary Engineering and Water Pollution Control, Vienna, and my colleagues from IFA-Tulln from the Institute of Environmental Biotechnology.
I also thank Norbert Weissenbacher and Thomas Ertl for giving me the opportunity to work on the DEKO project and supporting me with my thesis. Their ongoing trust and support allowed me to have this valuable experience.
Furthermore, I thank Werner Fuchs, who has guided me with his practical advice since my master thesis and who together with Johannes Busek helped me in so many ways when I needed support.
Moreover, I thank Karin Schitzenhofer, Agime Beqaj, Martin Goriup, and Thomas Zingerle for the efforts they put into the success of this project. Their contribution is the backbone of this thesis, and without them it would not have been possible to do this research.
Additionally, I thank Friedrich Kropitz who helped me by teaching me many practicalities and giving me a helping hand when I needed it. His great work on the pilot plant should be mentioned in particular at this point. I further thank Alexander Haider for his patience during the implementation of the UV–VIS probe.
The lab work would not have been possible without the great lab team at SIG and their great company at the coffee kitchen where most problems were solved. In particular, Wofgang Stach and Falko Ziegenbalg practically guided me and my colleagues with their lab expertise. At this point, the well maintained coffee machine of the lab team, which never runs out of beans—even in the most desperate moments, shall receive an honourable mention as the single most important tool besides the Internet in guiding me through my research.
I also thank Roza Allabashi and Marija Zunabovic-Pichler, who always had an open ear when I needed a chemical or micro biological sanity check and kept an eye on me when the lab work took longer than expected.
I further thank Sebastian Handl, Benedikt Schmidt, Sandra Nicolics, and Lena Simperler for their great company and moral support during numerous lunch and coffee breaks. Many problems were solved by drinking a coffee and cooking pasta with Hofer-pesto.
I also want to thank my friends who listened to my endless stories about my struggles. Whether it was keeping me company for a beer or cycling trough Austria, they helped keep my spirits up.
Last and most importantly I want to thank my parents, Friederike and Wolfgang Schöpp, who have continuously supported me throughout my life, and recently through my endless studies and academic endeavours. Without their constant support, this research would have never been possible.

Preamble

The studies conducted for this thesis investigated,small-scale biological wastewater treatment using the partial nitration anaerobic ammonia oxidation (ANAMMOX) process at the BOKU Institute of Sanitary Engineering and Water Pollution Control in Vienna. The experimental work was conducted from March 2015 to March 2017 in the DEKO Project led by Norbert Weissenbacher, and under the supervision of Thomas Ertl. The project was performed in close cooperation with the Institute of Environmental Biotechnology in Tulln, whereby additional co-supervision was provided by Werner Fuchs. The DEKO Project focused on small-scale partial nitration ANAMMOX, and involved the development of a novel reactor configuration at a lab and at pilot scale, and also the investigation of the greenhouse gas emissions of the novel reactor configuration. The DEKO Project was consulted by Bernhard Wett, who developed the DEMON® process at the WWTP in Strass Tyrol, which also provided the ANAMMOX seed sludge essential to this project.
The data evaluation and preparation of publications was conducted from 2017 to the beginning of 2019, which also formed the foundation for this thesis, and the final writing was conducted at the beginning of 2020.
The scientific output related to ANAMMOX comprises one first-author SCI publication involving the evaluation of the greenhouse gas emissions of the pilot plant, the central experiment of this study (Schoepp et al. 2018), and one co-authored publication in an SCI journal about the lab-scale implementation of the novel reactor configuration (Fuchs et al. 2017). In addition, the author co-authored two project reports, one conference proceeding, and an article in the Institute's communications, which altogether form the basis for this thesis. To fulfil the scope of this thesis, additional data analysis was conducted, and previous results were put in context to each other to further develop the conclusion about the small-scale implementation of partial nitration ANAMMOX.
Moreover, the author conducted side projects during his thesis in the field of environmental biotechnology, which led to three co-authored SCI publications (Montgomery et al. 2016; Bousek et al. 2018; Gruber-Brunhumer et al. 2019).

Abstract

Partial nitrification anaerobic ammonia oxidation (ANAMMOX), also known as deammonification, has the potential to become one of the key processes in wastewater treatment. However, the application of the technology is limited to large wastewater treatment plants. To offer the advantages of resource and energy efficiency to small-scale treatment facilities, this thesis investigates the small scale (<20.000 PE) implementation of the partial nitrification–ANAMMOX process. The aim was to improve process stability, minimize greenhouse gas emissions, and simplify the process to be applicable at a small scale.
The first part comprises two different lab-scale implementations, one being a conventional single chamber sequencing batch reactor and the other a novel mesh separated reactor design. The lab-scale single chamber system showed that the downscaling of a pH bases control, successful at a large scale, was prone to disturbances from pH artefacts. The mesh separated system was less affected by pH artefacts, and it demonstrated that stable continuous operation comparable to a large-scale system is achievable.
In the second part, ANAMMOX specific monitoring tools were compared by testing the effect of additives commonly used upstream of the partial nitrification–ANAMMOX process during sludge dewatering, revealing that measuring the heme concentration is more suitable than measuring the ANAMMOX activity for monitoring PNA systems.
In the third pilot plant part of the study, a single chamber sequencing batch reactor and a mesh separated reactor were implemented and optimised. Furthermore, the study summarised and investigated the impact of a small scale on pH-dependent process control and highlighted the importance of alkalinity for the process, especially at a small scale where stripping may severely affect and limit the process. Furthermore, process control strategies for coping with pH imbalances and the feasibility of pH-dependent feed control were tested, altogether forming an interrelated topic.
In the final part of this study, the pilot-scale mesh separated reactor configuration was compared with a pilot-scale single chamber sequencing batch reactor with regards to process stability, operation mode, and greenhouse gas emissions. A system that allows for continuous operation, such as the mesh separated system, was demonstrated to significantly reduce the nitrous oxide emissions of the process.
Overall, it was shown that continuously operating partial nitrification–ANAMMOX systems should be favoured due to the increased process stability and reduced emissions. Furthermore, it was shown that small-scale systems are especially dependent on influent characteristics. This highlighted that good practices in sludge dewatering should be enforced, especially for small-scale partial nitrification–ANAMMOX implementations.

Kurzfassung

Die partielle Nitrifikation ANAMMOX (anaerobe Ammonium-Oxidation) bzw. Deammonifikation hat das Potenzial, zu einem Schlüsselprozess in der Abwasserbehandlung zu werden. Bislang ist die Anwendung jedoch auf relativ große Kläranlagen beschränkt. Daraus folgt das Ziel dieser Dissertation, die Anwendung der partiellen Nitrifikation und ihrer Vorteile, Ressourcen und Energie-Effizienz auch kleinen Kläranlagen (< 20 000 EW) zugänglich zu machen. Hierfür wurde die Implementierung eines Kompaktsystems untersucht mit der Absicht, die Prozessstabilität zu erhöhen, die Emission von Klimagasen zu reduzieren und den Prozess für die Kompaktanwendung zu vereinfachen.
Der erste Teil der Arbeit umfasste die Implementierung von zwei Laborsystemen – einem konventionellen Einzelkammersystem im Batch-Betrieb und einem neuartigen Zweikammersystem mit einem Trenngewebe. Während die auf dem pH-Wert basierende Belüftungsregelung des Einkammersystems regelmäßig Störungen durch pH-Artefakte aufwies, wurde das kontinuierlich betriebene Zweikammersystem hierdurch wenig beeinträchtigt. Weiters zeigte sich, dass ein stabiler Betrieb möglich ist, der eine mit industriellen Systemen vergleichbare Leistung aufweist.
Im zweiten Teil wurde die Anwendung von ANAMMOX-spezifischen Monitoringtools untersucht. Hierfür wurde der Effekt von Hilfsmitteln, welche stromaufwärts in der Schlammentwässerung verwendet werden, auf ANAMMOX betrachtet, da der ANAMMOX-Anteil der Mikrobiologie als der empfindlichste gilt. Dabei wurde deutlich, dass für das Anlagenmonitoring die Bestimmung der Hämkonzentration besser geeignet ist als die Messung der ANAMMOX-Aktivität.
Im dritten Teil wurden das Einkammersystem und das Zweikammersystem im Pilotmaßstab umgesetzt, wobei der Effekt des kleinen Maßstabs auf die pH-Belüftungsregelung untersucht wurde. Hier wurde die Bedeutung der Alkalinität speziell im kleinen Maßstab deutlich, da Strippingeffekte den Prozess beeinflussen. Weiters wurde gezeigt, wie die Steuer- und Regelstrategien angepasst werden können, um den Effekt von pH-Artefakten zu reduzieren, und wie der pH-Wert für die Beschickung des Reaktors verwendet werden kann.
Abschließend wurden beide Systeme in Bezug auf ihre Prozessstabilität, ihr Treibhausgas-Emissionsverhalten und die Betriebsweisen verglichen. Hierbei zeigte sich, dass Systeme, welche sich für eine kontinuierliche Betriebsweise eignen, zu einer maßgeblichen Reduktion der Lachgasemissionen beitragen.
Zusammenfassend kann festgestellt werden, dass kontinuierliche Systeme zu bevorzugen sind, da sie die Prozessstabilität erhöhen und zu einer Reduktion der Emissionen beitragen können. Weiters wurde deutlich, dass kleine Systeme besonders stark von den Zulaufcharakteristika beeinflusst werden. Dies unterstreicht die Bedeutung der Schlammentwässerung für den Betrieb kompakter Deammonifikations-Anlagen.

List of Abbreviations

AA	ANAMMOX activity
ANAMMOX	anaerobic ammonia oxidation
AOB	ammonia-oxidising bacteria
CO_2	carbon dioxide
COD	chemical oxygen demand
DO	dissolved oxygen
EF	emission factor
GHG	greenhouse gases
HCO_3-	bicarbonate
N	nitrogen
N_2O	nitrous oxide
NGS	next generation sequencing
NH_4^+	ammonia
NH_4-N	ammonia nitrogen
NO_2^-	nitrite
NO_2-N	nitrite nitrogen
NO_3^-	nitrate
NO_3-N	nitrate nitrogen
NOB	nitrate oxidising bacteria
O_2	oxygen
OHO	ordinary heterotrophic organisms
OTE	oxygen transfer efficiency
PCR	polymerase chain reaction
PE	population equivalent
PID	proportional, integral, and derivative
PNA	partial nitration ANAMMOX
SBR	sequencing batch reactor
TKN	total Kjeldahl nitrogen
TOC	total organic carbon
WWTP	wastewater treatment plant

Authors contributions

The basic concept of this study was developed by Norbert Weissenbacher and Werner Fuchs. The author was involved in the subsequent parts of the study, and the respective contributions are declared hereinafter. Furthermore, the development of this study was guided by Thomas Ertl, Werner Fuchs, and Norbert Weissenbacher, as well as Bernhard Wett who provided consultancy.
The basic structures of Chapter 1 (**General introduction)** and Chapter 2 (**Targets and motivation)** are based on the final DEKO project report (Weissenbacher et al. 2017), which the author co-authored, and were revised to fit this thesis.
The subsection titled **Lab-scale single-chamber system** (4.1.1.1) is partly based on the interim and final report and presentations of the DEKO project. It describes the implementation and results of the lab-scale single chamber system, which was implemented in parallel to the mesh-based lab-scale reactor prior to setting up the pilot plant. The author practically contributed by establishing the monitoring regime, evaluating the process data, setting up the process automation, and continuously improving the setup. The work was done in close cooperation with Thomas Zingerle, Karin Schitzenhofer, and Friedrich Kropitz.
This subsection titled **Lab-scale mesh reactor** (4.1.1.2) is based on a paper (Fuchs et al. 2017) published in *Water Science and Technology* (Vol. 76 No. 6 1409-1417). The author practically contributed during the setup period by organising the initial inoculum and substrate together with Benedikt Kleibel as well as by providing lessons learned from the single-chamber lab-scale system. Furthermore, monitoring methods were used to assess the effect of the mesh. In addition, the author regularly visited the project partners Werner Fuchs and Johannes Bousek at the Department of Agrobiotechnology, IFA-Tulln to discuss the findings from the lab-scale mesh system and incorporate them into the design of the pilot plant version of the mesh system.
The work described in the section titled **Evaluating process monitoring tools** (4.2) was performed in close collaboration with Karin Schitzenhofer. The author was practically involved in developing the basic concept of the study and testing and providing the basic lab setup. The detailed implementation and optimization of the laboratory methods, as well as the detailed planning of the experiment, were conducted by Karin Schitzenhofer (Schitzenhofer 2016). The author performed a final statistical evaluation, data arrangement, and proof of data consistency, and also further developed the initial study.
The section titled **Start up, optimisation, and** monitoring (4.3.1) and **Adjusting the aeration control algorithm for small-scale application, and studying the impact of different ammonia-to-alkalinity ratios** (4.3.2) are partly based on the interim and final report and presentations of the DEKO project, and they discuss the problem in greater detail and rigour and involve additional data analysis. They are based on the optimisations that were necessary to achieve increased nitrogen loading rates during the start-up of the pilot plant, which was performed by the author. Friedrich Kropitz, Martin Goriup, and Agime Begaj were major contributors during the experimental work.
The section titled **Comparing the mesh implementation with the conventional single-chamber system at the pilot scale in performance, stability, N2O emissions, and biomass composition** (4.3.3) is based on a paper (Schoepp et al. 2018) published in *Water Science and Technology* 78, 2239–2246, which the author practically contributed to by setting up the pilot plant together with Friedrich Kropitz. The author wrote the programme for automatising the reactor control and data acquisition. He incorporated the lessons learned from the lab-scale mesh system, which were provided by the project partners Werner Fuchs and Johannes Bousek at IFA. Furthermore, he was responsible for optimising the reactors and bringing them up to the desired level of nitrogen load with the help of Martin Goriup. He was

responsible for calibrating and integrating the N_2O measurements and he performed reactor monitoring and operation with the assistance of Agime Beqaj. The sequencing of the biomass was performed by Christina Fiedler, and final data evaluation was performed by the author, who was the lead author of the paper.

Contents

1 General introduction

Removing nitrogen from wastewater to protect natural water bodies is a crucial task of wastewater treatment plants (WWTP). Many WWTP configurations have two different streams of wastewater that carry a nitrogen load to the plant. The mainstream, representing the major volume of wastewater to be treated, and secondly the side stream, also called reject water, which represents a relatively small volume but a relatively high nitrogen load. Usually reject water is also treated together with the mainstream wastewater. Reject water is a by-product of the mainstream treatment process, where bacteria bind or consume soluble and insoluble impurities of wastewater, thereby generating a sludge that is separated by settling from the wastewater before the treated water leaves the WWTP. In larger WWTPs (ca. > 20.000 PE), the concentrated sludge is usually treated in anaerobic digesters, where biogas is generated from the organic carbon inside the sludge and thus removed. At the same time, nitrogen in the form of ammonia (NH_4^+) remains. In the subsequent step, the leftover fraction of the sludge which remains after anaerobic digestion is separated by filtration or centrifugation from the remaining reject water rich in NH_4^+. While the remaining solids are usually combusted elsewhere, the NH_4^+ inside the reject water remains to be treated, either in the mainstream through the process of denitrification or in a separate side stream treatment process which involve anaerobic ammonia oxidation (ANAMMOX), such as partial nitration ANAMMOX (PNA).
PNA is increasingly applied to treat high-strength reject water (Lackner et al. 2014), and is thus used to improve the energy efficiency of WWTPs (Siegrist et al. 2008). Energy efficiency is improved through making use of the distinct metabolism of microorganisms, which allow reject waters rich in NH_4^+ to be treated with reduced energy input and a small areal footprint. Until today, their application is limited to large-scale WWTPs because of their increased demand on process operation. However, the technology also has potential for small-scale WWTPs, considering the trend towards anaerobic digestion even in smaller WWTPs (Füreder et al. 2014), which will increase the necessity of treating anaerobic sludge from reject water in smaller WWTPs. Furthermore, small-scale WWTPs are facing increasing environmental standards concerning nitrogen treatment targets, while often receiving increased amounts of wastewater because of the growth of settlements. This often pushes these plants mainstream nitrogen removal capacities to their limits, requiring plant expansion or process optimisation in the long run. However, plant expansion of the mainstream is often not possible due to the rather large areal footprint. The NH_4^+-rich reject water that remains after dewatering the sludge from anaerobic digestion has been identified as a major contributor to the mainstream nitrogen load. Furthermore, reject water contains an unfavourable carbon-to-nitrogen ratio, which reduces the potential of the mainstream to eliminate nitrogen through the process of denitrification.
Despite the advantages of PNA systems in reducing the nitrogen load in the mainstream and increasing the energy efficiency of a WWTP, PNA is a relatively demanding process to operate. Furthermore, it is known to potentially emit problematic amounts of greenhouse gases (GHGs), which may outweigh the benefits of energy savings (Paredes et al. 2007). Therefore, to achieve successful implementations in small-scale WWTPs, the process operation must be simplified while maintaining low GHG emissions.

1.1 Partial nitration ANAMMOX

PNA is a nitrogen removal process that consists of the combination of two distinct metabolisms. In a first aerobic step, air is supplied to oxidise NH_4^+ to nitrite (NO_2^-) —a process called nitritation or partial nitration performed by ammonia-oxidising bacteria (AOB).

The term partial nitration stems from the fact that the NO_2^- is usually further oxidised to nitrate (NO_3^-) by nitrate-oxidising bacteria (NOB), which must be suppressed in this process. In a second anaerobic step, the remaining NH_4^+ is oxidised with NO_2^- to form nitrogen gas (N_2) using bacteria, which perform ANAMMOX (Figure 1) and thereby remove the nutrients from the reject water.

The history of ANAMMOX started with the assumption by Hamm and Thompson (1941) that anaerobic nitrogen oxidation could be the missing link for explaining nitrogen loss in oceans. Four decades later, the thermodynamic feasibility of the metabolic pathway was proposed (Broda 1977). Up to the 1990s, those findings had no further relevance until in 1995 ANAMMOX was discovered in a fluidized bed reactor, where NO_3^- was assumed to serve as the electron acceptor (Mulder et al. 1995). One year later, it was shown that NO_2^- was the actual electron acceptor by cultivating a red culture of as of yet unidentified cells. From 1998 to 1999, the first physiological stoichiometric characterization of enriched culture became available (Strous et al. 1998). The most recent evaluation (Lotti et al. 2014) reads as follows:

$$NH_4^+ + 1.146NO_2^- + 0.071HCO_3^- + 0.057H^+ \rightarrow 0.161NO_3^- + 0.982N_2 + 0.071CH_{1.74}O_{0.31}N_{0.2} + 2.002H_2$$

Another year later, it was identified that the bacteria belonged to the phylum of *Planctomycetes*, inside the phylum ANAMMOX resembles a deep branch (Strous et al. 1999). Shortly after, the first industrial implementation of ANAMMOX in Rotterdam, the Netherlands followed (Dongen et al. 2001), where it was combined with the SHARON process, to achieve partial nitration before the ANAMMOX process. Here, the stoichiometry read as follows:

$$NH_4^+ + HCO_3^- + 0.75O_2 \rightarrow 0.5NO_2^- + 0.5NH_4^+ + CO2 + 1.5H_2O$$

Balancing the abovementioned processes is a key element for achieving a stable PNA process. The ratio of NH_4^+ to NO_2^- must be balanced according to the stoichiometry. Furthermore, there must be a sufficient supply of inorganic carbon, especially for partial nitration, which also requires the suppression of NOB. NOB can be suppressed by increased temperatures of approximately 30°C to 35°C as well as a limited oxygen supply, which kinetically selects AOB over NOB (Third et al. 2001) and reduces the chance of reversibly inhibiting ANAMMOX bacteria (Strous et al. 1997). Therefore, intermittent aeration is commonly applied to suppress NOB and balance NO_2^- production and consumption (Zekker et al. 2012). Another problem may arise if too much organic carbon is present in the reject water as ordinary heterotrophic organisms may hinder the process, only by quickly overgrowing the ANAMMOX biomass. Furthermore, ANAMMOX growth is much slower in comparison to that of other species involved. Therefore, sludge selection mechanisms such as granular selection, which favour ANAMMOX growth and retain them within the reactor, as well as the continuous removal of the other faster-growing bacteria, play essential roles in maintaining a stable process.

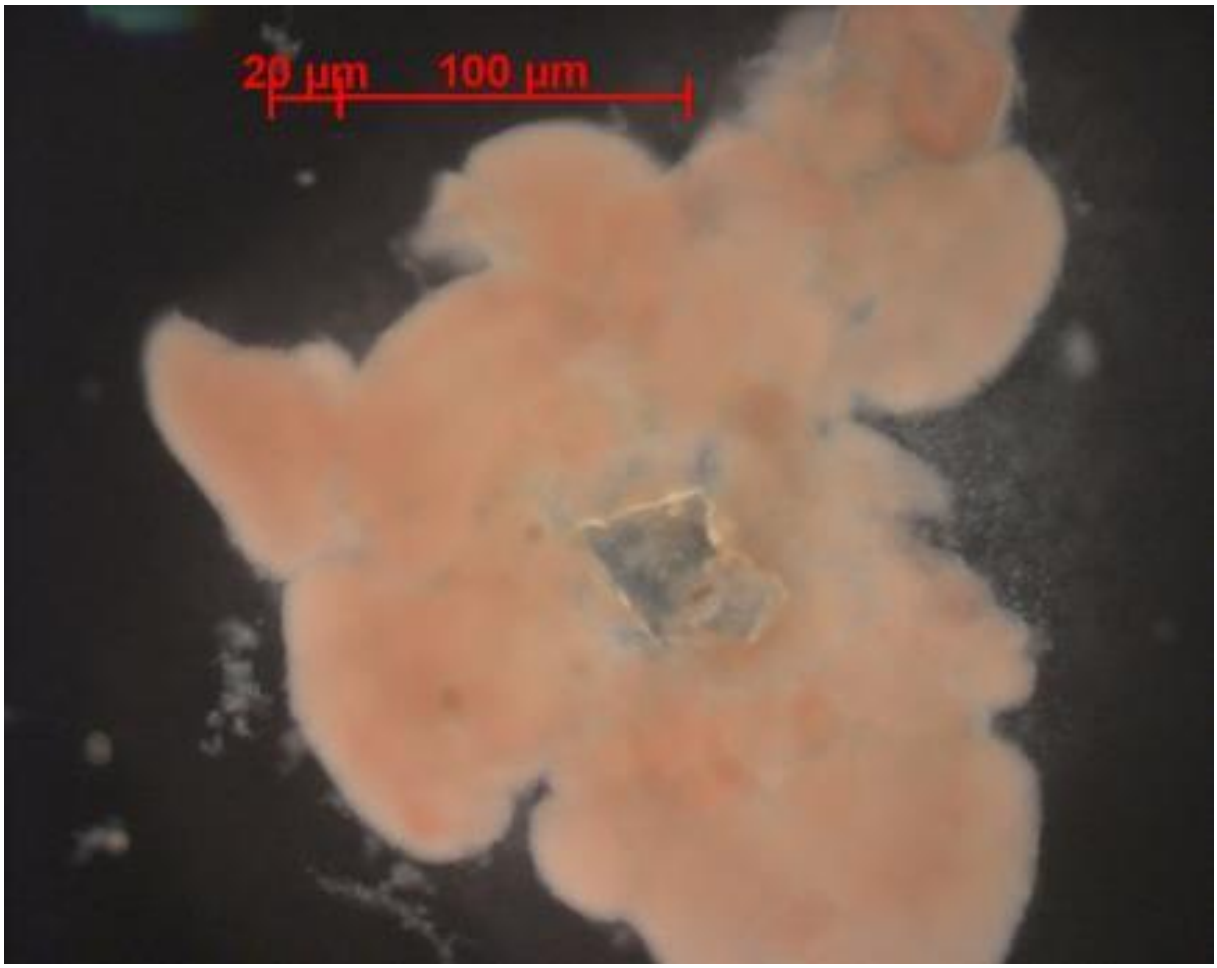

Figure 1: ANAMMOX granule from the DEMON® process at WWTP Strass (Schitzenhofer 2016)

1.2 Process configuration of PNA

Since the first implementation of the first ANAMMOX-based process, there has been ongoing development that has resulted in several process implementations. The first successful implementation was based on a two-stage system (van der Star et al. 2007), which was motivated by the possibility of optimizing each step of the process individually. However, there has been a shift from two-stage systems to single-stage systems (Hippen et al. 2001; Hao et al. 2002; Wett 2006) due to the more straightforward setup, and also the fact that it is easier to balance the process as the biomass thrives close to each other.
Various other system configurations have been developed such as downflow hanging sponge (Chuang et al. 2007), airlift (Jin et al. 2013) and membrane (Trigo et al. 2006) reactors. However, the majority of the industrial process implementations are dominated by single-stage systems, with suspended growth and moving bed biofilm reactors; for example, ANITAMOX®, DEMON®, and OLAND®, which vary in details such as process control parameters and biomass retention and selection. These processes are currently undergoing continuous development, such as the DEMON® process, which intensified its ANAMMOX selection starting with the control of the settling time in sequencing batch reactor (SBR) mode, then by a hydro cyclone (Wett 2007), and today by continuously operating reactors with micro sieves (Han et al. 2016a).

These implementations have focused on reject water from anaerobic digestion because of its characteristics favouring the process (high temperature, low carbon-to-nitrogen ratio, and high NH_4^+ concentration). However, because of the increased knowledge, there is a drive to extend the advantages gained from ANAMMOX to more difficult process situations such as the mainstream (Wett et al. 2013; Lotti et al. 2015).
Although much progress has been made, problems still occur on a regular basis, such as the following:

- NO_2^- build-up,
- loss of biomass,
- insufficient NOB suppression,
- sludge flotation.

These problems give PNA technology the reputation of being difficult to control, and therefore provide a challenge especially for small-scale implementations where process operation must be as simple as possible.

1.3 N_2O emissions

Nitrogen removal processes are known to possibly emit a severe amount of the greenhouse gas nitrous oxide (N_2O; Ali et al. 2016). Life cycle analysis showed that applying a PNA system may increase the overall impact on climate change of wastewater treatment even though energy savings may be achieved (Hauck et al. 2016). The production of N_2O occurs during the different metabolic steps that lead to the conversion of NH_4^+ to N_2 during PNA. Those steps involve a series of intermediate products. If one of those conversion steps is hindered, those nitrogen species may accumulate, whereby the volatile fraction may be emitted from the system. One of those intermediates happens to be nitrous oxide, a GHG 265 times stronger than CO_2 according to IPPC AR5 (related to the 100-year horizon), making it one of the most relevant GHGs. The range of N_2O emissions from the PNA processes varies largely from 0.001% up to 90% of the influent nitrogen load (Kampschreur et al. 2009). This demonstrates that N_2O emissions have to be evaluated when developing nitrogen removal systems.

2 Targets and motivation

2.1 Project targets and research questions

The overall target of this study was to improve and investigate the limitations of the small-scale implementation of PNA, which consisted of three sub-targets:

- To increase process stability
- To improve biomass retention
- To reduce GHG emissions

These targets were worked on in two phases. The first was the lab-scale phase involving the implementation of a lab-scale single chamber and a mesh separated system, and the implementation and testing of monitoring tools. Then, in the second phase, the lessons learned from the lab-scale phase were implemented at the pilot scale. The pilot plant consisted of a single chamber and a mesh separated system. During the start-up period, constant improvements were made to the reactor configuration and process control until stable operations were achieved. Different modifications of the pH-based control strategy were tested, such as PID-based feed control, and a robust algorithm to increase the tolerance of the aeration against process disturbances. Once performances similar to industrial-scale plants were achieved, the GHG emissions under different operational modes were closely monitored. Finally, the impact of different alkalinity concentrations was investigated at the pilot and lab scales, as this has been suspected of playing a crucial role regarding the limitations of small-scale plants with respect to the interplay of process control, process performance, and the impact of CO_2 stripping.
During the process, a set of research questions was developed:

1. What are the problems associated with small-scale implementations of PNA processes, and what can be done to circumvent them?
2. What are the conditions necessary for pH-dependent control algorithms to function under small-scale conditions?
3. What are the advantages of mesh-based reactor configurations for small-scale implementations?
4. What is the effect of a mesh separated reactor configuration and operation mode on N_2O emissions?
5. Are ANAMMOX activity and heme concentration suitable methods for detecting process disturbances and do they offer more information compared with regular monitoring of influent and effluent values?

2.2 The lab-scale phase

The following section describes the motivation for the experiments performed during the initial lab-scale phase of this thesis.

2.2.1 Comparing a lab-scale single chamber with a mesh separated lab-scale system[1]

PNA can be run as a two-stage or single-stage process. During the two-stage process, AOBs aerobically convert halve of the influent NH_4^+ to NO_2^- in the first stage and pass it on to a second ANAMMOX stage where it is anaerobically converted to N_2. It is also possible to

[1] This section is based on Fuchs et al. 2017

combine both stages into a single stage (Jaroszynski and Oleszkiewicz 2011; Lackner et al. 2014). A two-stage process overs the possibility of optimising the conditions individually for AOB and ANAMMOX, while a single chamber process has to balance both processes, such as by intermittent aeration.
Losing the balance can lead to product inhibition, especially by NO_2^- (Jin et al. 2012; De Prá et al. 2016), which is a severe problem for PNA systems (Strous et al., 1999). Single chamber systems offer the advantage that the proximity of AOB and ANAMMOX reduces the risk of problematic concentrations, whereas a two-stage system runs a much greater risk of supplying overly high concentrations of NO_2^- to the ANAMMOX stage or destabilising the carbonate buffer system as the partial recovery of alkalinity in the ANAMMOX stage is decoupled from the first nitrifying stage, where alkalinity is consumed.
The intention of separating the single-chamber system with a mesh was to create two distinct zones, one aerated favouring AOB activity and the other anoxic, to facilitate an increase of ANAMMOX activity. While the biomass is retained to some degree, NH_4^+; NO_2^- and HCO_3^- easily pass through and thus reduce the chance of process inhibition. Therefore, combining the single- and the two-stage approach into one hybrid system, the intention is to increase process stability.
In contrast to using a membrane, a mesh is a simple technology. For example, textile filters are commonly used at WWTPs to separate particles, such as in the dewatering step of the filter press, or a polishing step of the effluent. Replacing the final settler has also been investigated (Loderer et al. 2012) but not applied at an industrial scale. Although a mesh does not allow the separation of very small particles, they are a cost-efficient option for separating activated sludge. Therefore, they are an interesting option for small-scale PNA processes.
The mesh reactor was compared with a single-chamber reactor configuration at lab scale to investigate the impact of the mesh on the PNA process. The single-chamber system emulated the implementation of the DEMON® process in Strass in Tyrol, which has been successfully operated for several years using pH-dependent aeration control to facilitate intermittent aeration, along with an SBR operation to achieve sludge retention and selection by settling (novel developments have included hydro-cyclones and micro sieves).

2.2.2 Evaluating process monitoring tools

The process performance of a PNA system is generally accessed by monitoring the influent and effluent N parameters NH_4^+, NO_3^-, and NO_2^-. However, these parameters only indirectly inform about the wellbeing of the bacteria responsible for the PNA process. Having additional information on the status of microbiology could help in maintaining the delicate microbiological balance between aerobic and anaerobic microorganisms (Strous et al. 1997; Third et al. 2001; Zekker et al. 2012). Thus, the detection of process disturbances, such as those caused by substances present in the process water, could be performed before severe disturbances occur, and therefore assist the target of increasing the process stability.
Although any impact on the ammonium oxidising microbial community is essential, impacts on the ANAMMOX community are generally considered more troublesome. The slow recovery of ANAMMOX from disturbances has motivated several studies that investigated the effect of various inhibitors on ANAMMOX, where the inhibition caused by increased NO_2^- levels was the most prominent (Strous et al. 1999). Regarding substances other than NO_2^- or NH_4^+, most of those studies focused on the conditions occurring during industrial wastewater treatment (Daverey et al. 2014; Sabine Marie et al. 2015; Gonzalez-Estrella et al. 2017), such as the impact of heavy metals. Such substances are of little relevance for processes at municipal wastewater treatment plants.

This study attempted to cover the knowledge gap that exists for monitoring the conditions of municipal PNA systems through comparing the impact of possible disturbances on ANAMMOX, with two commonly used methods suitable for labs at WWTPs in a batch test. Difficulties were experienced during the start-up of the lab-scale single chamber reactor, which destabilised after switching to a process water source of a WWTP that relied on the intense use of additives during the dewatering step. Thus, it was presumed that the influence of the chemicals used directly upstream of PNA during sludge dewatering (to increase precipitation and coagulation of the sludge before filtration or centrifugation), namely $FeCl_3$ and polyamide polymer, are those most interesting under such conditions. Furthermore, it was assumed that increased NO_2^- concentrations caused by system imbalances are also a likely source of inhibition and that their known negative effect would serve as a reference for comparing methods. Two methods were chosen for comparison, ANAMMOX activity (AA) for monitoring the short-term impact on the metabolism, and the quantification of the heme group for addressing the general impact on the metabolic protein apparatus. AA is determined by providing a well-defined substrate to the biomass and recording its specific turnover rate. On the other side, heme is known to be the prosthetic group of central enzymes responsible for ANAMMOX metabolism (Strous et al. 2006; Kartal et al. 2007; Ferousi et al. 2017; Xu et al. 2019). Although heme analyses and AA have been used in numerous studies, only a few studies have used both methods simultaneously (Chen et al. 2012; Zhang et al. 2014; Sabine Marie et al. 2015); therefore, little is known about the differences between those two methods. In addition, both methods were used to monitor the start-up of the pilot plant, which is described as follows.

2.3 The pilot-scale phase

The following section describes the motivation for the experiments performed during the pilot-scale phase of this thesis.

2.3.1 Pilot plant start-up, monitoring, and optimisation

After the lab-scale mesh reactor demonstrated its potential, the process was upscaled to the pilot scale and compared with a similarly scaled single-chamber system run in parallel, to gain data that are more representative for the application at a WWTP. Scale-dependent effects, which may interfere with the process, such as the settling of biomass caused by different hydrodynamics, or different surface-to-volume ratios, such as the transfer of processes intermediated through the mesh. Therefore, the pilot scale increases the representativity of N_2O emissions and allows larger samples to be drawn to study the application of ANAMMOX monitoring tools.
Furthermore, it was important to demonstrate that the mesh reactor could achieve biomass retention and granular selection due to the mesh, which was not possible at the lab scale. Granular selection is known to increase the process stability of PNA systems. Moreover, the pH-dependent aeration control strategy had yet to overcome issues experienced at the lab scale, which were thought to be more manageable at the pilot scale due to the reduced stripping phenomenon.

2.3.2 Adjusting a pH-dependent aeration control algorithm for small-scale application, and studying the impact of different ammonia-to-alkalinity ratios

The DEMON® process has successfully demonstrated that pH-based intermittent aeration control achieves a stable PNA process. It does this by exploiting the fact that the pH drops due to AOB activity when the aeration is turned on and increases because of the feed supply and ANAMMOX activity. While other approaches exist such as redox signal or conductivity measurements, which have their respective advantages and disadvantages (Paredes et al. 2007), changes in pH directly relate to the stoichiometry of the PNA process and therefore facilitate a well-balanced PNA process (Wett et al. 2007). Furthermore, pH sensors are a cheap and reliable technology commonly applied in WWTPs, and therefore they are an attractive option for small-scale implementations.

The pH signal is also affected by the variation of the influent, where the amount of alkalinity plays an important role. Sufficient alkalinity is a prerequisite for PNA. Firstly, nitrification and ANAMOX both require an inorganic carbon source to occur, and secondly, the bicarbonate system resembles the most important buffer of a PNA system. Under normal circumstances, it is assumed that sufficient alkalinity is present in the reject water; however, several reasons such as storage and chemicals added during sludge dewatering may lead to an insufficient supply of alkalinity. A wide variation of volumetric nitrogen removal rates is reported in the literature (Lackner et al. 2014). Some of these variations may be associated with the supply of alkalinity to the process, and some studies have even suggested utilizing the influent alkalinity as a measure of process control (Hwang et al. 2000; Bagchi et al. 2010). In this study, it was assumed that the impact of the NH_4-N to HCO_3^- ratio of the process is specific to the reactor geometry due to the different mass transfer properties during aeration, which could explain the wide range of pH setpoints found to be optimal in the literature (Jaroszynski et al. 2011; Jin et al. 2012). Because CO_2 is removed from the system when air is supplied to it, scale-specific stripping occurs, which may affect the pH signal of the aeration control and the availability of alkalinity.
The impact of scale and alkalinity on the established aeration control strategy was therefore investigated, which led to the development of adaptations necessary for downscaling. In addition, whether pH-based aeration and feed control were possible simultaneously was tested.

2.3.3 Comparing the novel mesh implementation with a conventional single-chamber system at pilot-scale, with respect to performance, stability, GHG, and biomass composition[2]

After the lab-scale version of the mesh reactor had shown its potential, and after succeeding in solving the remaining issues at pilot-scale, it was necessary to investigate its N_2O emissions. This is because these processes can lead to major emissions in which nitrous oxide (N_2O) usually represents the biggest and most significant mass fraction (Weissenbacher et al. 2012; Wang et al. 2016). Depending on the N_2O emission factor, the GHG effect of these emissions may outweigh the advantages of PNA (Thibodeau et al., 2014). The emission factor sets the N_2O emission in relation to the influent nitrogen load of the treatment system. Several studies have attempted to quantify the N_2O emission factors of single-stage partial nitration and reported values ranging from 0.1% up to 6 % (Ali et al. 2016). This shows that nitrogen removal systems such as PNA may lead to severe emissions. Nevertheless, the reported

[2] This section is based on Schoepp et al. 2018

values in the lower range also indicate that it is possible to maintain small GHG emissions in PNA processes.
While some operational factors such as influent characteristics may not be altered to reduce N_2O emissions, process engineering and control systems can be adjusted to foster low N_2O emissions. Several factors may be controlled by process engineering and that are linked to N_2O emissions, such as low dissolved oxygen level (Pijuan et al. 2014; Lv et al. 2016), intermittent aeration (Castro-Barros et al. 2015), pH and reactor configuration. Altogether, numerous PNA systems have been studied for GHG emissions, such as SBR biofilm (Third et al. 2001), membrane aerated biofilm reactors (Ma et al. 2017), two-stage (Okabe et al. 2011), as well as granular/suspended growth (Kampschreur et al. 2009) systems.

To show the impact of the novel configuration on N_2O emissions, the system was run in SBR and continuous mode in parallel to a single-chamber system operated in SBR mode. The systems were fed using reject water from a local WWTP, which was spiked with sodium bicarbonate ($NaHCO_3$) and ammonium bicarbonate (NH_4HCO_3) to simulate high-strength reject water. Both reactors received a nitrogen loading rate comparable to full-scale conditions of approximately 0.5 kg N m^{-3} d^{-1}. The microbial community composition of both systems was investigated using next generation sequencing (NGS). The N_2O gas emissions were measured online to calculate the corresponding N_2O emission factors.

3 Material and methods

3.1 Analytical procedures

3.1.1 Monitoring of routine values[3]

During the pilot plant operation (Section 4.3), the batch tests (Section 4.2) and lab-scale operation (Section 4.1.1) following routine analysis were performed; photometric analyses of nitrogen parameters were performed using a photometer and test tubes (Hach, USA); and COD was analysed according to DIN 38449 (H41):1:1980. Furthermore, alkalinity was determined according to DIN 38409 T7 (H7); TOC was analysed according to DIN EN 1484 (H3):1997; COD was sampled to obtain conversion factors for TOC to COD; and TNb was sampled for quality control of nitrogen parameters according to DIN EN 12260 (H34):2003. To characterise the activated sludge, grab samples of 100 mL for suspended solids (SS) and volatile suspended (VSS) solids were taken from each compartment as well as from the effluent tanks. The measurements were performed according to DIN 38409 (1987) and DIN EN 12879 (2001) during the lab-scale single-chamber operation, and the batch tests' sample size was reduced to 10 mL aliquots.

During the operation of the lab-scale mesh system (Subsection 4.1.1.2), dry matter was determined using an automatic moisture analyser with an infrared heating system (MA35, Sartorius, Germany). To correct for dissolved dry matter, samples were filtered and analysed in a similar manner. The difference in the two values obtained corresponds to the suspended solids concentration. In addition, NH_4-N and TKN values were periodically crosschecked according to standard methods using a Büchi distillation/titration unit (K370, Büchi, Switzerland). For TKN, determination samples were previously digested with sulfuric acid (Digestion Automat K-438, Büchi).

3.1.2 Microbial diversity analysis using next generation sequencing[4]

For the final evaluation (Section 4.3.3) of the pilot-scale single chamber and mesh system, an NGS analysis of the biomass was performed; 50 mL samples were taken in Falcon tubes from each chamber of the two systems while being aerated or mixed, respectively (three samples). Subsequently, the samples were centrifuged at 4,000 *g* for one minute. After the supernatant was discarded, DNA was extracted using the DNeasy PowerBiofilm® kit (Qiagen, US) according to the manual. DNA concentration was determined using a Qubit™ 2.0 fluorometer with a Qubit™ dsDNA HS Assay Kit (ThermoFischer Scientific, US) according to the manual and 199 µL of dye and 1 µL of DNA extract were applied.
The V3/V4 region of the 16S rDNA was amplified in two PCR steps, an Amplicon PCR followed by an Index PCR with intermediate clean-up steps. Amplicon PCR was implemented using forward and reverse fusion primers 341F_ill (5'-CCT ACG GGN GGC WGC AG$^{-3'}$) and 802R_ill (5'-GAC TAC HVG GGT ATC TAA TCC$^{-3'}$). Amplicon PCR was performed using 3.5 µL of DNA extract, 5 µL of each primer, and 12.5 µL of mastermix (KAPA HiFi Hotstart ready mix, Kapa Biosystems, CH) with the following conditions: initial

[3] This section is based on Schoepp et al. 2018 and Fuchs et al. 2017
[4] This section based on Schoepp et al. 2018

denaturation at 95°C for 3 min, followed by 30 cycles of denaturation at 95°C for 30 s, annealing at 55°C for 30 s, elongation at 72°C for 30 s, a final elongation step at 72°C for 5 min, and 4°C on hold. One mixture containing DNA free water was carried as a negative control. After the first PCR, clean-up was performed using the PeqGOLD Cycle Pure Kit, S-Line (Peqlab brand, Germany) according to the manufacturer's instructions with the following adaptations: the centrifugation time for drying of the silica membrane column was extended to 5 min, incubation time of the elution buffer was extended to 5 min followed by 2 min of centrifugation.
To monitor the quality of the PCR products, gel electrophoresis was implemented using a 2% agarose gel, loaded with a mixture of 3 µL of gel loading buffer and 4.5 µL of purified PCR products. To verify the length of the PCR products, a molecular weight size marker (100^{-1}000 bp) was loaded onto the gel. Gel electrophoresis was conducted at 80 V, 2000 mA, and 300 W for 50 min. The gel was dyed using GelRed (Biotium, CA, USA) and subsequently visualised using the Molecular Imager Gel Doc XR+ system (Bio-Rad, Austria).
For the Index PCR, PCR products were quantified and diluted with DNA free water such that 15 µL contained 20 ng of DNA. Then, 5 µL of each index primer (N7xx and S5xx, respectively) and 25 µL of master mix (KAPA HiFi Hotstart ready mix) were added to 15 µL of PCR product and subsequently subjected to the following PCR conditions: initial denaturation at 95°C for 3 min, followed by seven cycles of denaturation at 95°C for 30 s, annealing at 55°C for 30 s and elongation at 72°C for 30 s, a final elongation step at 72°C for 5 min and 4°C on hold. Different combinations of N and S primers were used to distinguish samples after sequencing. A second clean-up was performed as before, followed by DNA quantification.
Aliquots of each sample were taken and adjusted to a target concentration of 12 ng μL^{-1} using 10 mM TRIS buffer. Then, 5 µL of each sample was pooled to obtain the library, which was sent to Microsynth for sequencing with an Illumina MiSeq using the reaction kit V3, 2x300bp (Microsynth, Switzerland). Demultiplexing and trimming of Illumina adaptor residuals were conducted using Microsynth; trimming of locus specific adaptors and merging of forward and reverse reads were implemented using cutadapt v 1.8.1 and Usearch v 8.1.1861, respectively. Error filtering as well as OTU (operational taxonomic unit) picking (closed reference) were implemented using QIIME 2 (Quantitative Insights Into Microbial Ecology). After multiple libraries were compared, the taxonomy was assigned to the SILVA database as in here the fewest operational taxonomic units remained unknown bacteria.

3.1.3 Measurement of heme

During the pilot plant operation and batch testing of ANAMMOX, specific measurement of the heme concentration was conducted (the molecule responsible for the characteristic red colour of ANAMMOX). The heme measurement method was based on an adapted version by Sinclair et al. (2001), which itself was based on research by Sassa (1976) and Morrison (1965). Cytochrome C from equine heart (Sigma Aldrich) was used as a standard (1087 absorption units per mg L^{-1} cytochrome C). The extraction agent for the samples and the standard solution was modified from 100% (v/v) dimethyl sulfoxide (DMSO) to 60% (v/v) DMSO and 40% (v/v) H_2O. The ratio was experimentally determined because 100% DMSO did not dissolve the standard completely. Samples were drawn from the completely mixed system and stored at −20°C until analysis, made in the following manner. Thawed samples were centrifuged at 4000 rpm for 3 min. The supernatant was discarded and after refilling with 60% [v/v] DMSO the pellet was remixed. Then, 2 mL was inserted into a Precellys vial containing ten 2.4-mm ceramic balls. The samples were homogenised at 6000 rpm for 2 min

with five repetitions. Subsequently, samples were diluted in the range from 1:100 to 1:250 with 60% [v/v] DMSO, and 100 µL was transferred to a glass tube. In a subsequent step, a saturated oxalic acid solution was added and heated in a water bath for 30 min at 100°C closed with aluminium caps. In a similar manner but without the heating step, a blank was produced which served to subtract background noise. Finally, heme quantification was performed using a fluorescence scanning spectrophotometer (Cary Eclipse Fluorescence Spectrophotometer, Agilent Technologies, USA), with excitation at 402 nm, emission ranging from 500 to 700 nm, emission slit at 20 nm, scan velocity of 120 mm min^{-1}, and peaks at 596 nm and 652 nm. A detailed description of the method's optimisation can be found in Schitzenhofer (2016).

3.1.4 Measurement of ANAMMOX activity

The ANAMMOX activity was determined during the pilot plant operation and batch tests. During the batch tests, the background levels of nitrogen were determined at the start of each test. Pilot-plant samples were washed with media to remove background levels, and then the feed was added, the flasks were closed with a rubber septum, and the headspace was flushed with nitrogen and incubated as described above. The test lasted for 4 hours. During this period, five samples were drawn every 30 to 60 min through the rubber septum using a syringe. Samples were then analysed using the Berthelot method for the determination of NH_4-N and a plate reader (Tecan Multimode Reader Infinite 200 PRO, Tecan Trading AG, CH). The rate of NH_4^+ removal over time was multiplied by the respective stoichiometric factor (2.01) to calculate the ANAMMOX activity. Furthermore, NO_2-N and NO_3-N were measured with a Dr Lange photometer LASA 50 (Hach, USA) using the corresponding test tubes to also cross-check for the mass balance. A detailed description of the optimisation method can be found in Schitzenhofer (2016).

3.2 Inoculum source

The PNA inoculum for all experiments in this study was extracted from the DEMON® side stream treatment process, treating reject water rich in NH_4^+ (Figure 2) from the municipal WWTP Strass Tyrol Austria (170.000 PE), as described in Wett et al. (2007). It was taken from the recirculated fraction of the screen separating ANAMMOX biomass from the waste activated sludge stream (Figure 3).
At the time of extraction, the reactor was operated at 3–4 g VSS L^{-1}, and had a nitrogen removal efficiency of approximately 90% and loading rate of 0.5–0.7 kg N d^{-1}. With a simulated biomass composition of 26% OHO, 18% AOB, 0% NOB, and 55% ANAMMOX (Wett et al., 2010a). The presence of the genus *Candidatus Brocadia* was detected during pilot plant operation (Schoepp et al. 2018). After sampling, the sludge was stored and transported overnight at a temperature of 10–15°C until it was used for inoculation. Before the start of the batch test, background levels of nitrogen were removed from the sludge through two washing steps using media and centrifugation at 4 000 rpm for 3 min; no washing step was performed when inoculating the lab- and pilot-scale reactors.

Figure 2: The source of inoculum, the DEMON® side stream treatment process at the WWTP Strass Tyrol (Weissenbacher et al. 2017)

Figure 3: Extraction of biomass from the recirculated fraction of the screen separating ANAMOX biomass (Weissenbacher et al. 2017)

3.3 Experimental batch test procedure

To compare the monitoring methods, namely ANAMMOX activity and heme concentration, batch tests were conducted. The tests were simultaneously conducted in anaerobic flasks with 300-mL working volume and a sludge concentration of 0.5 g VSS L^{-1}. They were incubated at 35°C, and an orbital shaker kept the biomass in suspension. To capture the development over a prolonged time, the tests consisted of 3 consecutive cycles. After 4, 8, and 12 days, the same procedure was conducted: at the start of a new cycle, heme samples were drawn, and pH and DO measurements were conducted; then, after settling the biomass, the residual nitrogen concentration was sampled. Subsequently, fresh feed was adde, and the headspace was flushed with nitrogen gas to remove residual oxygen, before the biomass was resuspended. In the next step, the AA was determined by regularly sampling through the septum in the first 4 hours of a cycle. The reason for re-testing was that the different exposure times could alter the conclusions drawn from the monitoring methods. The reason for the rather long exposure time of a total of 12 days was that most studies used only short incubation times with extreme

concentrations, which were not considered to be relevant for the monitoring of communal treatment plants. This approach would allow for the determination of whether acclimatisation occurs.
With the results obtained after each feed cycle (4, 8, and 12 days), the effect of the independent variables NO_2-N, polymer, and FeCl3 on the dependent variables AA, heme, and nitrogen removal efficiency were evaluated, representing a 23-factorial design. This approach was chosen since it allows multiple substances to be tested in one test, and further increases the significance of the test compared with testing just one factor at a time. As several outcomes (heme, AA, and nitrogen removal) were recorded at a time, a multivariate analysis of variance (MANOVA) followed by the respective follow-up ordinary least squares (OLS) univariate linear regression for each statistically significant dependent variable (p threshold of 0.05) was conducted. The analysis was performed using R.

3.3.1 Media and treatment

The treatment concentrations were chosen in order to focus on the response to mediocre and small effects, as stronger disturbances rapidly become self-evident using the commonly performed monitoring of nitrogen in the effluent; thus, no advantage would be gained from testing monitoring tools under such conditions. Following this reasoning, concentrations were chosen.
First, 70 mg L^{-1} NO_2-N was selected as the base level for NO_2 as it is commonly used for performing ANAMMOX activity tests, and 105 mg L^{-1} NO_2-N was selected as the high level as the literature has reported inhibiting (Strous et al. 1999; Carvajal-Arroyo et al. 2013) as well as noninhibiting effects in this range (Fernández et al. 2012). With these concentrations, mediocre effects were expected, which would not overshadow the other test results.
Considering the addition of $FeCl_3$, another study observed negative effects on PNA systems already in the range of 1.5 to 2 mg L^{-1} (Liu and Horn 2012). For a an iron concentration of 6 mg L^{-1}, positive effects were also reported (Chen et al. 2014). In the present study, a concentration of 1 mg L^{-1} $FeCl_3$ was chosen. Considering the addition of polymer, Dapena-Mora et al. (2007) found that the addition of a polymer had a negative effect at 1 g L^{-1}. Because this concentration was rather high, it was decided that a lower concentration of 50 mg L^{-1} should be investigated. The polymer Poly Separ® PK 1455, Separ Chemie, was chosen because of its increased usage in a nearby WWTP, where reject water caused failure in a lab-scale PNA reactor operated by the author.
The medium was prepared in accordance with the frequently used media for ANAMMOX batch tests by Dapena-Mora et al. (2007) with a trace element solution by Van de Graaf et al. (1996). It was slightly adapted by adding 1.5 g L^{-1} $NaHCO_3$ and by setting the pH to 7.8 after spiking the treatments with a phosphate buffer system according to the protocol provided by Dosta et al. (2008) and Dapena-Mora et al. (2010). Before testing, 40 mg L^{-1} of anhydrous Na_2SO_3 was used to remove residual dissolved oxygen. To create the eight solutions necessary for the 23-factorial design, two distinct solutions were prepared, one spiked with 6 mg L^{-1} FeCl3 and a second without. The polymer was subsequently added to half of the solutions and homogenised. In each case, the pH was fixed at 7.8 by adding $NaHCO_3$, and 840 mg NH_4-N L^{-1} was added to all solutions. Half of the solutions were spiked with 630 and the other half with 420 mg NO_2-N L^{-1}. This resulted in the treatment concentrations applied at each test cycle presented in Table 1. A more detailed description can be found in Schitzenhofer (2016).

Table 1: Tested factors and their initial concentration levels

Factor	Low level	High level
NO_2^-	70 mg^{-1}	105 mg^{-1}
$Fe(III)Cl_3$	0 mg^{-1}	1 mg^{-1}
Polymer (Poly Separ® PK 1455, Separ Chemie)	0 mg^{-1}	50 mg^{-1}

Figure 4: Batch test setup (Schitzenhofer 2016)

3.4 Lab-scale single chamber reactor

The lab-scale single chamber system was used to first gain experience of the PNA process and to facilitate the comparison with the mesh reactor system later.
The reactor comprised a 6 L glass reactor with a working volume of 3 L (Figure 5). It was placed in a water bath to regulate its temperature (Haak C1, DE) at 35°C. A peristaltic pump (Minipuls 2, Gilson, UK) was used to supply the substrate from a storage tank to the reactor. The effluent was ejected similarly by a membrane pump (Gamma 4, Prominent, DE) and was transferred to a 240 mL tank for drawing composite samples. The reactor was aerated with an aeration stone and an air pump (ProSilent a 200, JBL, CH), and the aeration intensity was regulated using a screw valve. The reactor was mixed using a magnetic stirrer (M2-A, AGRO LAB, DE) placed beneath the water bath. The entire system was automatised using a data acquisition device (USB 6210, National Instruments, USA) and a PC. The automation software was written in LabView. The pH was recorded using a pH probe (SensoLyte SE, WTW, DE) with the corresponding measuring transducer (pH 293, WTW, DE). The oxygen and temperature were recorded using an optical sensor with a temperature probe (FDO 925, WTW, DE) with its corresponding measuring transducer (Multi 3410, WTW, DE) for measuring dissolved oxygen. Furthermore, the redox potential was recorded using a redox probe (SensoLyte PL, WTW, DE) and a measuring transducer (pH 293, WTW, DE). The offline operation data were recorded on a daily basis using Microsoft Excel and evaluated using the software package R and Microsoft Excel. NH_4-N, CSB, and pH were recorded in the influent, and NH_4-N, NO_2-N, and NO_3-N were recorded in the effluent. Remote control was performed using UltraVNC (Ver.10, UltraVNC). Furthermore, two 1.5 L bottles were installed to perform batch tests that could be controlled separately with the control programme.

Figure 5: 3 L single chamber system (right) and 1.5 L batch test bottles (left); the red colour is due to increased iron concentrations.

During the first lab-scale operation (2 months) (Subsection 4.1.1.1), the lab-scale single-chamber system was inoculated with sludge from the DEMON® process at the WWTP Strass and fed using reject water from the same WWTP. Later, the process water was changed to reject water from the WWTP Tulln in Lower Austria (Table 2). The biomass was transferred within one day. During this time, the control programme as well as the reactor parts were regularly optimised. The operational setting and the control programme attempted to emulate the setting of the DEMON® plant in Strass, especially aeration control. It operated in SBR mode with six cycles per day each lasting for 4 hours. Initially, eight and then 10 feed intervals were used to approximate a close to continuous feed, which was followed by one settling phase and a phase for ejecting the effluent. The initial working volume was 2.5 L, which was later changed to 3 L. Between 80 and 250 mL was supplied during each cycle.

Table 2: Substrate characteristics during lab-scale single-chamber operation

Substrate characteristics during lab-scale single-chamber operation						
Origen	NH_4-N	CSB	Ks [mmol L^{-1}]	pH	Time	Comment
WWTP Strass	1098–1275	633–798	96–21	7.6	8.5.15–2.7.15	Same source as biomass
WWTP Tulln	650–744	271–288	48–56	6.92–7.3	2.7.15–06.07.2015	Additives used during sludge dewatering

Subsequent operations were used to develop the control programme, which was later used in the pilot plant. Next, the system was equipped with the improved robust aeration algorithm developed at the pilot plant (Subsection 4.3.2.1) and used to study the scale-dependent effects of alkalinity limitation on pH-based aeration control (Subsection 4.3.2.2), where a synthetic medium was used (as described on p. 39).

3.5 Lab-scale mesh reactor[5]

The reactor was made of a 20 L rectangular plastic vessel (340 x 240 x 240 mm) and had a working volume of 13 L. It was dived into two equal compartments by an aluminium frame tightly squeezed into the reactor vessel. The frame was covered with a polyester mesh (opening size 1.0 x 1.2 mm). The reactor was immersed in a water bath to maintain a temperature of 35°C +/ 0.2°C using an immersion thermostat (ED, Julabo, Germany). Two stirrers (RW 20, IKA, Germany) were implemented to obtain homogenous mixing of both reaction zones. The inflow was initially provided from a 60 L barrel placed on a balance by means of a peristaltic pump (505U Watson Marlow, US); later, a 1.000 L bulk container served as a substrate storage tank. Two automated pinch valves (SCH284B015 Asco, US) allowed the distribution of the inflow either to the nitration or alternatively to the ANAMMOX compartment. The outlet was a simple overflow established within a small conical settling zone (upper-lower Ø 70/ 45 mm, height 140 mm). In its centre, a small slow-moving rabble rake was mounted to remove gas bubbles. Aeration was performed with a ceramic aerator (140 x 25 mm) immersed in the nitration compartment using pressurised air. The air flow was controlled using a flow indicator regulator (FIC, Aera FC-PA7800c, Hitachi, Japan) and a variable area flow meter for visual control. The plant was equipped with an optical oxygen measurement device with two needle-type fibre-optical oxygen

[5] This section is taken from (Fuchs et al. 2017)

sensors (FireStingO2, Pyroscience, Germany) submerged in the two compartments. The device includes also a 4-wire PT100 temperature sensor. The pH in the nitritation compartment was measured using a standard pH meter (Mettler Toledo, US). In the start-up phase, pH was controlled within the two limits (pH 6.9, 7.8). For this purpose, two pH-controlled peristaltic pumps (101U/R Watson Marlow, US) were installed dosing 1 M HCl or 1.5 M NaOH into the nitritation zone, respectively. Online monitoring, data storage, and process control were conducted by means of a PLC (Melsec FX3G Mitsubishi). A scheme of the plant layout is presented Figure 6 and Figure 7.

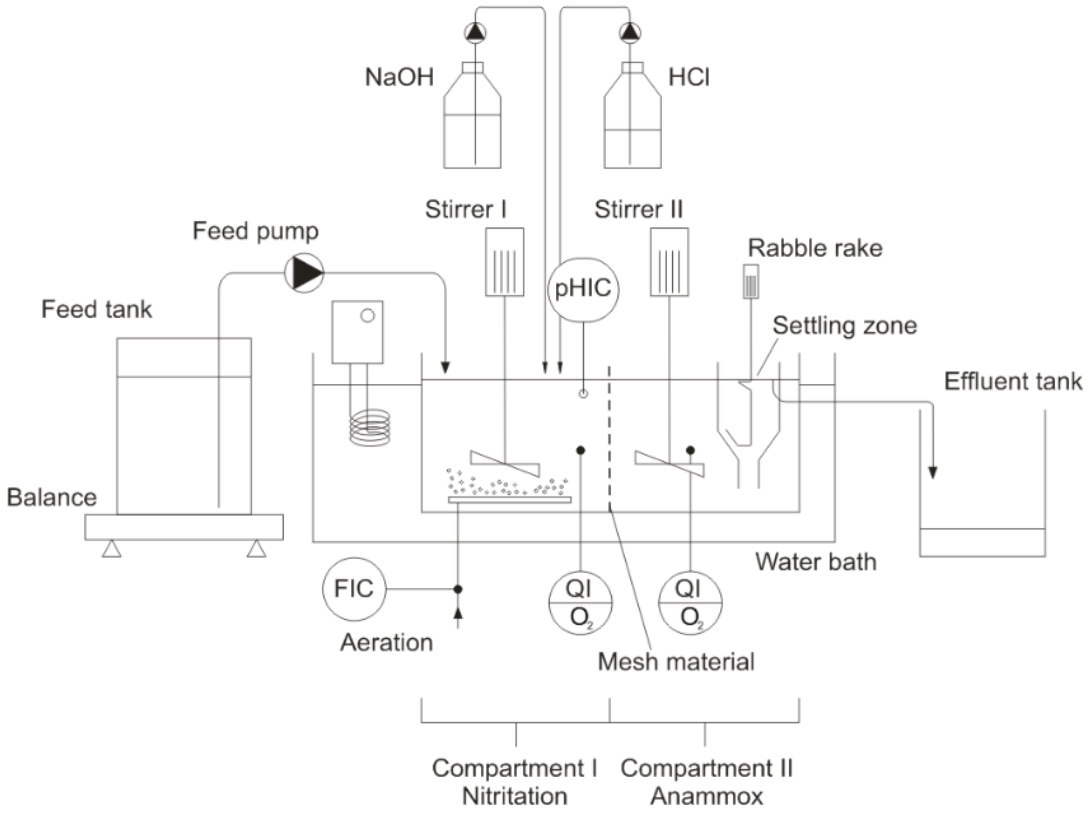

Figure 6: Schematic setup of the lab-scale mesh reactor configuration (Fuchs et al. 2017)

Figure 7: 13 L- Laborreaktor (Weissenbacher et al., 2017)

The substrate (feed) was sludge reject water derived from the anaerobic digester of the WWTP Klosterneuburg, Lower Austria (55,000 p.e.). Dewatering of digested sludge was performed by flocculation and a decanter centrifuge. To reduce variations in NH_4-N concentration, the reject water was artificially spiked with NH_4HCO_3 to achieve a NH_4-N level of approximately 750 mg.L^{-1}. The composition is provided in Table 3. The description of the reactor operation combined with the corresponding results are presented in Subsection 4.1.1.1.

Table 3: Composition of the substrate (sludge reject water) (Fuchs et al. 2017)

Parameter	Unit	Range
NH_4-N	mg L^{-1}	(407–748*) 726–758**
TKN	mg L^{-1}	(430–791*) 773–825**
ortho-P	mg L^{-1}	11.0–16.0
TP	mg L^{-1}	13.0–17.9
COD	mg L^{-1}	260–414
pH	-	(7.8–8.1*) 7.8–8.1**
Alkalinity	mmol L^{-1}	(45–78*) 63–82**

*Original sample, **After spiking with ammonium bicarbonate

3.6 Pilot plant single-chamber and mesh reactor[6]

The pilot plant consisted of two reactors: a single chamber and a two-compartment mesh system (Figure 8 and Figure 9). Both had a working volume of 375 L during SBR operation and 395 L during continuous operation. Each reactor was equipped with a hood for collecting the off-gas of the reactor. The effluent of each reactor was collected in separate containers for drawing composite samples and measuring effluent flows according to the water level.
The single-chamber system was equipped with an impeller, a plate membrane aerator (Aquaconsult, AT), and an influent hole at the bottom. Both reactors were fed from an influent tank of 1.3 m^3 using a peristaltic pump (Watson Marlow, US) for each reactor, which were regularly readjusted to maintain the defined volumetric loading rates. The influent tank was equipped with an impeller to allow substrate manipulation by spiking, whereas the influent tank was supplied by two 5 m^3 storage tanks containing reject water.

Figure 8: Pilot plant before start-up consisting of a single chamber (right) and a two-compartment mesh system (left) (Weissenbacher et al. 2017).

[6] This section is based on Schoepp et al. 2018 and Weissenbacher et al. 2017

The mesh system was divided by an aluminium frame with a polyester mesh (0.2 to 0.3 mm in width), which was supported by a net (1 mm in width) (Figure 10). The aerated side was equipped with a plate membrane aerator (Aquaconsult, AT). The nonaerated side, where the effluent was also located, was equipped with an impeller. This allows the creation of two distinct zones, one being turbulent and the other being relatively laminar in the top section and turbulent in the lower section being anaerobic. Furthermore, this was used to induce a granular selection process when the reactor was operated in a continuous mode as the effluent was taken from the upper section of the reactor. The initial intention behind this reactor configuration and potential advantages are discussed in (Fuchs et al. 2017) and summarized in Section 2.2.1.

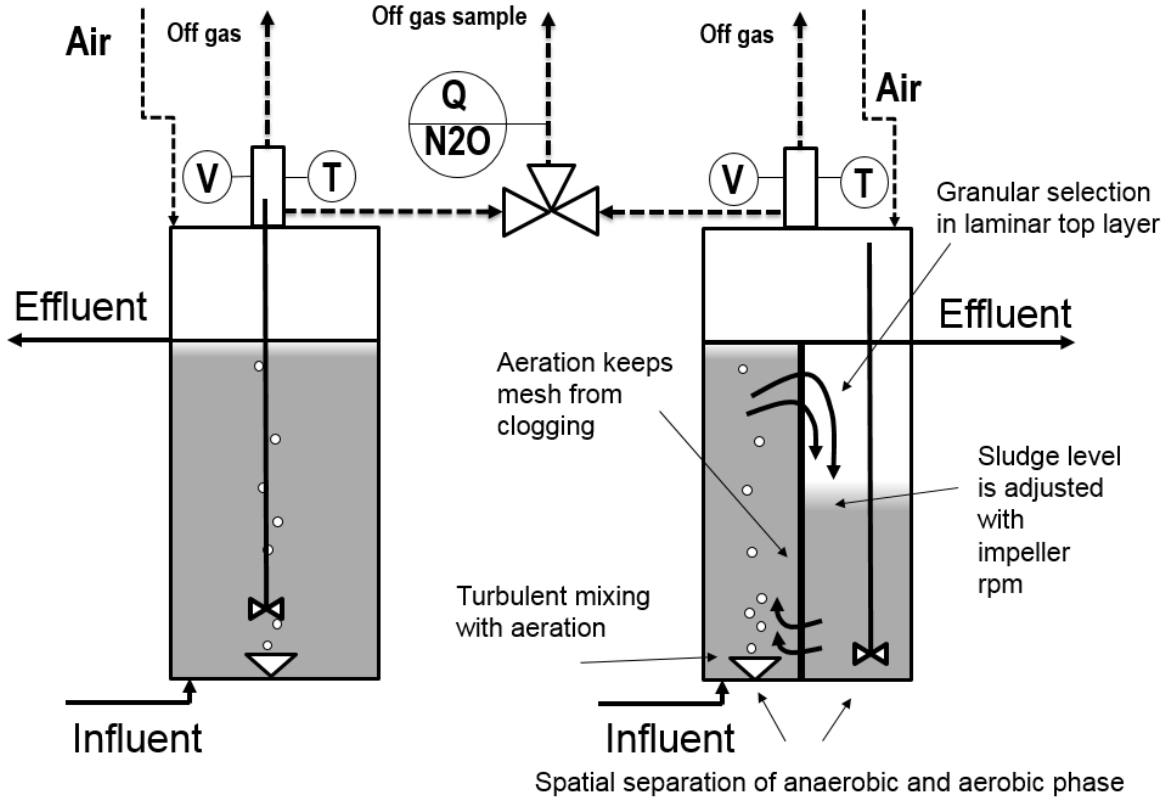

Figure 9: Scheme of the pilot plant reactors with N_2O monitoring single chamber (left) and the mesh reactor (right) (Schoepp et al. 2018).

Figure 10: The mesh in its final configuration, separating the aerated from the nonaerated side.

The pilot plant was controlled using a PC-based USB data acquisition device (USB 6210, National Instruments, US). The pH of each reactor was measured online (Orbisint CPS11, Endress Hauser, CH) and the dissolved oxygen was measured using an Oxymax W COS61 (Endress Hauser, CH). The airflow was switched using a magnetic valve at a preset flow rate, and the aeration volume was recorded using a positive displacement meter.

3.6.1 Substrate source and supply of the pilot plant

Initially, this study planned to use the process water from the WWTP plant in Tulln for the pilot plant operation. However, due to the loss of process stability during the first lab-scale operation of the single chamber reactor (Subsection 4.1.1.1), this plan was discarded. To prevent the problems, the lab-scale mesh reactor was switched to process water from the WWTP in Klosterneuburg, achieving stable operations. Unfortunately, it was technically not possible to extract the larger quantities required for the pilot plant operation from this plant. Therefore, process water supply had to be changed to reject water from the WWTP in Stockerau. The water was taken directly from a screen filter press (Figure 11) and stored in containers. A lorry (Figure 12) was regularly used to transport the reject water to the pilot plant station where it was pumped into the storage tanks (Figure 13). Compared with the reject water used in Strass Tyrol, its NH_4-N (290–510 mg L^{-1}) concentration was relatively low for a PNA application. To reach higher loading rates, NH_4HCO_3 and $NaHCO_3$ were used to adjust the ammonium and alkalinity concentrations (Table 4).

Table 4: Influent characteristics after spiking (Schoepp et al. 2018).

		Influent
Parameter	Unit	Average (range)
Influent NO_3-N	mg L^{-1}	3.2 (1.8–7.5)
Influent NO_2-N	mg L^{-1}	3.1 (1.28–4.85)
Influent NH_4-N	mg L^{-1}	1241 (1068–1448)
Influent TOC	mg L^{-1}	266 (211–364)
Influent Ks	mmol L^{-1}	126 (110–141)

Figure 11: Reject water was collected at the WWTP in Stockerau using a submersed pump (Weissenbacher et al. 2017).

Figure 12: Loading of onsite storage of reject water collected in 10 m^3 IBC tanks (Weissenbacher et al. 2017).

Figure 13: Takeover of reject water at the pilot plant station (Weissenbacher et al. 2017).

3.6.2 Monitoring of N_2O

During the N_2O monitoring period, the gas sampling was regularly changed between the reactors and combined with an intensified regular sampling campaign of the influent and effluent. The total off-gas flow was measured using an anemometer (EE75, EE Elektronik, AT). A suction tube collected the off-gas sample from the off-gas stream of the sealed reactor headspace, as shown in Figure 9. The off-gas sample was pumped into an insulated chamber containing a gas cooler and a Clark-type N_2O sensor (Unisens, Denmark).

3.6.3 Pilot plant reactor operation

Both reactors were operated using the same controller settings for the SBR mode. The SBR mode consisted of a 210 min reaction phase followed by 15 min of settling and 15 min of decanting. The inflow was evenly distributed to the two reactors during the SBR mode. During the continuous operation of the mesh reactor, the inflow to the continuous reactor was adjusted to ensure the same daily loading rates of both systems.
An improved time and pH bases robust aeration algorithm was implemented during the process of continuous optimisation of the pilot plant, which was to cope with pH artefacts

that, prior to implementation, regularly hindered stable reactor operation, especially after the aeration was interrupted due to malfunctions. In a subsequent step, a PID-based feed control strategy was tested with the single chamber system (Subsection 4.3.2.1). Furthermore the mesh reactor was optimised (Subsection 4.3.1.2).
After a process of continuous optimisation, nitrogen loading rates of 0.5 kg N m^{-3} d^{-1} were achieved and gaseous N_2O emissions were monitored to test for the impact of reactor configuration and operation mode (Section 4.3.3).
Finally, at the end of the pilot plant operation, an alkalinity limitation experiment was conducted to gain further information on the scale-dependent effects, and the single-chamber lab scale reactor was inoculated with an aliquot of the pilot plant single chamber system.
To control the molar NH_4-N to HCO_3^- ratio, tap water was spiked with NH_4HCO_3 until a NH_4-N concentration similar to the previously used process water was achieved.
By adding less $NaHCO_3$ with each reduction step, a ratio from 0.75 to close to 1 was tested.
By adjusting the $NaHCO_3$ concentration, the NH_4-N to HCO_3^- ratio was adjusted during the alkalinity reduction experiment (Subsection 4.3.2.2).
A summary of the different operation phases of the pilot plant is provided in Table 5.

Table 5. Summary of pilot plant operation phases (adapted from Weissenbacher et al. 2017).

Name	Time	Target
Start-up	4 weeks	To establish a stable process, solve remaining technical issues, and test monitoring tools.
First increases of N load	9 weeks	To optimise the mesh, test continuous operation, increase N load, and test monitoring tools.
Test of control strategies	4 weeks	To implement and finetune robust aeration control and pH-based feed control.
Increase of N load comparable to large scale	5 weeks	To increase the N load by increasing the NH_4-N to alkalinity ratio from 0.9 to 0.8, and to implement N_2O measurements.
Investigation of N_2O Emissions	4 weeks	To perform intense monitoring and N_2O monitoring, change the mesh reactor to continuous operation, and evaluate the biomass composition and particle distribution.
Variation of influent alkalinity	4 weeks	To investigate the impact of alkalinity reduction and measure the oxygen transfer efficiency.

3.7 Determination of oxygen transfer efficiency

During the investigation of alkalinity reduction, the oxygen transfer efficiency (OTE) of the lab-scale single chamber, the pilot-scale single-chamber, and the pilot-scale mesh system was measured to determine its impact of the pH-based aeration control.
The OTE of the single-chamber lab-scale and pilot-plant reactors was determined by reducing the reactor to endogenous respiration, followed by a subsequent aeration test. First, the feed of the system was stopped while aeration and mixing continued. Once all substrates were used and the systems were reduced to endogenous respiration, the aeration was turned off and

the DO was allowed to drop to zero. Once the DO had dropped to zero, the aeration was turned on again and the time to reach 1 mg L^{-1} DO was recorded. By considering the reactor volume and aeration volume that was used to reach 1 mg L^{-1} DO, it was then possible to express an estimate of the OTE.

4 Results and discussion

4.1 Lab-scale phase

4.1.1 Comparing the lab-scale single-chamber system with the mesh separated lab-scale system

This section describes the results of the first attempts at implementing lab-scale PNA systems. First, a lab-scale single-chamber system was implemented, and shortly afterwards a lab-scale mesh separated system was implemented. Both systems were used to gain the process know-how necessary for the later comparison of both systems at the pilot scale. Furthermore, they allowed the first conclusion to be drawn about the achievable process stability.

4.1.1.1 Lab-scale single-chamber system

Stable periods

The lab-scale single-chamber system (Figure 5) was inoculated with sludge from the DEMON® process at the WWTP Strass and was fed using reject water from the same WWTP; initially, it was possible to achieve a relatively good process performance (Figure 14).

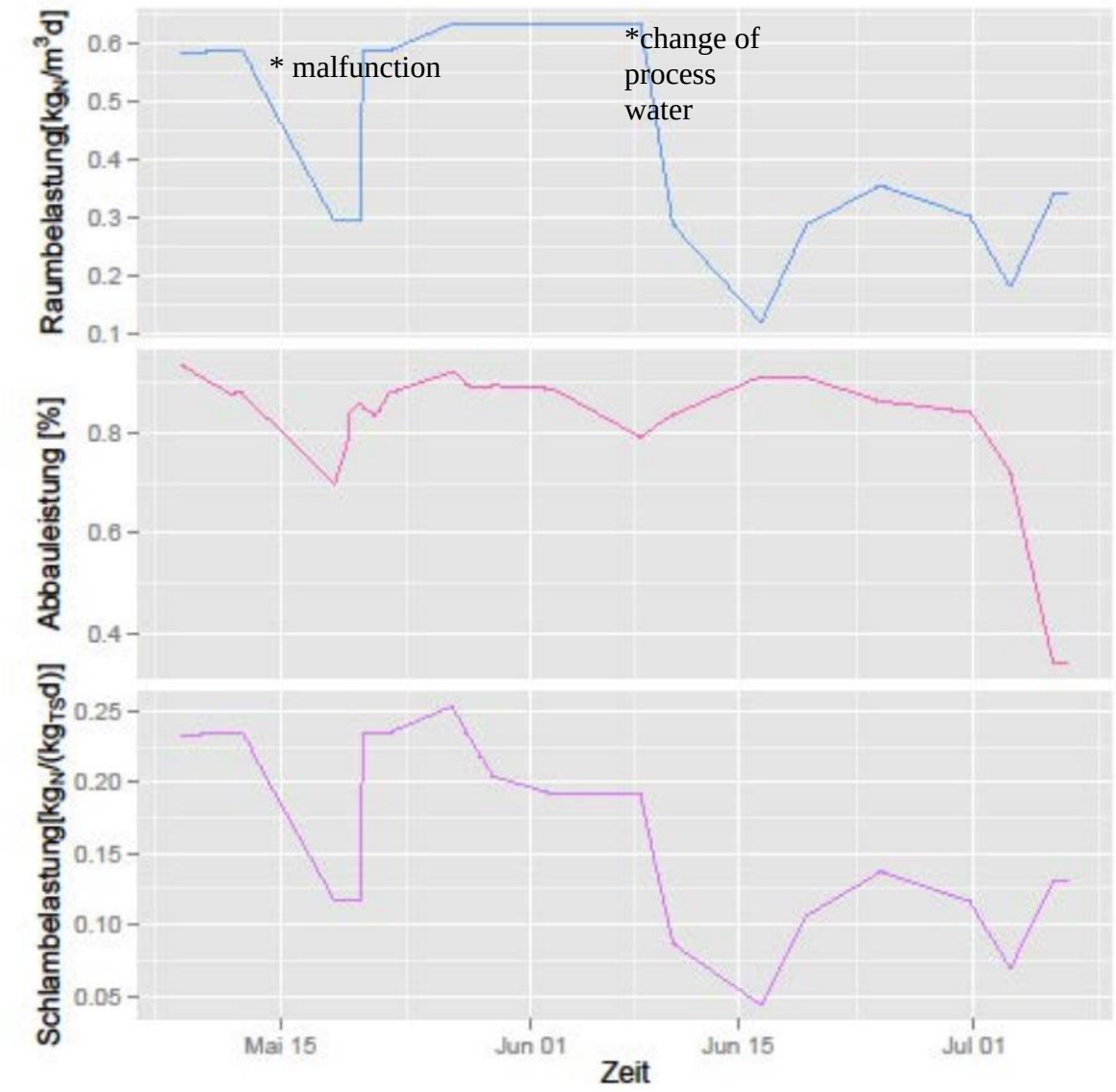

Figure 14: Overview of the volumetric loading rates and nitrogen removal rate of the lab-scale single-chamber system during the first operation, with sludge from WWTP Strass (a change of process water occurred on Jun 06–08); adapted from Weissenbacher et al. 2017.

During the stable periods (May 7–10, May 19–Jun 6), a nitrogen removal rate of 90% at a volumetric loading rate of 0.5 kg $m^{-3}d^{-1}$ was achieved, which corresponded to a sludge loading rate of 0.2 kg NH_4-N kg^{-1} VSS d^{-1}. The average concentrations were 22 mg L^{-1} NH_4-N, 1 mg L^{-1} NO_2-N, and 70 mg L^{-1} NO_3-N. Characteristic pH and ORP patterns became apparent, which resulted from the pH drop during aeration that stopped once the lower limit of the pH was reached. At this point, it rose again during the anaerobic phase until the upper limit of the pH interval was reached and the aeration was turned on again. A setting which emulated the aeration control of the large-scale DEMON® implementation at the WWTP Strass (Figure 15). The stable period was interrupted by a malfunction of the aeration (May 11). By reducing the loading rate and regularly readjusting the pH set point, it was possible to recover the process stability.

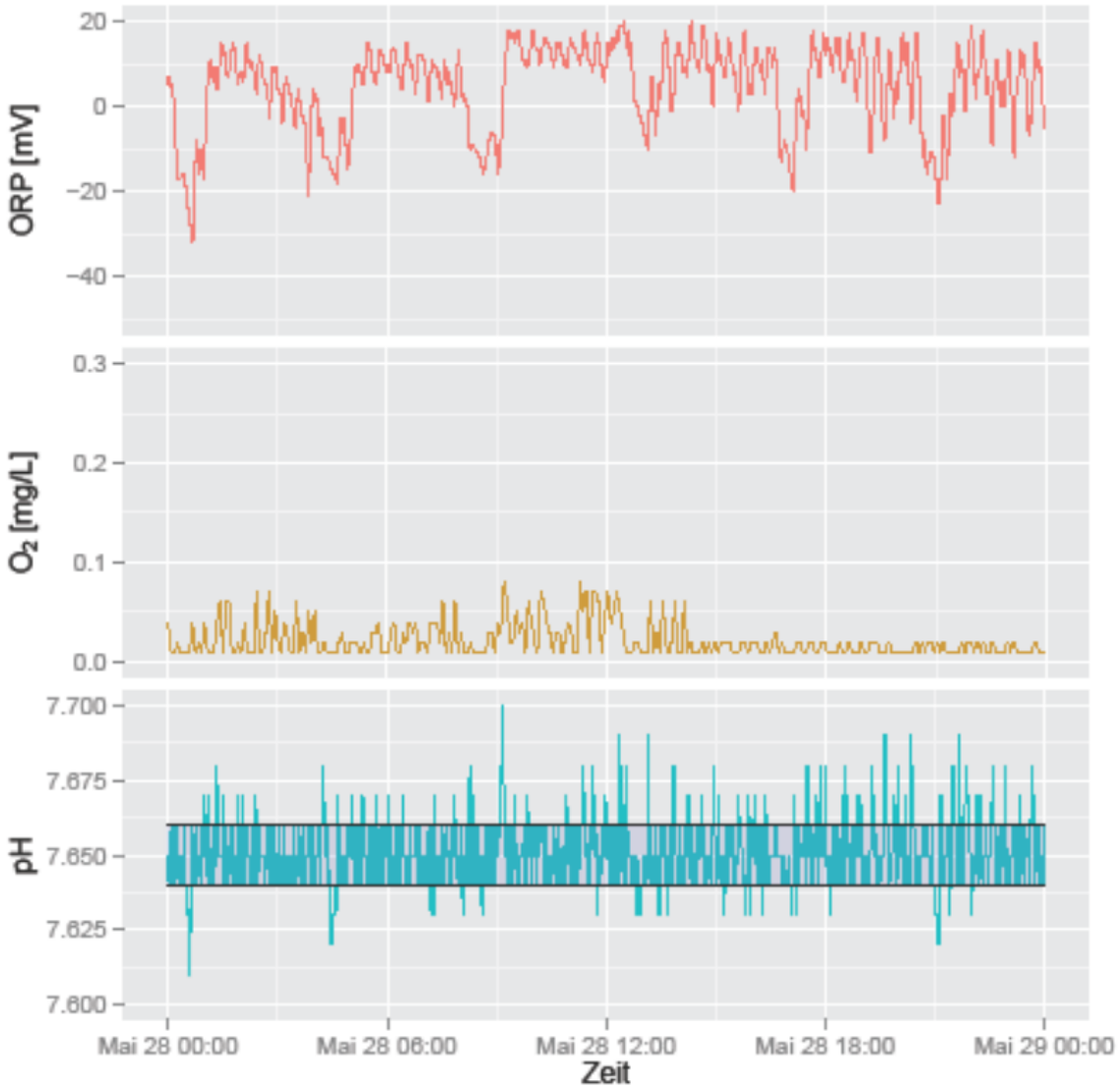

Figure 15: DO, pH, and ORP values during stable operation with reject water from WWTP Strass (Weissenbacher et al. 2017).

Change of process water

Once the reject water from the WWTP Strass had been used, it was switched to reject water from the WWTP Tulln (Jun 06–08). WWTP Tulln was supposed to serve as the future supplier of reject water during the later performed pilot plant operation, which led to a continuous loss of process stability. The aeration control could not maintain the pH limits, which led to regular under and over-aeration of the process. Even though the loading rate was reduced, NO_2^- started to accumulate. In addition, iron oxide started to enrich in the reactor, a reminder of the dewatering process. This observation motivated subsequent tests of dewatering additives on ANAMMOX activity (Section 4.2). Furthermore, the control strategy was changed to a combined pH- and DO-based control algorithm. Nevertheless, it was not possible to establish a stable process using the reject water from the WWTP Tulln. This also

made it necessary to evaluate alternative options for suppling the lab-scale mesh reactor as well as the pilot plant with reject water.

Impact of malfunction on aeration control

The loss of process stability due to changing of the reject water, or the impact of a malfunction that stopped the reactor operation for several hours, showed that the pH-based aeration control led to the over aeration of the system once the pH equilibrium of the process was disturbed, because the response of the pH to aeration was inverted. Figure 16 depicts the typical situation after a malfunction had occurred where the aeration had stopped, in this case because of a power surge that shut down the control computer for approximately 24 h. Thus, it was necessary to regularly reset the pH set point until an equilibrium was reached. Although an additional DO set point was used, and the loading rate was reduced to limit the possibility of over aeration, increased NO_2^- concentrations could be detected in the effluent. A solution to the problem was found later on (Subsection 4.3.2.1).

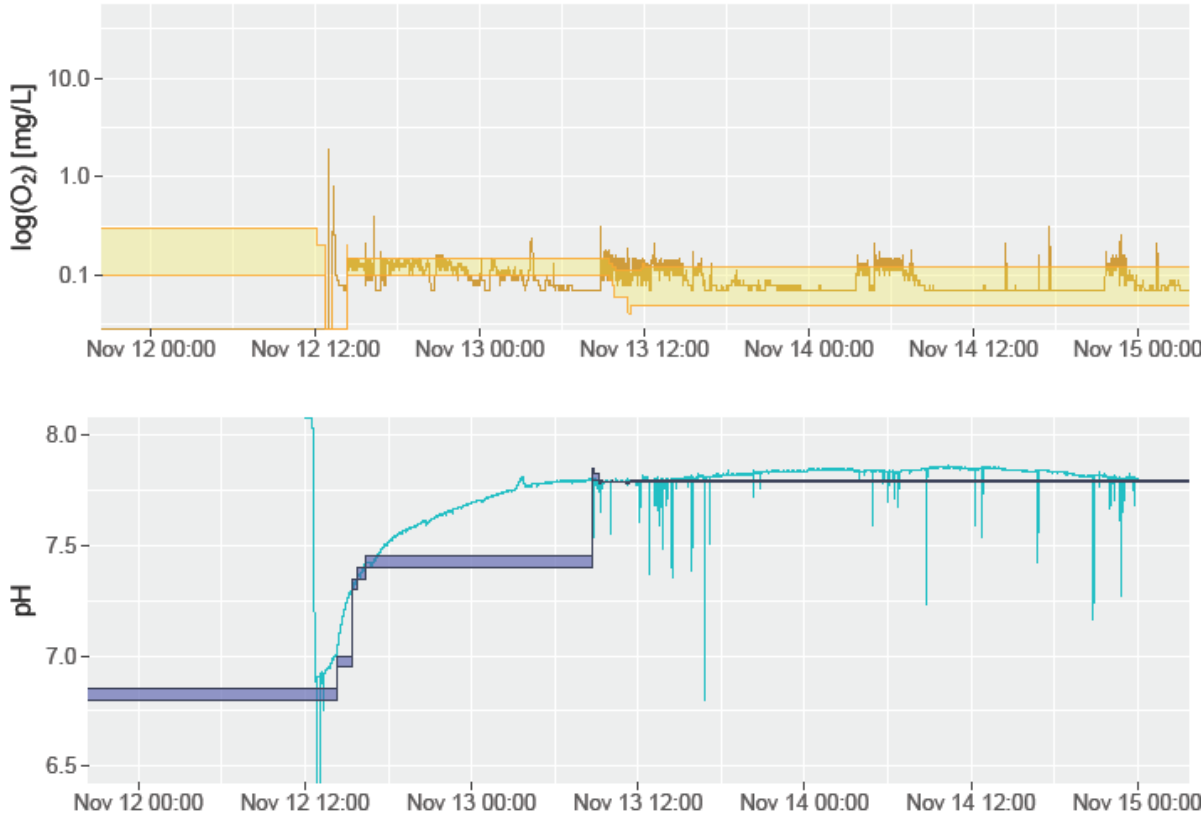

Figure 16: pH Stripping effect after a malfunction.

4.1.1.2 Lab-scale mesh reactor[7]

Because of the difficulties experienced during the start-up of the lab-scale single chamber system with the reject water from WWTP Tulln, synthetic medium was used to get the lab-

[7] This section summarizes the results of Fuchs et al. 2017 and puts them into context with this study

scale-mesh reactor started (Figure 7), whereby a volumetric nitrogen removal rate of 0.2 kg m^{-3} was achieved. Later, the process water source was changed to reject water from the WWTP Klosterneuburg. Similar fluctuations to those of the lab-scale single-chamber system followed by an NO_{2-} (100 - 150 mg L^{-1}) build-up were experienced. However, in contrast to the lab-scale single-chamber system, the mesh system's aeration control employed time-dependent intermittent aeration, which was limited by a DO signal to 0.2 mg L^{-1} due to the poor performance of the pH-dependent aeration control of the lab-scale single-chamber system.

To protect against pH fluctuations, an acid-base dosing device was installed during start-up. In addition, the influent was split to the aerobic and anaerobic sides according to stoichiometry 60:40. The initially installed mesh (0.12 x 0.12 mm), used to separate the anoxic from the aerated side, had to be changed to a wider mesh (1.0 x 1.2 mm) due to blocking by biofilm. A biofilm quickly formed, adding to the barrier properties of the mesh. Subsequently, 120 days of stable operation were possible; however, similar to the lab-scale single-chamber system, stable operation was terminated by NO_2^- accumulation, which indicated the substrate inhibition of ANAMMOX. This is a system failure common to PNA systems (Lackner et al. 2014).
Subsequently, the start-up strategy was changed to avoid further system imbalances. Instead of directly supplying the substrate, tap water was used to dilute the influent until the desired loading rate of 0.5 kg N m^{-3} d^{-1} was achieved within 21 days, whereby a loading rate comparable to the lab-scale single chamber system was achieved—a start-up strategy later applied at the pilot scale.
With an increasing loading rate, aeration intervals were manually changed to maintain the pH within the desired range, resulting in a behaviour similar to pH-dependent aeration. The separate feeding of the anoxic and aerobic sides of the mesh reactor was changed to only feeding the anoxic phase to reduce the risk of process inhibition. No change in the process performance was observed due to the permeability of the mesh. Therefore, splitting the influent was discarded and it was all directed to the first aerobic chamber.

After the abovementioned changes were implemented, the lab-scale mesh reactor did not experience further problems with process stability. When the lab-scale mesh system operated comparably to the lab-scale single chamber (0.5 kg N m^{-3} d^{-1}), the N removal rate was on average between 80% and 85%, with concentrations of 40 mg L^{-1} NH_4-N, NO_2-N < 5 mg^{-1} L^{-1}, and 86 mg L^{-1} NO_3-N. This indicated slightly lower N removal and increased NO_3-N formation compared with the lab-scale single-chamber system; however, achieved much more consistently. Altogether, those NO_3-N values were well in line with the process stoichiometry, and 11% was transformed into NO_3- N.

When those results were achieved (around day 175), the pilot plant was in its final stage of construction. The results achieved at this point in time were implemented into the pilot plant version of the mesh reactor, such as maintaining intermittent aeration, which resulted in a behaviour similar to the DEMON® plant. Nevertheless, it was decided to keep the pH-dependent aeration at the pilot scale because pH control by acid-base addition was unfeasible at a large scale and it was suspected that pH artefacts compromising the pH-controlled aeration would diminish at a large scale. Future operations showed that the lab-scale mesh system was able to maintain process stability without the control of pH by acid and base. Similar to the lab-scale mesh system, the implementation of a relatively wide mesh and feed all influent to the first aerobic chamber of the pilot-scale system was selected. However, the problem of sludge retention was yet not solved at the lab scale. The settler that was installed

could not effectively retain the heavier ANAMMOX granules inside the system, which was partly attributed to N_2 bubbles rising in the anoxic zone. To maintain stable operation, the granules that were washed out had to be returned manually to the system.

Further development of the system and testing of the limits

After the basic understanding for running a mesh system was developed and implemented at the pilot scale, the lab-scale mesh system was further developed and its performance limits were tested. Because of the successful adaption of the pH-dependent aeration at the pilot scale (Subsection 4.3.2.1) and the fact that the aeration intervals had relatively short aeration breaks at the higher loading rates, it was decided to omit the intervals all together and switch to pH-controlled continuous aeration using a mass controller. In addition, the DO signal was removed because it did not contribute to the aeration control as it remained below the limits of detection in the pilot plant systems, as well as in the lab-scale system. It was possible to reach loading rates up to 1.5 kg N m^{-3} d^{-1} with an 80 to 90% nitrogen conversion rate (Figure 17). During those 7 months of continuous operation, the lab-scale mesh reactor was able to demonstrate its process stability and recalcitrance to NH_4^+ and NO_2^- built up due to technical malfunctions. Further details and an in-depth discussion and comparison of the lab-scale mesh system can be found in Fuchs et al. (2017).

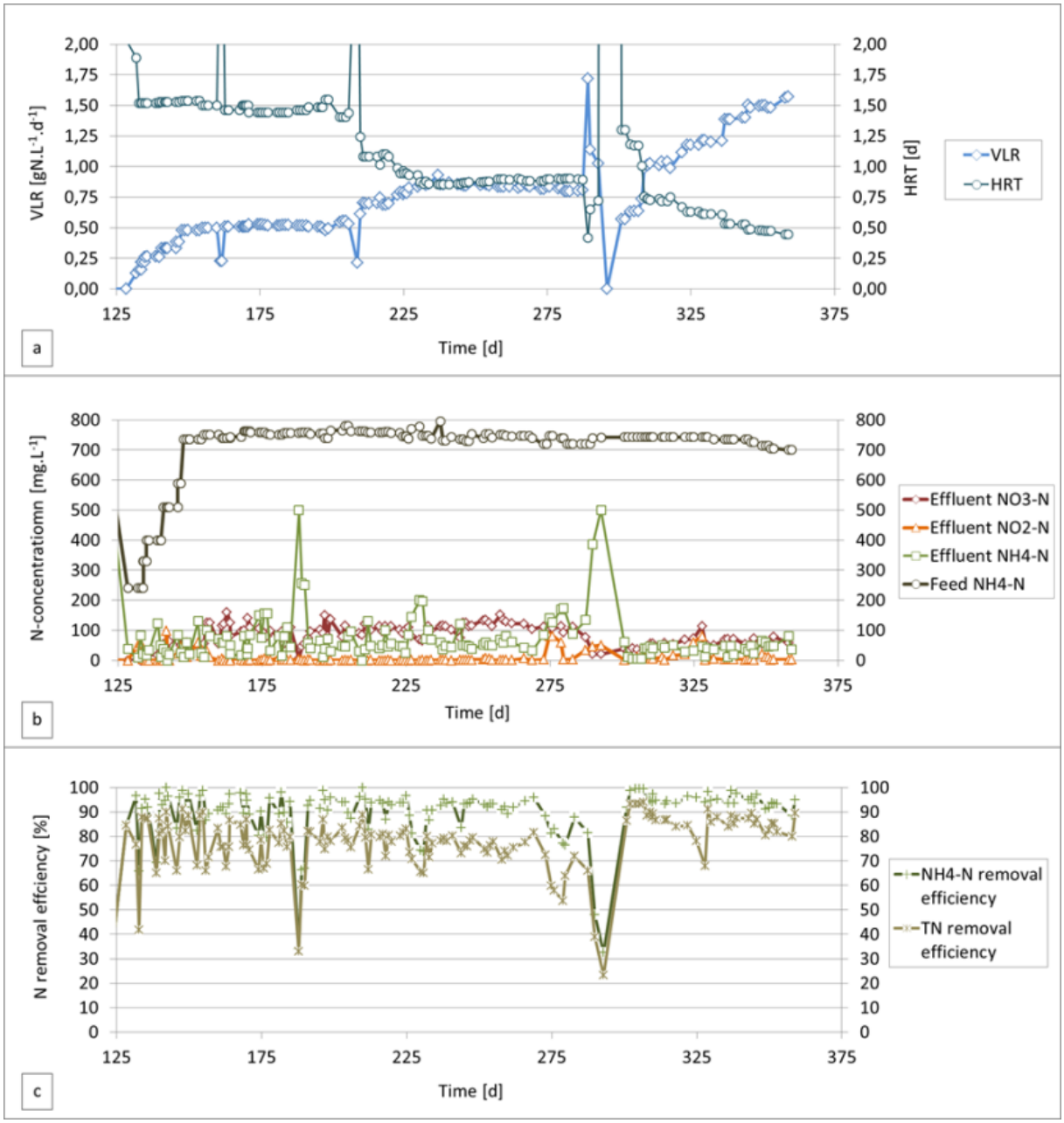

Figure 17 a-c: Performance data of the lab-scale mesh reactor: (a) NH_4-N volumetric loading rate (VLR) and hydraulic retention time (HRT), (b) concentration of nitrogen parameters in effluent and influent; (c) removal rate for ammonia (NH_4-N) and total nitrogen (from Fuchs et al., 2017).

4.2 Evaluating process monitoring tools

Applying additional monitoring methods, in contrast to just monitoring effluent and influent values, was intended to increase the process stability through increased process information. As the ANAMMOX fraction is commonly referred to as being the sensitive bottleneck of the process, it was selected for implementing ANAMMOX specific monitoring tools. AA and heme concentration were promising methods as they were simple enough to be performed in small scale WWTPs.

Due to the difficulties experienced after switching the lab-scale reactor to a reject water source where dewatering additives were intensely used, it was decided to investigate polymer and $FeCl_3$ and increased NO_2^- levels during a batch test to compare the suitability of both methods. The batch test consisted of three consecutive test cycles to evaluate the development of both monitoring values over time, before they were applied during the start-up of the pilot plant later (Figure 28).

4.2.1 Treatment effects on AA and heme

The batch test results after 4 days, 8 days, and 12 days (Table 12) were analysed using MANOVA (Table 14) and follow-up post-hoc regression (Table 15). The significant results are discussed herein and the magnitude of the effect is given as the relative difference of the high and low group of the respective treatment, such as the 70 mg L-1 and 105 mg L-1 NO_2-N treatment levels (

Table 13).

After 4 days, the polymer had a relatively positive effect of +28 % on heme, and $FeCl_3$ and NO_2-N had positive effects of +47 % and +15 % on AA. After 8 days, the relatively positive effect of NO_2-N of +110 % on N removal increased, whereas no significant effects on heme and AA were detected for $FeCl_3$ and polymer, which turned into a relatively negative effect of –53 % until the end of the batch test. The initial positive effect after 4 days of NO_2-N was presumed to be caused by the increased substrate supply due to elevated NO_2-N concentrations. However, while higher concentrations were beneficial in the beginning, the effect of NO_2^- inhibition prevailed in the end. In this context, it must be noted that in AA batch tests, NO_2^- levels are always problematic as they require a sufficient supply of NO_2-N, which may lead to problematic concentrations of NO_2-N at the beginning of a batch test. The positive effect of $FeCl_3$ on AA could be attributed to some protective effect, as iron is an important cofactor of ANAMMOX metabolism (Kartal and Keltjens 2016). Recent studies have found a similar positive effect when adding iron (Zhang et al. 2019; Erdim et al. 2019; Yan et al. 2019).
A short-term positive effect can explain the positive effect of polymer on heme at the beginning due to the increased agglomeration of biomass. This increased agglomeration could have protected the ANAMMOX population against the elevated NO_2-N concentrations right after feeding. A post-hoc regression test for heme indicated a positive interaction of NO_2^- and polymer supporting this explanation. This suggested that the state of agglomeration of the biomass, among exposure time, should be taken into account when evaluating increased NO_2^- levels.
In contrast to expectations, the additives polymer and $FeCl_3$ used during sludge dewatering may also have had beneficial effects on the ANAMMOX population. However, this result should be interpreted with particular caution as the equally crucial nitrite-forming fraction of the biomass was not assessed in the test. For example, $FeCl_3$ addition may severely reduce the amount of alkalinity, which could limit the performance of the entire PNA system if the alkalinity drops too low (Klaus et al. 2017). This is because the alkalinity is central to meeting the inorganic demands of nitrification as well as stabilising the pH of the PNA system.

4.2.2 N parameters and VSS

All treatments showed an increase NH_4-N concentration with an ongoing duration of the experiment. As expected, a larger increase was observed for those treatments where less NO_2-N was provided (Table 13). In all treatments, NO_2-N was wholly consumed. Furthermore, NO_3-N concentration remained lower than expected by ANAMMOX stoichiometry, which indicated denitrification, either by denitrifiers or the facultative denitrification of ANAMMOX. This effect was also reported by Kartal et al. (2007) and requires the consumption of organic carbon. Such consumption is in line with the VSS levels which dropped throughout the experiment. This drop can be attributed to endogenous respiration and presumably also to the cell lysis caused by the starvation of the aerobic fraction of the sludge. Here, organic carbon was released by the latter process, allowing for denitrification to take place. Furthermore, the heme concentration dropped with the duration of the experiment, indicating generally unfavourable conditions for the ANAMMOX biomass as heme is a central element of the electron transport chain (Strous et al. 2006; Kartal et al. 2007; Ferousi et al. 2017). The nitrogen removal efficiency indicated a drop in the middle

followed by a catch up at the end of the experiment. Although this observation was not in line with the decline of AA, it could be attributed to a parallel increase in denitrification activity caused by the COD available through cell lysis.

4.2.3 Comparison of AA and heme for the suitability of monitoring

By comparing the development of AA and heme, their suitability for process monitoring could be examined (Figure 14). Whereas the heme concentration indicated a clear downward trend throughout the experiment, the AA values gave a less clear image. In contrast to heme, AA showed an increase of variance throughout the experiment and no clear trend regarding the effect of polymer and $FeCl_3$. Regarding the treatment effect of NO_2-N, AA allowed the observation that recovery occurred for the group treated with low NO_2-N from day 8 to day 12. This was not observed by monitoring the heme values.

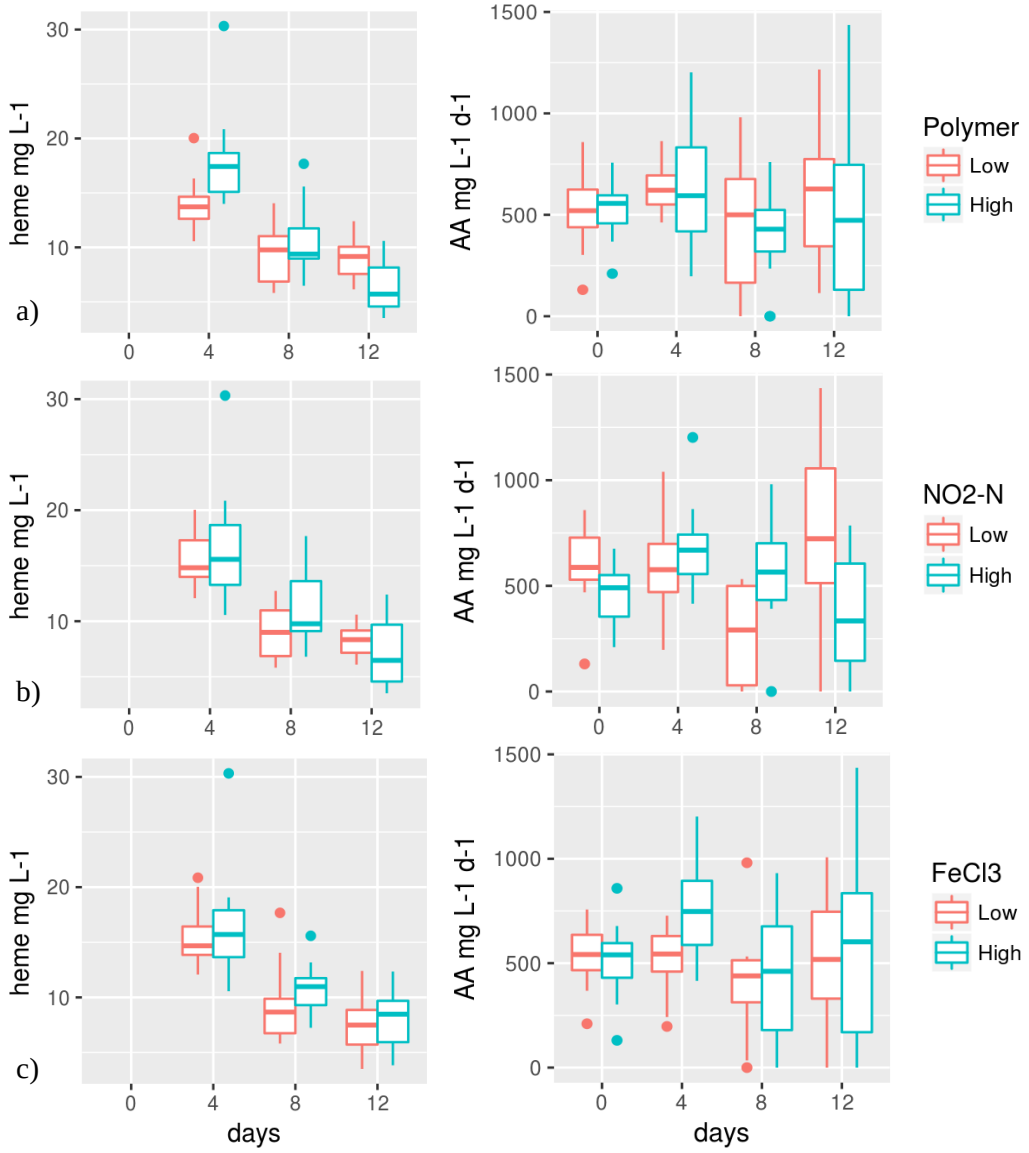

Figure 18: Development of heme and AA grouped by polymer (a), NO_2-N (b), and $FeCl_3$ (c) treatment.

The results of the batch test suggested that AA responded quickly to disturbances, as was observed by Chen et al. (2012), but also that it is less suitable for detecting general trends. Said trends are of greater interest to process operators because short-term fluctuations are already identified by the routine monitoring of effluent values. This was also observed when monitoring the pilot plant's start-up, where the nitrogen removal rate based on the effluent values showed similar values to the nitrogen removal rate based on AA (Subsection 4.3.1.1). A recent study similarly concluded that heme C is a good indicator of ANAMMOX performance (Ma et al. 2019).

4.3 Pilot scale

4.3.1 Start up, optimisation, and monitoring[8]

The pilot-scale single chamber and the mesh system were inoculated simultaneously. Both systems used pH-dependent aeration control. Until the improved robust aeration control algorithm was implemented (Subsection 4.3.2.1), a lower DO limit was introduced to prevent the prolonged unaerated phases when the pH signal destabilised (later discarded). Similar to the start-up of the lab-scale mesh system, the influent concentration was gradually increased by diluting the influent with tap water to allow the biomass to adapt. Moreover, the mesh system was operated in SBR mode with the intention of first establishing a dense biofilm, whereby the anoxic zone should become more laminar and the application of a settling device was possible (Subsection 4.3.1.2). Additionally, ANAMMOX monitoring methods were applied to gain additional information (Subsection 4.3.1.1).
The comparison of both systems showed that they behaved very similarly (Figure 19Figure 20), achieving a removal rate of 0.2 kg N m^{-3} with an 80% removal rate in the first month of operation. The NO_2-N concentrations were maintained below 5 mg L^{-1} (Figure 22) but relatively increased NH_4-N was observed (Figure 23), which indicated that the system was limited by AOB activity.

Table 6: Pilot plant process parameter during start-up (Weissenbacher et al. 2017)

Parameter	Single chamber	Mesh separated
TSS	2.6–4.9 g L^{-1}	3.3–3.8 g L^{-1}
VSS	2.18–4.2 g L^{-1}	2.9–4.2g L^{-1}
Volumetric Loading rate	0.05–0.27 kg N m^{-3} d^{-1}	0.05–0.20 kg N m^{-3} d^{-1}
Sludge loading rate	0.01–0.07 kg N kg^{-1} TS d^{-1}	0.01–0.04 kg N kg^{-1} TS d^{-1}
Upper pH Limits	7.01–7.015	7.01–7.015
Lower pH limits	7.26–7.265	7.125–7.13
Aerated reactor volume	100%	50%
Lower DO set point	0–0.3 mg L^{-1}	0–0.3 mg L^{-1}
Upper DO set point	0.1–0.5 mg L^{-1}	0.1–0.5 mg L^{-1}

[8] The section is based on results already published in the final report of the DEKO project, Weissenbacher et at. 2017

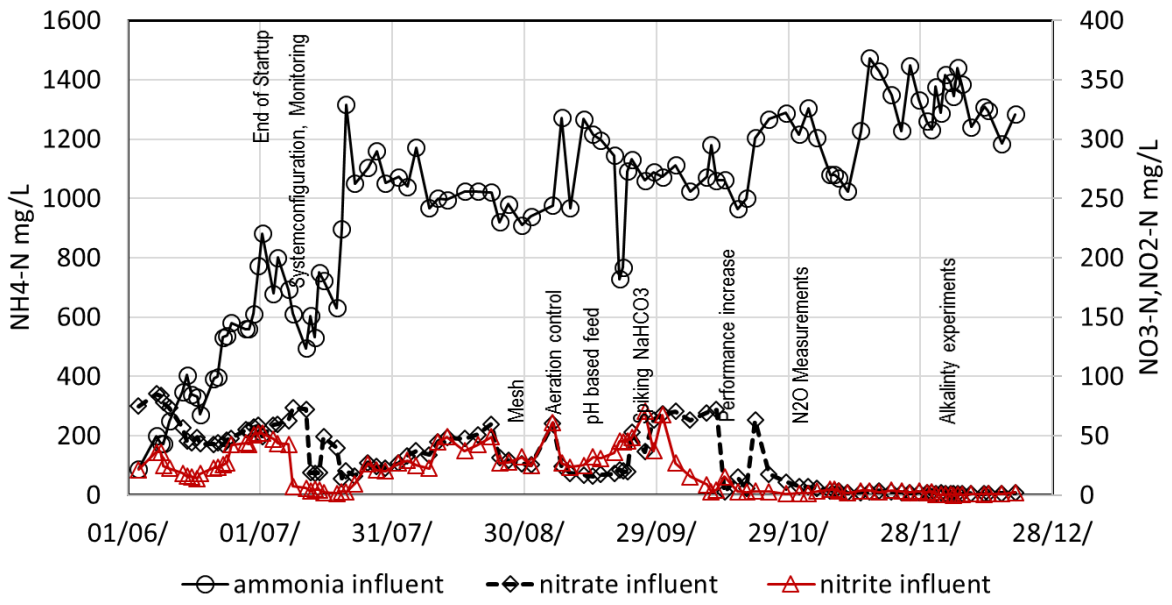

Figure 19 : Influent composition during pilot plant operation.

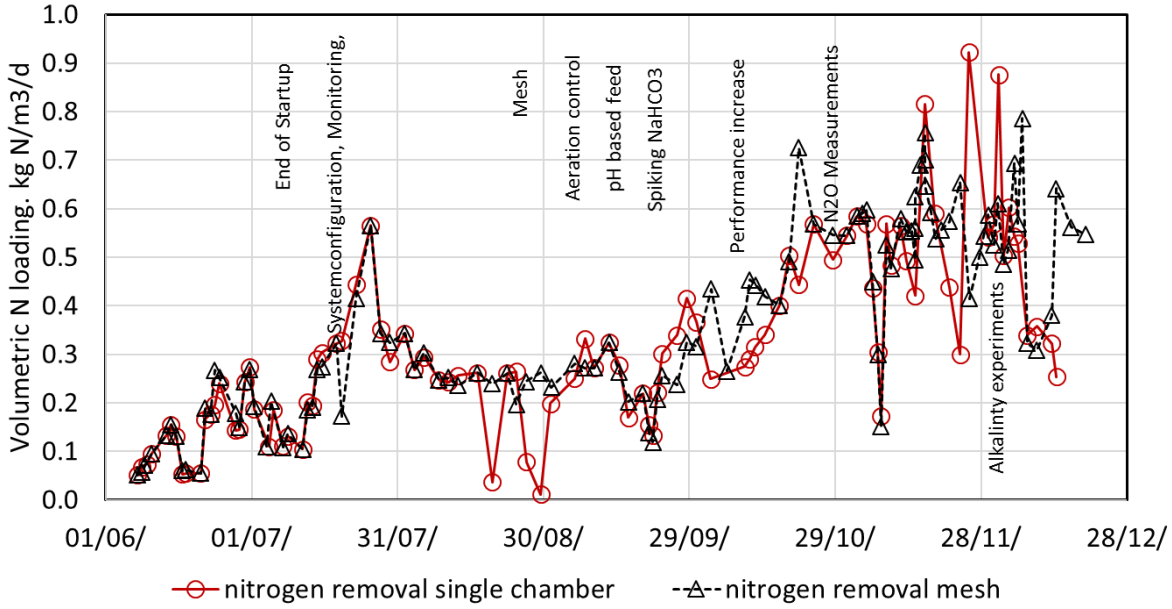

Figure 20: Development of volumetric nitrogen loading rate.

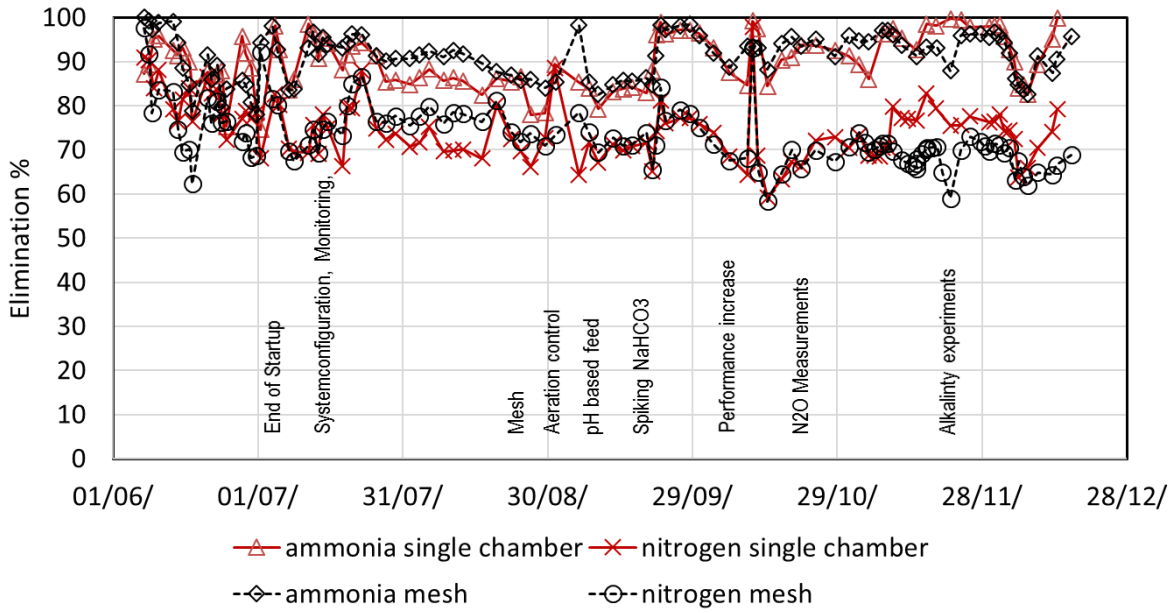

Figure 21: Development of ammonia and nitrogen elimination rate.

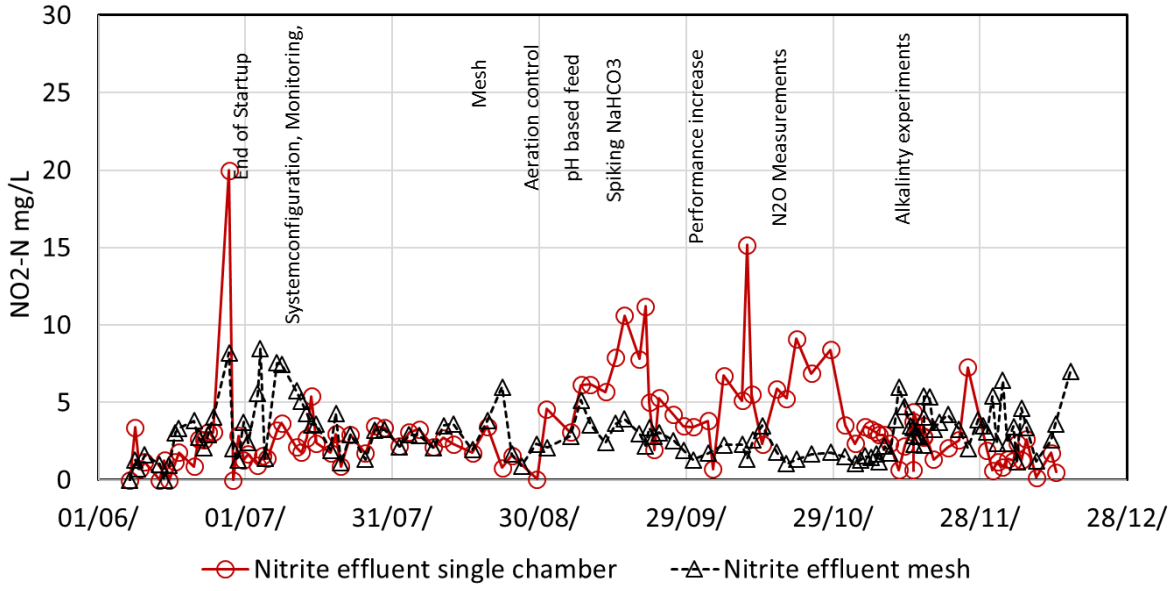

Figure 22: Effluent NO_2-N concentrations (NO_2 spike of 31.7 not included; see Figure 27).

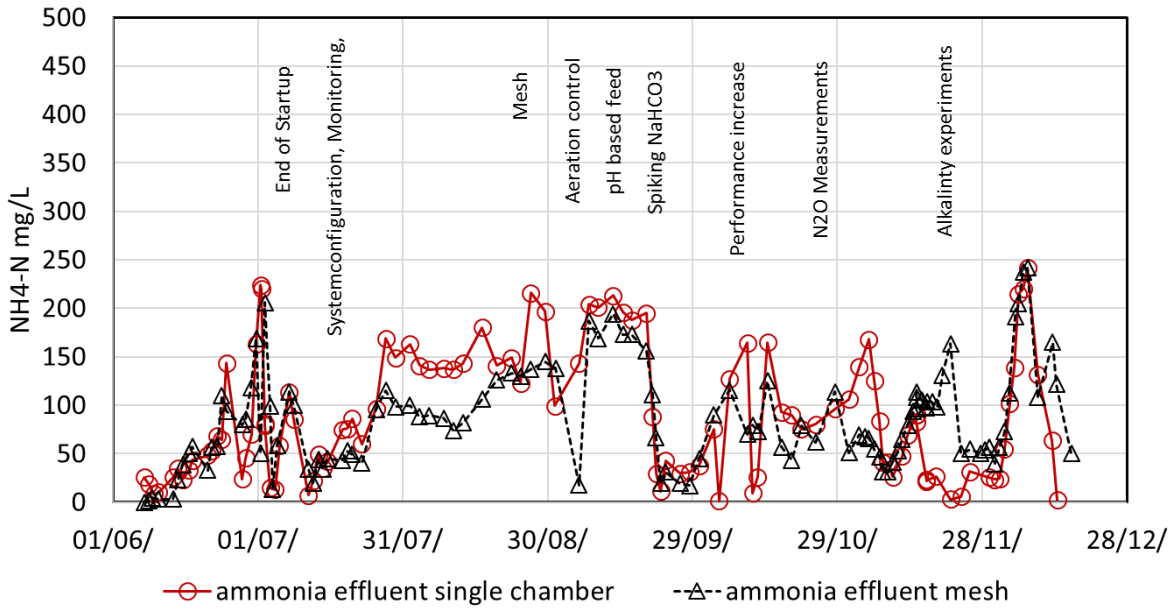

Figure 23: Effluent ammonia concentration.

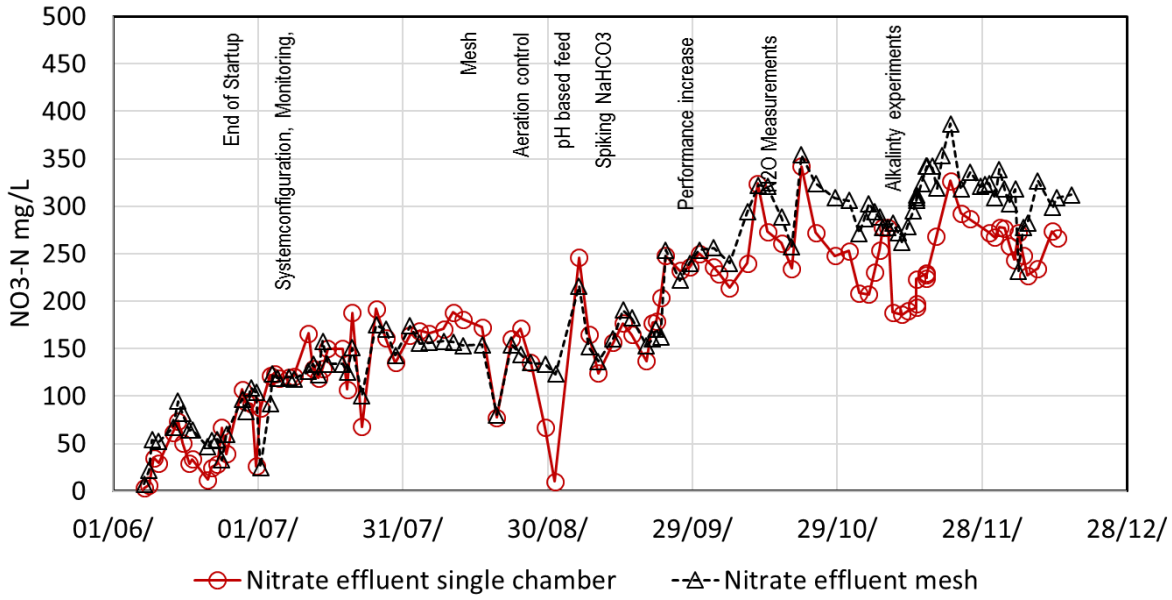

Figure 24: Effluent nitrate concentration.

The pH bases aeration delivered stable results for the single-chamber and mesh systems in the first weeks of operation; only minor adjustments were necessary. However, the problem remained that the stability of the aeration control was lost, when increasing the loading rate or changing to a new batch of process water was attempted. This motivated the development of the robust aeration algorithm to improve aeration control. After its implementation, a manual intervention was no longer necessary and process stability increased. Furthermore, a pH-based feed control was tested (Subsection 4.3.2.1).

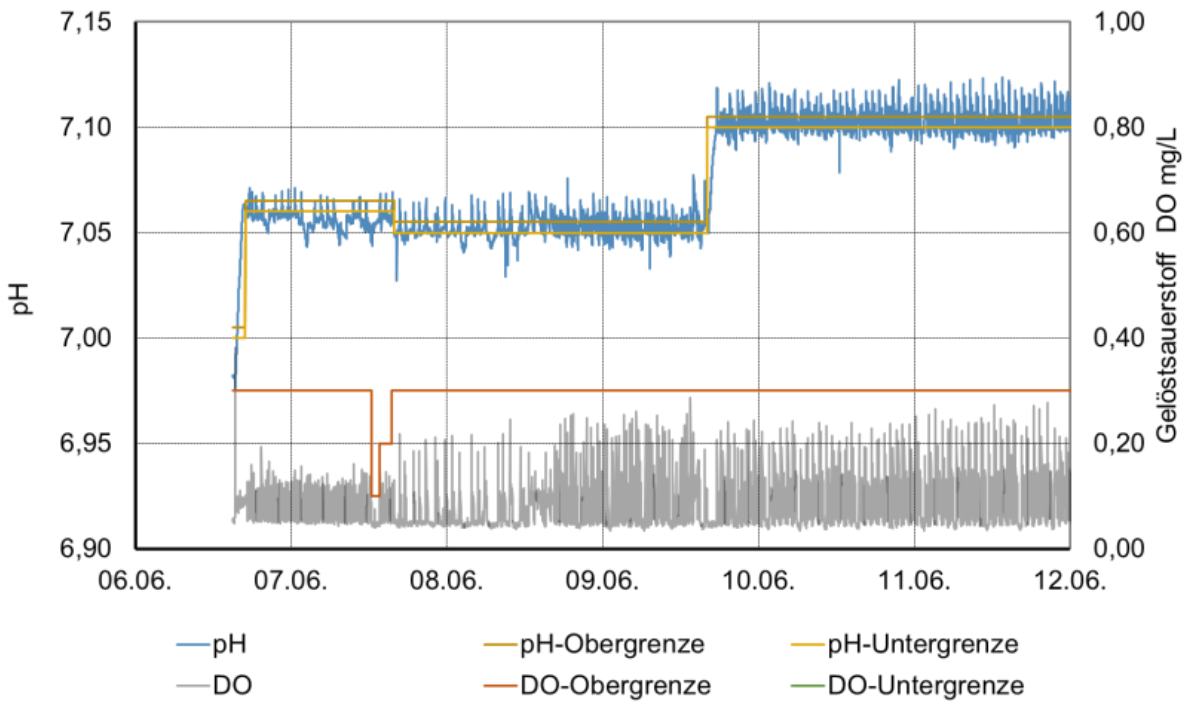

Figure 25: Controller setting and pH and DO measurements during the first week of the startup period of the single-chamber system (*Figure translation: Obergrenze = upper limit, Untergrenze = lower limit, Gelöstsauerstoff = dissolved oxygen*).

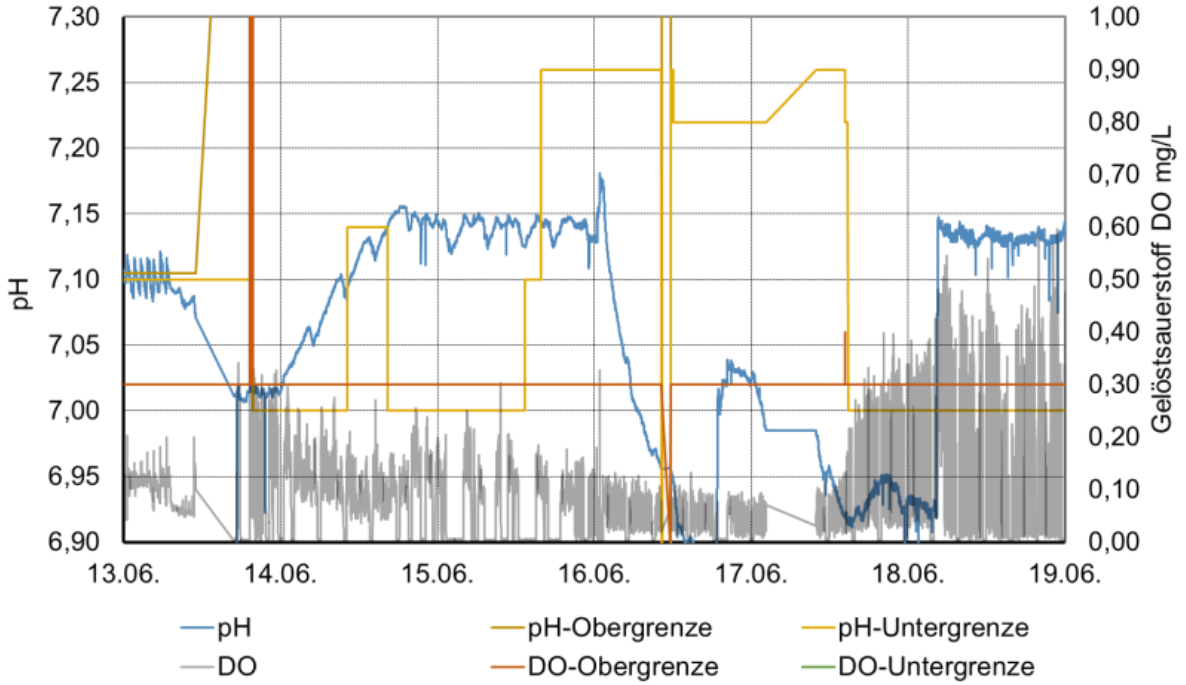

Figure 26: Controller setting and pH and DO measurements during the second week of the startup period of the single-chamber system (*Figure translation: Obergrenze = upper limit, Untergrenze = lower limit, Gelöstsauerstoff = dissolved oxygen*).

The robust aeration algorithm increased process and pH stability, yet the NH_4-N removal rate and N loading rate remained below expectations, with NH_4-N above 100 mg L^{-1} in both systems. The ANAMMOX specific monitoring tools indicated no problem in the ANAMMOX population (Figure 28); thus, AOB activity was suspected to be limited by alkalinity (Wett and Rauch 2003), although using stoichiometry sufficient alkalinity was present. By spiking with $NaHCO_3$ to decrease the molar NH_4-N to HCO_3^- ratio from 0.9 to 0.8 it was possible to quickly increase NH_4-N conversion and the N loading rate to reach the desired level of 0.5 kg N m^{-3} d^{-1}, comparable to large-scale plants. The impact of different NH_4-N to HCO_3^- ratios was investigated later (Subsection 4.3.2.2). Furthermore, stable operation and the desired loading rate made it possible to move on to comparing the N_2O emissions of both plants (Section 4.3.3). However, a certain batch-by-batch variation of effluent values remained when a new batch of process water was supplied every 3–4 days.

4.3.1.1 Pilot plant heme and AA monitoring

During the start-up of the pilot plant, heme and AA samples were regularly sampled in parallel to conventional reactor monitoring. The highly active seed sludge of the mesh and single-chamber system lost some AA and heme concentration as it took some time to establish a stable process at the beginning of the start-up. Figure 27 depicts the trend for the single chamber system, where the mesh system showed similar values. The comparison of nitrogen removal rate by effluent values and AA showed that it followed the same trend and that after an initial adaptation period N elimination by AA started to rise again (Figure 28, around 31.7).

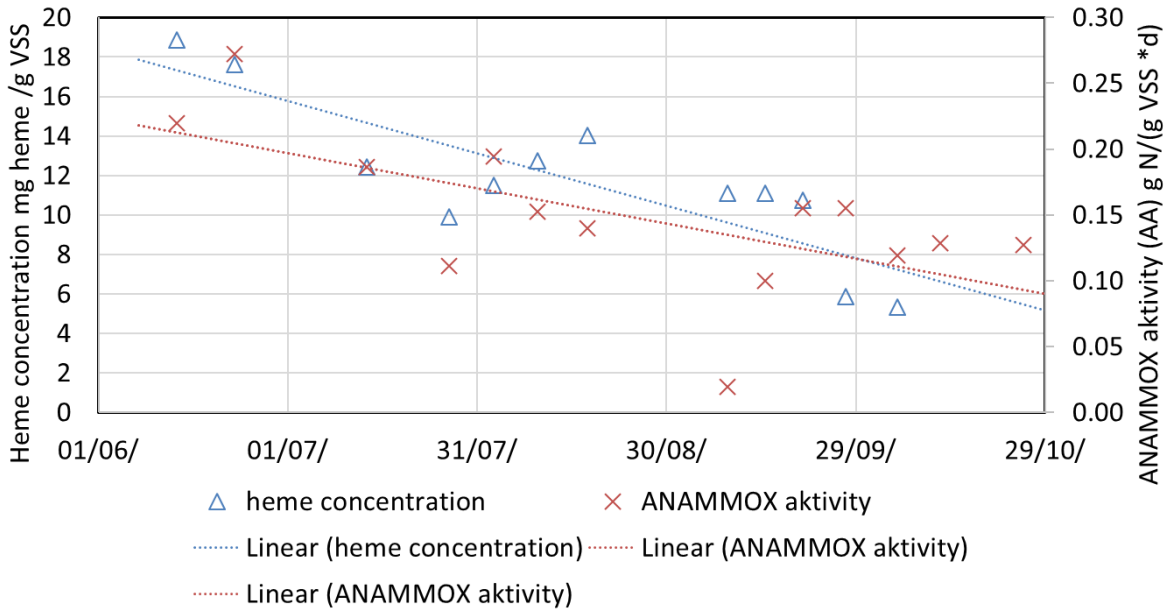

Figure 27: Development of heme concentration and AA of the pilot-scale single-chamber system.

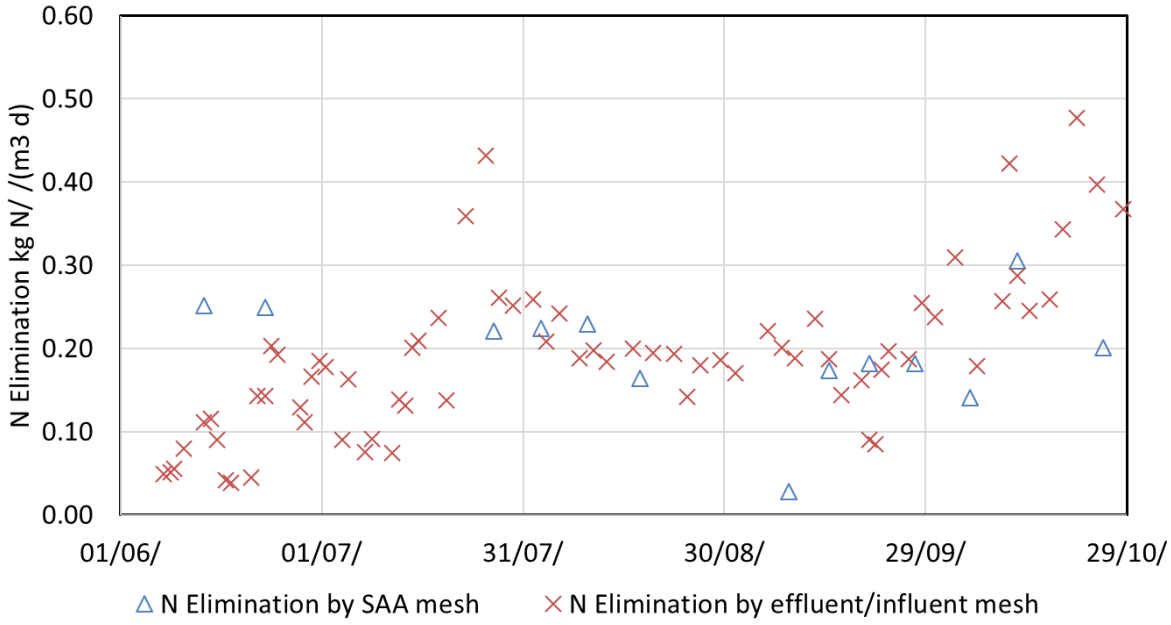

Figure 28: Comparison of the nitrogen elimination rate based on influent and effluent values and on ANAMMOX activity of the pilot-scale mesh system.

Similar to the batch test (Section 4.2), it was possible to observe the difference in response speed of AA and heme when a process disturbance occurred in the single-chamber pilot plant. The pressurised air valve of the aerator malfunctioned, which led to over-aeration and NO_2-N accumulation inside of the reactor. This allowed the observation of the response of the monitoring parameters. While AA quickly responded to the disturbance and quickly regenerated, the heme value did not react to the short-term process disturbance, which fitted

the observation that was apparent in the batch test (Section 4.2.3). However, little additional information for operating the system was generated in relation to the lab work required to apply the monitoring tools, and thus they were discarded during the future operation of the plant.

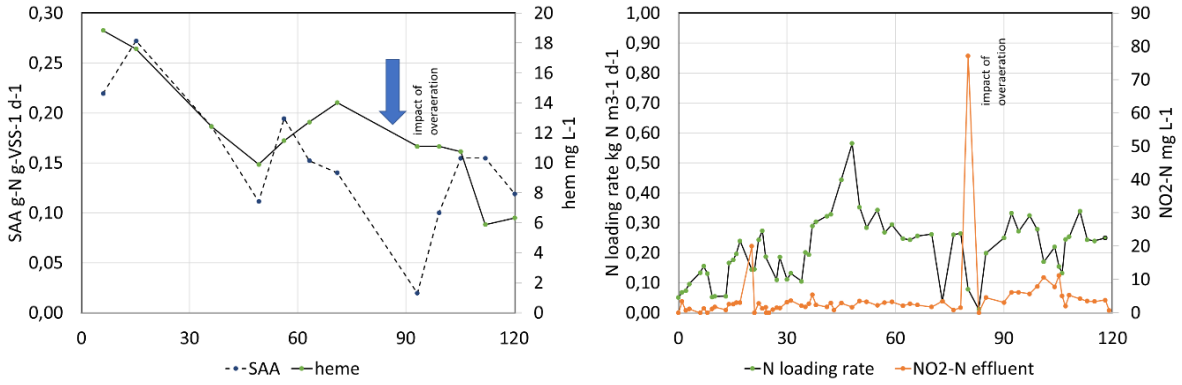

Figure 29: Impact of over-aeration on AA, heme, N loading rate, and NO_2-N effluent.

4.3.1.2 Optimising the implementation of the mesh separated reactor at the pilot scale

The lab-scale mesh reactor demonstrated that it is possible to achieve the creation of two distinct zones, one aerobic and the other anoxic, due to the formation of a biofilm on the mesh separating both zones. However, the plan to cultivate a biofilm on the mesh did not succeed at the lab scale. Only a minor biofilm formation was visible after 2 months of operation and no difference in DO could be detected between the aerobic and anaerobic sides. This was attributed to the higher shear forces of the aeration at the pilot scale. Using a finer mesh did not succeed either because it was torn after a few days of operation. However, using a synthetic curtain supported by the initially installed mesh solved the issue (Figure 10). This allowed the creation of two distinct zones, one aerobic and turbulent and the other anaerobic (no DO was detected even during intense aeration) and relatively laminar in the top section and turbulent in the lower section. Both zones interchanged volumes within 15 to 30 min (estimated by the time to reach pH equilibrium after manipulating the pH with HCO_3^-. The mesh prevented a rapid interchange of sludge, but in principle it was more permeable for the smaller fraction of the granular sludge. When the sludge passed the mesh, the heavier granules quickly settled in the laminar top section of the anaerobic zone, while the small solids remained suspended in the top section of the anaerobic side. The size of the laminar zone could be controlled by changing the intensity of agitation. Some of the granular sludge that settled into the moving bed moved back to the aerated side of the reactor, and thus equilibrium of the different mass fractions was maintained. To avoid clogging of the mesh, the aeration was placed close to the mesh, allowing only for minor biofilm formation in the subsequent 3 months of operation (Figure 9).

The creation of the laminar top layer in the anaerobic side allowed the issue of sludge retention to be solved, which could not be solved in the lab-scale mesh reactor; thus, a change to continuous operation was enabled without the initially intended settling device being integrated. By taking the effluent from the laminar layer it was possible to retain larger granules inside the system. Removing the small particles from the system is a process known to increase the process stability of PNA systems because the larger particles are known to contain ANAMMOX, whereas smaller particles containing OHO, AOB, and NOB are removed from the system (Han et al. 2016b). Effluent grab samples did not exhibit any larger particles and the laminar layer was visible to the eye. The observation could be confirmed by taking grab samples during continuous operation (Figure 31) and measuring the particle size distribution (Figure 30).

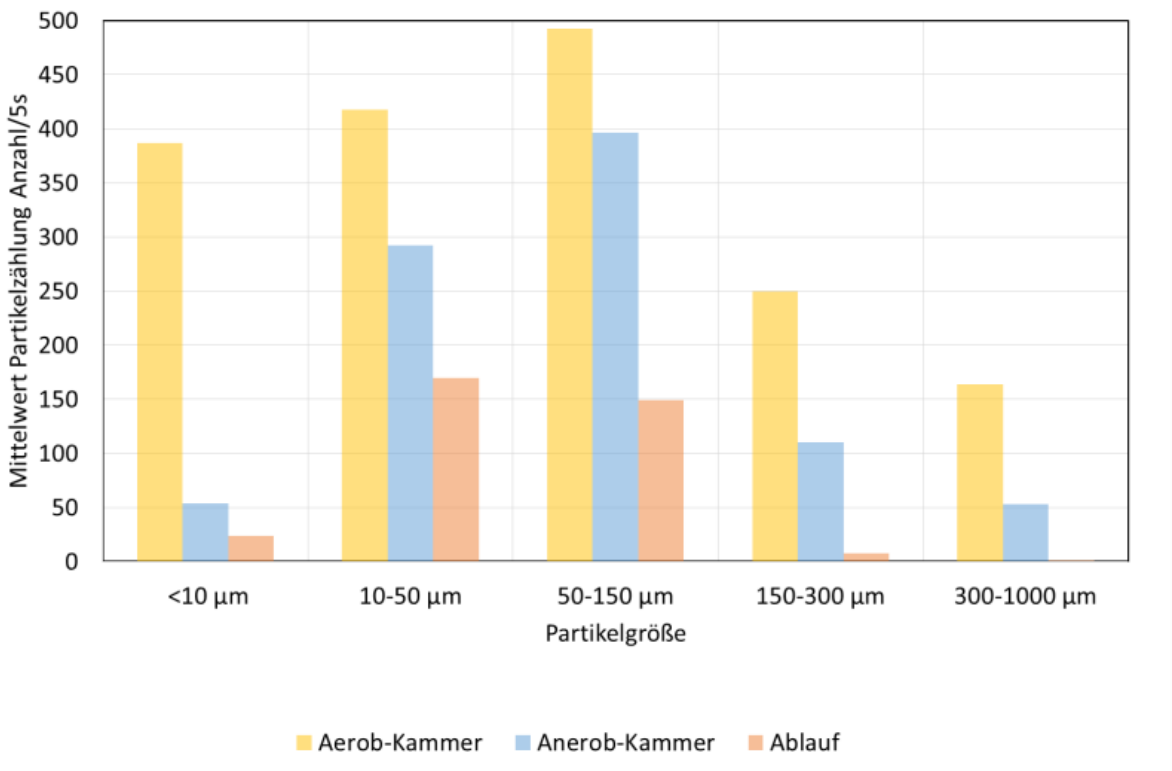

Figure 30: Results of particle distribution during continuous operation of the pilot-scale mesh system.

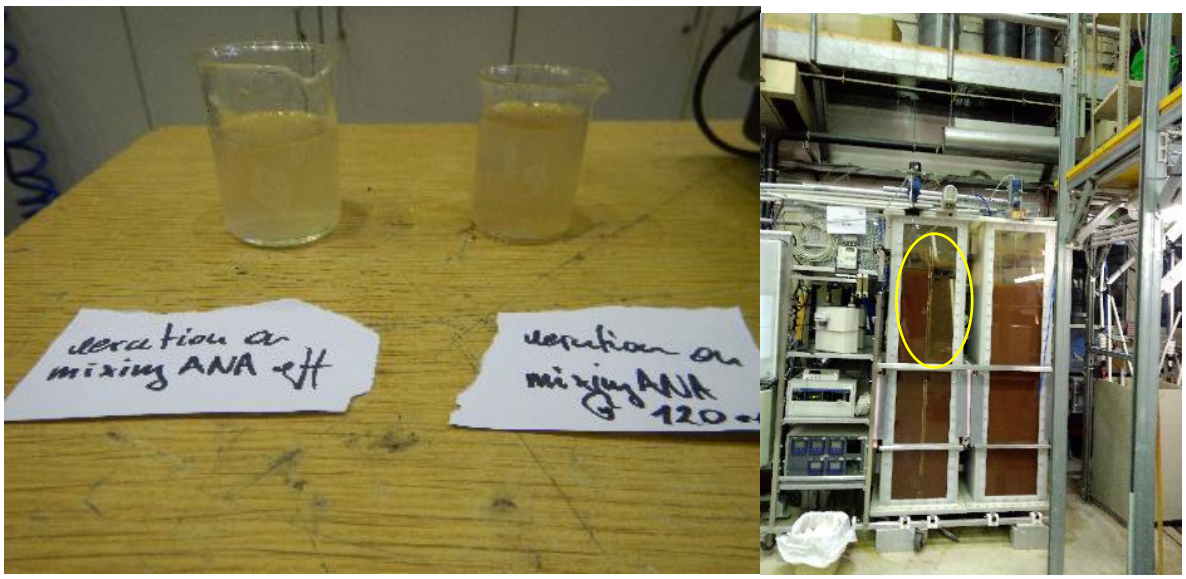

Figure 31: (Left) Effluent grab samples indicating good sludge retention during continuous operation; (right) sludge retention visible to the eye during continuous operation.

4.3.2 Adjusting the aeration control algorithm for small-scale application, and studying the impact of different ammonia-to-alkalinity ratios

4.3.2.1 pH control of small-scale implementations and coping strategies

During the operation of the pilot plant and in previous lab-scale trials, it became apparent that pH patterns typical for a stable PNA process were lost when process disturbances occurred. Several causes were observed, such as when the process was changed to a new batch of reject water, the process stopped for some time due to a malfunction, a sensor was recording faulty signals caused by things such as air bubbles that got stuck beneath the DO sensor, or biofilm was attached to the pH probe. After fixing the problem a typical phenomenon occurred; instead of a regular interchange of aerated and nonaerated phases every 5 to 30 min due to the change of pH caused by nitrification, ANAMMOX, and influent feed, the pH rose for several hours once the aeration started, thereby leading to an inversion of the pH signal (Figure 16), which disabled the principles of the control strategy that worked successfully at a large scale (Wett et al. 2007). This situation led to a phase of prolonged aeration and nonaeration, thereby destabilising the process because too much aeration eventually led to the accumulation of NO_2^-, which is known to inhibit ANAMMOX. The situation was combated by manually resetting the pH upper and lower limits until a new equilibrium was reached. In doing so, it was discovered that the process stability was best regained if the aeration was turned off and on regularly, irrespective of the pH, until stable patterns re-emerged. This led to the development of a time-dependent heuristic, which turned the aeration either on or off for a given amount of time irrespective of the pH signal if no change to the status of the aeration had occurred for a defined time; 15 min and 5 min proved to work best. This resulted in a mode in which the aeration was either turned on for 15 min with a pause of 5 min if the pH stayed above the limits or it turned on for 5 min with a pause of 15 min if the pH was below the pH limits (Figure 32).

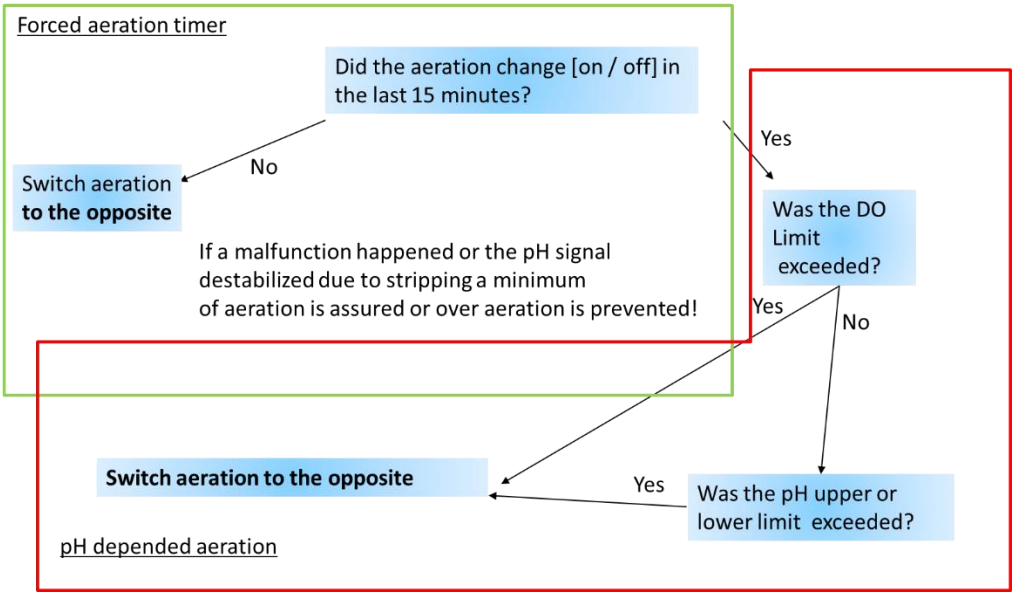

Figure 32: Time- and pH-based robust aeration algorithm.

Figure 33 shows how the signal started to stabilise once the time- and pH-based robust aeration control method was implemented. Because of this the process stability of the pilot

plant significantly increased due to the method acting as a safety net when the narrow pH equilibrium was lost. This occurred when changing to the next batch of process water, which led to situations in which the system was dominated by stripping after operational pauses or the pH or the DO signals had malfunctions.
In this study, the flow rate was manually adjusted proportionally to the increasing nitrogen loading rates of the process. (If an aeration with a flow rate controller was available, the author suggests utilising a moving average of the last days of operation if the logic switches to forced aeration.)

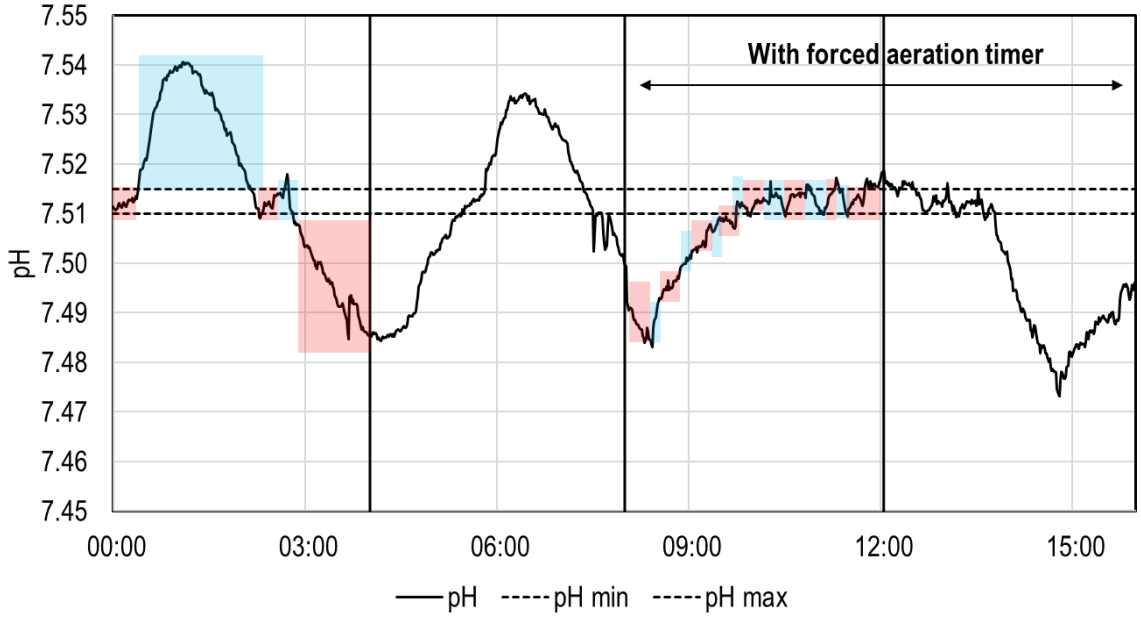

Figure 33: Destabilised pH pattern (blue = aeration on, red = aeration off) and recovery after the robust aeration algorithm was applied (pH is relative due to the offset after calibration).

However, the system still lacked the ability to automatically adjust the feed, and it became apparent that small-scale systems with varying influent characteristics may benefit from automatically adjusting the volumetric loading rate of the process, especially during start up when the loading rate has to be regularly readjusted. Manual operation showed that an overloading of the reactor corresponded to a rapid increase of the pH above the pH limits. Thus, a feed control strategy was developed that could exploit the long-term trend of the pH, while the aeration logic utilised the short-term movement of the pH. It was assumed that a PID controller operating on sufficiently smoothed pH signals could be used to continuously load the reactor to the limits of its capacities if a pH set point was put to the upper limit of the aeration control algorithm.
First, a moving average was implemented to smooth the pH signal that was continuously influenced by short-term fluctuations in the aeration. By trial and error, a reasonably smooth signal was determined whereby a moving average of 2 h provided a good compromise of reacting to trends without incorporating short-term fluctuations.
In a subsequent step, a Ziegler–Nichols Test was performed to obtain the initial settings of the PID. The test was performed during a stable period by suddenly increasing the loading rate from 4 L h^{-1} to 5 L h^{-1}. After fine tuning the parameters during operation, the following settings for the PID controller provided the desired responsiveness: 0.027 for the integral term, 100 for the proportional term, and 22254 for the derivative term, using a loop rate of 5 min. In addition, integral windup was prevented by inserting upper and lower boundaries to the integral error term.

After a week of stable operation (Table 7), the concept described above could serve as the basis for completely automatising the feed of the pilot plant. Figure 34 shows how the controller tests the limits of the reactor by increasing the loading rate and then reducing it once the limit has been passed for too long.

Table 7: Average process parameters during PID-based feed control.

Influent:	
NH_4-N mg L^{-1}	1100
NO_3-N mg L^{-1}	70
NO_2-N mg L^{-1}	26
Ks mmol L^{-1}	104
TOC mg L^{-1}	86
Effluent:	
NH_4-N mg L^{-1}	38
NO_3-N mg L^{-1}	212
NO_2-N mg L^{-1}	4
Nitrogen removal rate %	76
Nitrogen loading rate kg m^{-3} d^{-1}	0.3

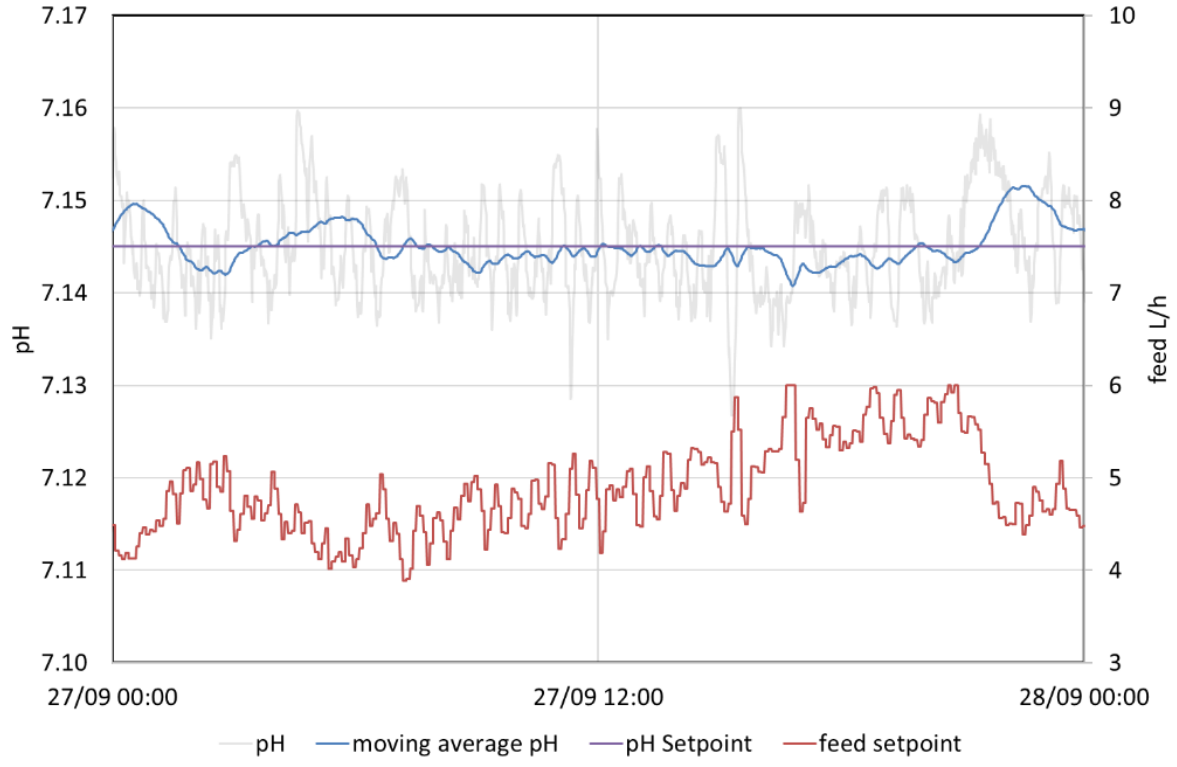

Figure 34: pH-based feed control.

This study demonstrated how to create more autonomous PNA systems. In a first step it was shown how a timer- and pH-based aeration algorithm can be used to overcome aeration control disturbing pH artefacts, where small-scale systems are especially vulnerable, which thus represents a key feature for the autonomous operation of the PNA process. In a second step it was shown that pH-dependent aeration control and feed control produce a stable

process which automatically adjusts the feed to the plant's capacities, while using the same pH signal for the aeration. Yet, further optimisation and testing would be necessary to fine tune the existing controller or implement a more robust control algorithm.
Furthermore, the framework through which the strategy was implemented deserves further consideration. This study demonstrated that the combination of two relatively simple methods resulted in a robust aeration control algorithm. However, there are methods that are potentially more suited to coping with the situation of small-scale PNA plants. Especially pH artefacts due to stripping, and the varying response of the pH to different influent alkalinity ratios, would ask for the implementation in a fuzzy controller framework such as that described by Bai and Wang (2006). Boiocchi et al. (2015) chose to implement a control strategy in a fuzzy framework for a PNA system, and demonstrated its use with a computer simulation. While that study provided valuable insights into the implementation of a fuzzy controller, it was based on the assumption that influent and effluent nitrogen parameters are known to the controller. This implies that online measurements for NO_3^-, NH_4^+, and NO_2^- are available. Those measurements, although principally possible with devices such as UV probes, significantly increase the costs and increase the maintenance work necessary. Practical experience in this study has shown that implementing a UV–VIS probe with a reliable calibration, although possible, is a time-consuming process due to the tedious process of calibration, and especially cumbersome if the influent characteristics change regularly.

4.3.2.2 Alkalinity limitation experiment

After the problem of maintaining process stability with the robust aeration control algorithm was solved, some fluctuation of the effluent remained, and it was suspected that the batch-by-batch variations of the influent NH_4^+ to HCO_3^- ratio affected the pH-based aeration control. Furthermore, this required the occasional reset of the pH set point (between 7.2–7.5) to increase the quality of the pH signal (typical sawtooth pattern). After the final comparison of the pilot plant system was performed (Section 4.3.3), it was possible to investigate the influence of the influent NH_4^+ to HCO_3^- ratio on the improved pH-based aeration control, and thereby risk an irreversible process disturbance.
The investigation was conducted using a stepwise reduction of the influent alkalinity. It was applied in parallel to the pilot-scale mesh and pilot-scale single-chamber reactors as well as the lab-scale single-chamber reactor. The pH setpoints, influent composition, and sludge and volumetric loading rates were maintained the same to ensure comparability between the reactors. Reference measurements confirmed that the systems were operating within a 0.1 range of the pH. The step-wise reduction of the alkalinity led to a systematic decrease in the quality of the pH signal of the pilot plant reactor. Figure 35 shows how the pH signal of the single-chamber system changed when increasingly less alkalinity became available, keeping everything else constant. It became apparent that with decreasing alkalinity, the pH regularly increased due to stripping followed by a rapid decline due to buffer depletion, and then a long recovery. Surprisingly, the pH signal of the lab-scale single-chamber system did not show any signs of instability of the pH signal, even when no extra alkalinity was provided to the system. This result was unexpected because the lab-scale reactor had the highest aeration requirements for removing nitrogen; thus, it was expected that the pH signal would be most affected by the stripping of CO_2.

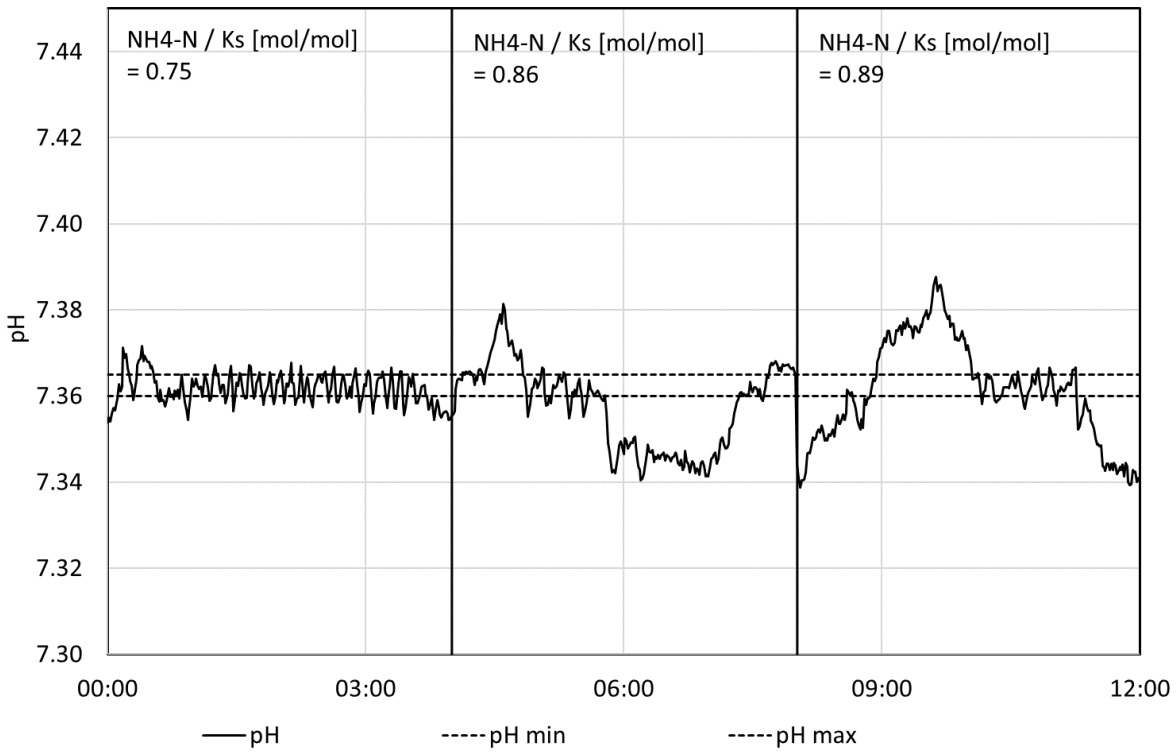

Figure 35: Effect of decreasing alkalinity on the pH signal of the pilot-scale single-chamber system (alkalinity decreases from left to right).

Figure 36 shows that the removal efficiency of all reactors decreased when less alkalinity was provided and that the lab-scale single-chamber system was the least sensitive as it showed the lowest decline.

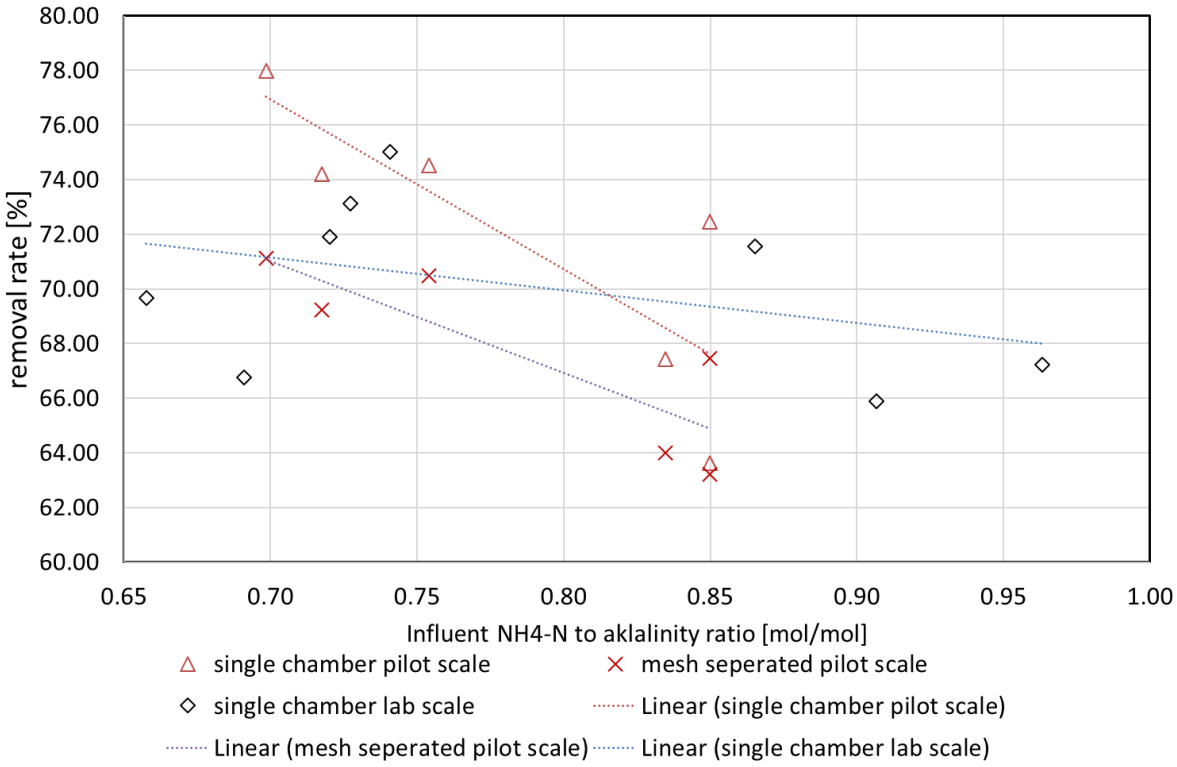

Figure 36: Removal compared with influent NH_4-N to alkalinity ratio.

The effluent alkalinity was measured together with the NH_4-N concentration of the effluent. By applying PNA stoichiometry to the influent NH_4-N concentration, one can calculate the stoichiometric requirements of alkalinity. After adding them to the remaining effluent alkalinity and subtracting them from the influent alkalinity, an approximation of the alkalinity that was stripped was obtained. Figure 37 shows that the pilot plant systems behaved relatively similarly, stripping 15–20% of the influent alkalinity when alkalinity was supplied in excess, whereby the lab-scale single-chamber system stripped 20–30% of the influent alkalinity. The same system which stripped the most showed the smallest decline in process performance due to a reduction of alkalinity; however, the nitrogen removal rate was lower to begin with. In each case, none of the reactors was limited stoichiometrically by alkalinity (Table 8). In part this could be due to a kinetic limitation of the AOB by alkalinity. The other factor could be a relative change in the response of the pH signal to aeration due to changes in the carbonate puffer system.

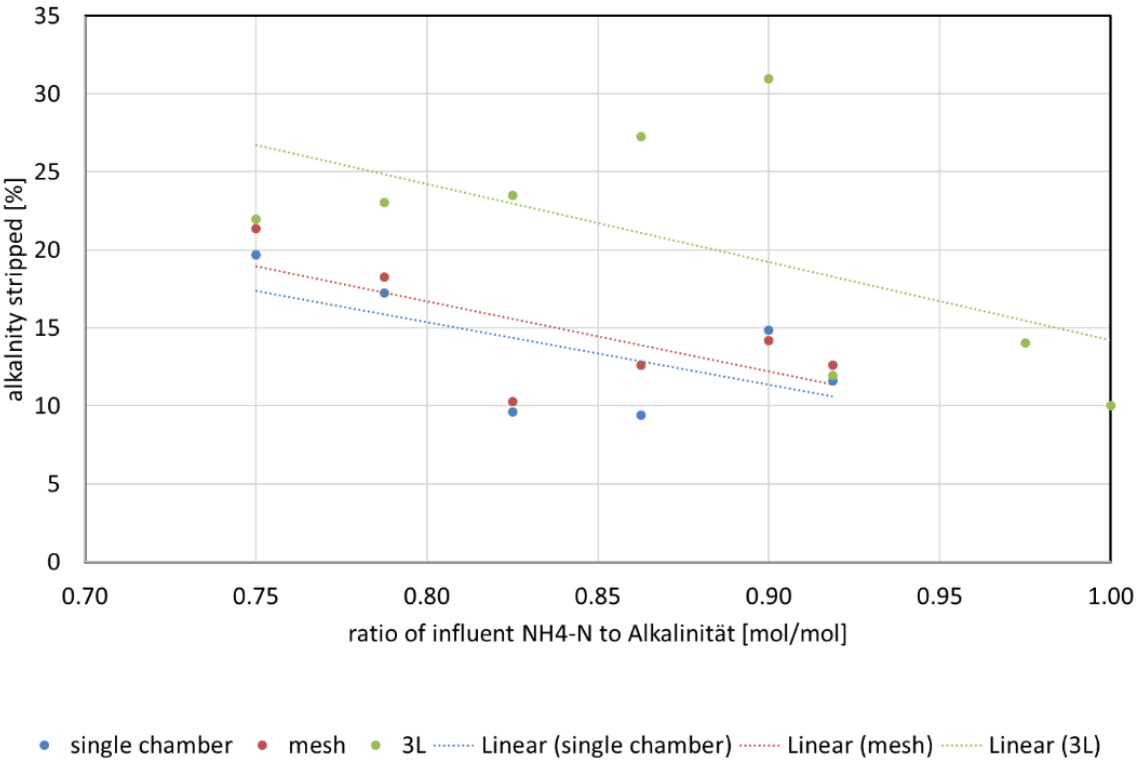

Figure 37: Alkalinity stripped in relation to the influent ammonia-to-alkalinity ratio.

All reactors exhibited a tendency to decrease their nitrogen removal efficiency (Table 8), whereas the NO_2-N concentration remained relatively constant and the NO_3-N concentration decreased proportionally to the reduced turnover of NH_4-N, which highlighted that the robust aeration control algorithm (Subsection 4.3.2.1) was capable of coping with the alkalinity depletion. However, the NO_3-N concentration of all systems exceeded the stoichiometry of PNA. The pilot-scale single-chamber system produced on average 91%, the pilot-scale mesh system 112%, and the lab-scale single-chamber system 139% more NO_3-N^- due to NOB activity (the performance of the pilot-scale systems is discussed in detail in Subsection 4.3.3.2). The comparison of the lab-scale single-chamber and pilot-scale single-chamber system is particularly interesting because the lab-scale system was inoculated with an aliquot of the single-chamber system, and thus resembled a very similar system besides the scale and geometry. The lab-scale system was less sensitive to a decline in alkalinity but produced much more NO_3-N, with NO_2-N concentrations two times higher than those of the single chamber system. This suggested that due to the different response of the pH to aeration, more oxygen was supplied to the system compared with the single-chamber system. The comparison of the pilot and lab-scale single chamber system showed that NOB suppression decreased when more stripping occurred. To verify whether those differences could be attributed to the efficiency of the aeration, the oxygen transfer efficiency of each system was determined: 5% for the pilot-scale single-chamber system, 6% for the pilot-scale mesh system, and 1% for the lab-scale single-chamber system. Contrary to initial expectations, this showed that systems with lower oxygen transfer efficiency are not automatically the most sensitive systems to alkalinity reduction with regards to their removal efficiency, but the data suggested that NOB activity may increase with decreasing oxygen transfer efficiency.

Table 8: Summary of the alkalinity limitation experiment

	Reduction step	NH_4-N influent	NH_4-N/alk.	Removal rate	Volumetric N load	NH_4-N effluent	NO_3-N effluent	NO_2-N effluent	N removal per m^3 aerated	Effluent alkalinity	Alk. stripped
	[d]	[mg L^{-1}]	[mol mol^{-1}]	[%]	[kg m^{-3}]	[mg L^{-1}]	[mg L^{-1}]	[mg L^{-1}]	[kg m^{-3}]	[mmol L^{-1}]	[%]
Single chamber pilot-scale	0	1376	0.75	78	0.88	24	278	1	0.0121	13.50	20
	1	1288	0.79	74	0.50	55	277	1	0.0160	12.90	17
	2	1416	0.83	75	0.60	102	258	1	0.0093	13.70	10
	3	1392	0.86	72	0.54	139	244	1	0.0146	16.50	9
	4	1344	0.90	64	0.53	215	272	2	0.0134	17.30	15
	4.5	1440	0.92	67	0.83	220	248	1	0.0101	17.20	12
Mesh continuous pilot-scale	0	1376	0.75	71	0.61	57	339	2	0.0172	11.10	22
	1	1288	0.79	69	0.49	73	318	6	0.0172	11.80	20
	2	1416	0.83	70	0.52	113	303	2	0.0166	15.80	12
	3	1392	0.86	63	0.69	192	318	3	0.0182	15.30	13
	4	1344	0.90	67	0.57	205	232	1	0.0208	15.20	16
	4.5	1440	0.92	64	0.79	237	277	5	0.0183	0.66	14
Single chamber lab scale	0	1348	0.75	75	0.58	15	318	4	0.0029	6.28	22
	1	1200	0.79	72	0.58	16	318	3	0.0026	7.03	23
	2	1232	0.83	73	0.57	17	312	3	0.0026	5.75	24
	3	1064	0.86	67	0.47	23	327	4	0.0019	5.69	27
	4	1068	0.90	70	0.51	27	294	3	0.0022	5.71	31
	5	1284	0.92	72	0.63	59	303	3	0.0026	5.83	12
	6	1240	0.98	66	0.61	136	285	4	0.0021	5.08	14
	7	1292	1.00	67	0.66	147	274	3	0.0024	4.38	10

The observations made in this study revealed that the influent NH_4-N to HCO_3^- ratio critically influenced the process performance and stability. This is in line with other studies; for example, a lab-scale PNA study by Bagchi et al. (2010) used this effect to control PNA by manipulating the DO and alkalinity of the influent. Similarly, Hwang et al. (2000) demonstrated in a nitrifying reactor that, given constant aeration, the more the NH_4-N to HCO_3^- ratio decreased, the more the NO_2^- built up and pH inside the reactor increased. Jin et al. (2013) also manipulated the influent NH_4-N to HCO_3^- ratio and found that DO had a greater influence on the removal rate of a PNA plant than did the influent NH_4-N to HCO_3^- ratio. Although those findings are not directly comparable to those of the present study, as none of them tried to control the aeration via pH, they highlight the importance of the availability of sufficient alkalinity.

By systematically reducing the alkalinity of the pilot-scale single chamber system and the lab-scale single chamber system inoculated with an aliquot (no difference due to biomass composition) of the pilot-scale system, it was shown that the pH response due to aeration was influenced by scale. Otherwise, very similar systems concerning the control programme, pH and DO setpoint, reject water, volumetric nitrogen load, biomass concentration, and biomass composition showed relevant differences regarding the pH signal stability. Furthermore, different NH_4-N conversion rates and NOB activities at an equal reduction of influent alkalinity were observed. This could be explained by two nonexclusive factors; first, due to the difference of oxygen transferred in relation to the change in the pH signal, and second by kinetically favouring NOB due to different NH_4^+ to HCO_3^- ratios because of stripping, which would be in accordance with the observation by Tokutomi et al. (2010).

Acknowledging the effects of scale and influent alkalinity on pH-based aeration control raises the question of to what extent adjustments of the pH set point could be used to compensate. However, investigating the optimum pH setpoint is a challenging task due to the complexity involved. The equilibrium of the carbonate system depends on the pH. Furthermore, the pH change due to AOB and ANAMMOX activity depends on the current state of the carbonate buffer system. In addition, the influent pH depends on the NH_4-N to HCO_3^- ratio. Furthermore, stripping effects are scale- and geometry-specific, which again influence the pH signal; for example, the hydrostatic pressure shifts the partial pressure of CO_2 (depth of the pH probe). Stripping is also influenced by the surface to volume ratio of the reactor as it provides an area for CO_2 stripping, and the aeration efficiency affects the amount of turbulence. Furthermore, the turbulence impacts concentration gradients of the air–liquid interface and therefore the rate of CO_2 stripping. For example, lowering the pH setpoint to account for the reduced increase of pH when the NH_4-N to HCO_3^- ratio increases. One must consider that this would also reduce the availability of alkalinity due to increased stripping through a shift in the bicarbonate system towards CO_2, and thus also the proportional response of the pH set point to aeration (Wett and Rauch, 2003). Furthermore, COD is a factor affecting the system by introducing CO_2 by respiration, thereby changing the equilibrium of the bicarbonate buffer system. This highlights that conclusions drawn from other studies regarding the optimum pH set point and optimum alkalinity to NH_4-N ratio are system-specific properties, where this effect is presumably reduced the larger the system becomes, and thus the relative amount of stripping is reduced along with its impact on the control algorithm.

4.3.3 Comparing the mesh implementation with the conventional single-chamber system at the pilot scale in performance, stability, N_2O emissions, and biomass composition[9]

After the pilot plant was sufficiently optimised to assure process stability at nitrogen loading rates comparable to those of large-scale installations with both reactor configurations, the final target of evaluating the impact of the mesh reactor configuration on N_2O emissions was performed. To demonstrate the impact of continuous operation, now possible with the pilot-scale mesh reactor, it was decided to switch the operation mode from SBR to continuous operation after evaluating both systems in SBR mode. In addition, the influent and effluent monitoring was intensified. Both systems were operated with the same feed and aeration control settings to allow direct comparison. Furthermore, grab samples for sequencing the biomass were taken to show whether biomass composition or the operation mode was more likely to influence GHG emissions.

4.3.3.1 Microbial community composition of the pilot-scale single chamber and mesh system

The presence of bacteria generally associated with nitrogen removal in PNA plants was confirmed by NGS (Table 11). Each chamber of the mesh system and single-chamber system contained similar amounts of VSS, and thus NGS results which correlated to the relative abundances of DNA are compared directly herein. Since NGS provides information on DNA ratios only, a direct reference to the absolute biomass composition in terms of VSS cannot be provided because the fraction of VSS representing living cells remains unknown. The ANAMMOX bacteria present in both systems belong to the genus *Candidatus Brocadia* (Pereira et al. 2017); this type of microorganism has been frequently identified in ANAMMOX processes. The nonaerated chamber of the mesh system exhibited the highest abundance of 12.4%, followed by 5.6% inside the single-chamber system and 4.3% at the aerated side of the mesh system. The average ANAMMOX concentration of the mesh system was 8.35%, which suggested that the mesh system selected ANAMMOX more efficiently given the equal distribution of VSS and similar VSS levels between reactors. AOB represented by the genus *Nitrosomonas* were identified in both systems. Among them, the species *Nitrosomonas europaea* was the most abundant. The highest abundances were found in the aerated side of the mesh system at 1.9%, followed by 1.3% in the single-chamber system and 0.8% in the nonaerated side of the mesh system. In total, both systems showed comparable amounts of AOB. NOB represented by the genus *Nitrospira* were also present in both systems: 1.1% in the aerated chamber of the mesh system, which was shown to be the highest abundance, followed by the nonaerated side of the mesh system at 0.7% and the single-chamber system at 0.8%. This indicated that in total the single chamber system achieved superior suppression of NOB. This was consistent with the higher effluent NO_3-N concentrations observed at the mesh reactor. The average difference was 40 mg L^{-1} in SBR mode and 69 mg L^{-1} in continuous operation.

[9] This section is based on (Schoepp et al. 2018)

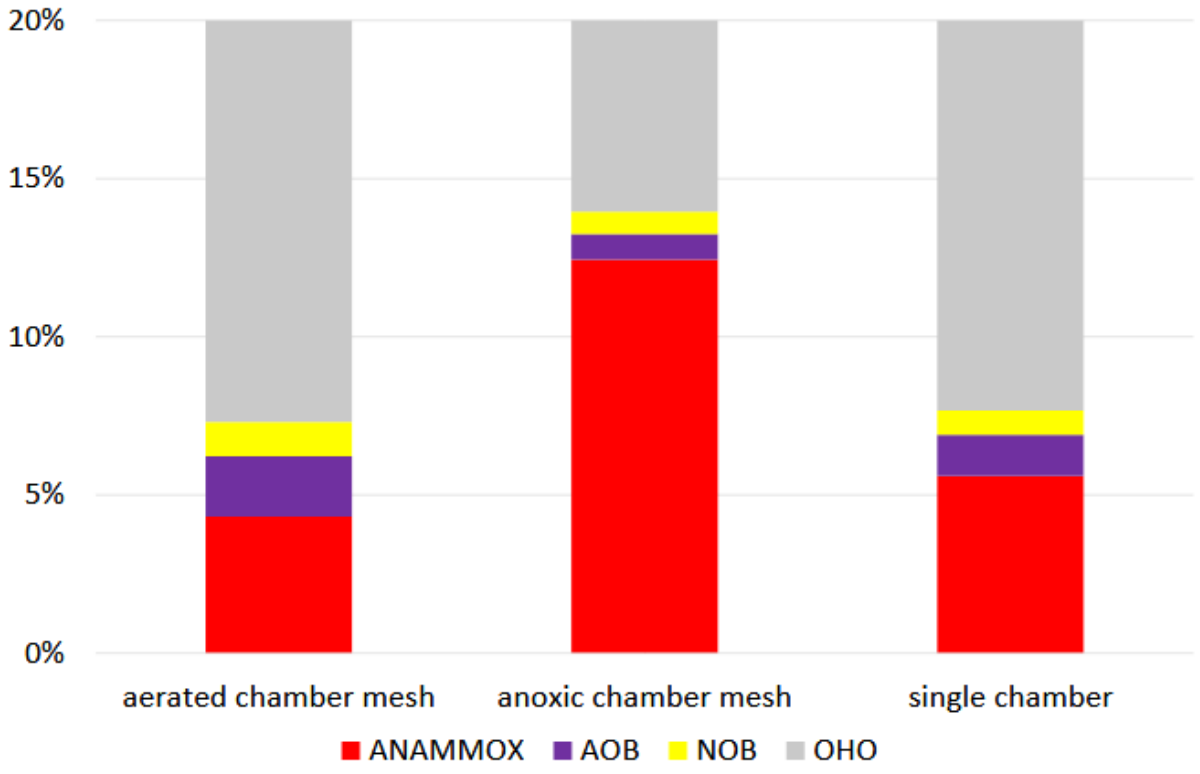

Figure 38: Relative species distribution of biomass: ANAMMOX, ammonia-oxidizing bacteria (AOB), nitrite oxidizing bacteria (NOB), and ordinary heterotrophic organisms (OHO).

A comparison of the relative abundances of ANAMMOX, AOB, ordinary heterotrophic organisms (OHO), and NOB for all samples revealed (Figure 38) that the biomass composition of the pilot plant reactors differed significantly from the composition of full-scale PNA plants as described in Wett et al. (2010a). For the full-scale plant, 26% for OHO, 18% for AOB, 0% for NOB, and 55% for ANAMMOX were reported. This direct comparison of the biomass composition was likely subject to some bias as DNA data were compared with simulation results. However, part of the difference might be explained by the long-term operation and optimisation of this reactor. In particular, more efficient biomass selection was achieved by hydro-cyclones (Wett 2007) or screens (Han et al. 2016a) established at full-scale.

Nevertheless, the mesh reactor achieved nitrogen loading rates around 0.5 up to 0.7 kg N m^{-3} d^{-1}, in the range of performances reported from full scale (Fuchs et al. 2017), a difference that could be partly explained by the two times larger VSS fraction inside the pilot-scale system (4 g VSS L^{-1} vs. 2 g VSS L^{-1}).

An even more important aspect is the relative abundance of ANAMMOX that may be achieved in relation to the AOB, which can be expressed as an AOB:ANAMMOX ratio. The aerated side of the mesh had an AOB:ANAMMOX ratio of 0.44, the nonaerated side had one of 0.06, and the single-chamber system had one of 0.23. These results indicated that the separation of the aerobic and anoxic zones did have an influence on the biomass composition. Although NOB suppression was not completely achieved and the concentration of OHO was much higher than in full-scale systems with external biomass selection, the ratio of AOB:ANAMMOX was comparable to the 0.33 of the large-scale system.

The composition of the heterotrophic biomass varied largely between the two systems, especially the class *Acidobacteria*, which accounted for 28.3% of the mesh system and only 7.3% of the single-chamber system. Belonging to the phylum of *Acidobacteria*, it is a

versatile aerobic heterotroph capable of thriving in low carbon environments (Ward et al. 2009). On the other hand, the single-chamber system consisted of 26.1% of bacteria belonging to the class *Spartobacteri*a, about which little information exists. It must be mentioned that little is known about the physiology of many bacteria that have been detected, especially due to the difficulties in cultivation and long replication times of waterborne bacteria. Nevertheless, it could be shown that the reactor configuration had an impact on the composition of the microbial community. Although knowledge of the community composition in ANAMMOX-based processes (Pereira et al. 2017) has increased over recent years, the implications for process performance are vague. Furthermore, it must be mentioned that NGS data may be subject to a bias as no distinction is made between DNA from living and dead cells. Regarding the abundances of most relevant organisms for N conversion being AOB, NOB, and ANAMMOX, it could be shown that distinct differences existed that could partly explain the differences of N_2O emissions that were observed.

4.3.3.2 N_2O emissions and reactor performance

After comparing the N_2O emissions of both systems operating in SBR mode for the duration of 1 week, the mesh system was switched to continuous operation and after 2 days of acclimatisation the systems were compared for 3 weeks. During the first week, similar N_2O emission patterns were observed during the SBR operation of both systems, albeit with different magnitudes of emission peaks (Figure 39). During SBR operation, both reactors showed a steep increase of emissions at the beginning of each cycle when the aeration was turned on again following the settling phase of the previous cycle. The emission peaks strongly varied in magnitude; whereas the SBR had higher initial peaks, the slope in the cycle-pattern of the mesh system was less pronounced. The emission peaks of the mesh system strongly decreased once the system was changed to continuous operation.

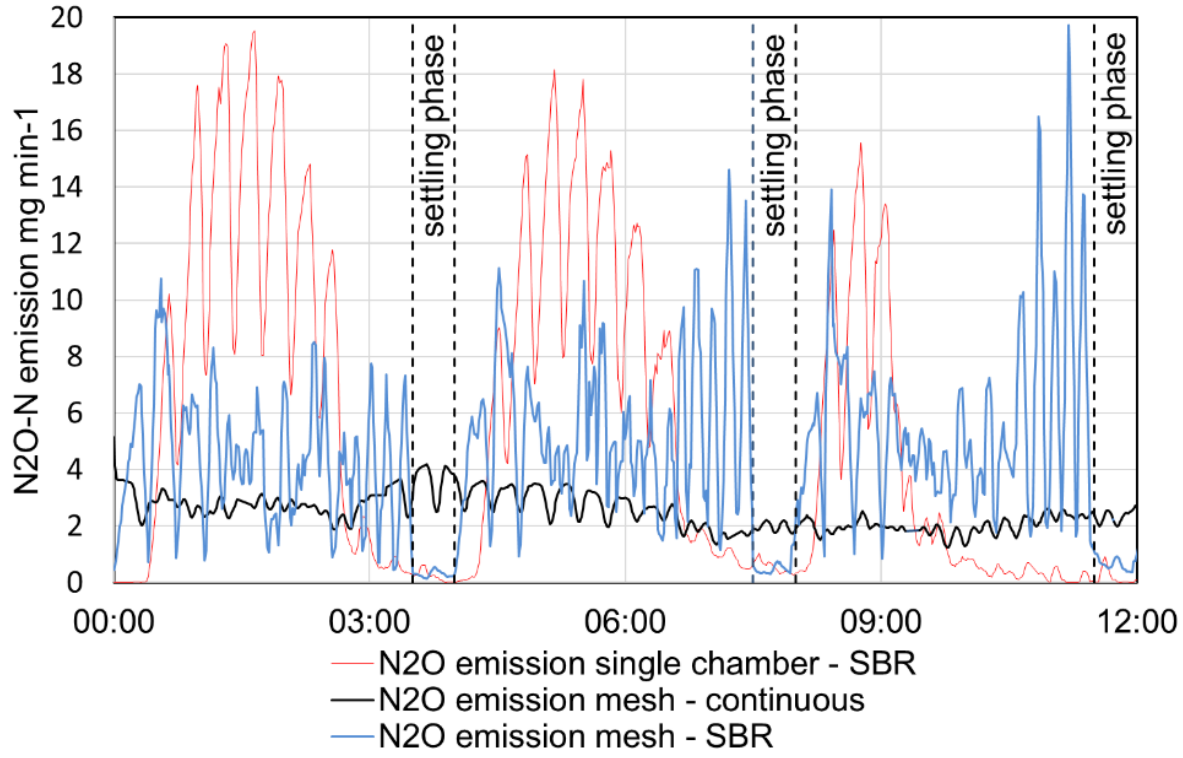

Figure 39: N_2O emission pattern of the single chamber in SBR mode, and the mesh system in SBR and continuous mode.

When both systems were operated in SBR mode, the single chamber system had an average N_2O emission factor (EF) of 4.3% and the mesh system had an average N_2O EF of 3.7% related to their influent N load. A severe change was observed after switching the mesh system from SBR to continuous operation. Once the system had stabilised again, the continuous operation of the two-chamber mesh reactor reduced the N_2O EF to 1.8%, which corresponds to an average reduction of 50% of the N_2O emissions (Table 9). The single chamber system had a nitrogen removal rate of 76%, which was higher compared with the mesh system with a nitrogen removal rate of 71% in SBR mode and a nitrogen removal rate of 69% in continuous mode. The difference in N-removal efficiency was due to NOB activity (higher NO_3-production in the mesh system), whereas NH_4-N conversion was at a comparable level (Table 10). Measurements of the particle size distribution and the VSS of the effluent and of the fully mixed system indicated no decrease of VSS, as only the small particles were leaving the system.

The differences in N_2O emissions can only be partly explained by the differences in the community composition described above, influencing the balance between the production and consumption of process intermediates.

With a view to the fact that the switch to continuous operation of the mesh system resulted in a strong reduction of N_2O emissions (Table 9), the operation mode appears to be more relevant than the community composition (Figure 38). To a certain extent, this change can be associated with the different aeration requirements of the systems. In addition, when changing from anoxic to aerobic conditions, the increased emissions may be explained by the faster recovery of AOB compared with the NO_2^--consuming bacteria and the resulting accumulation of more intermediates compared with continuous conditions (Brotto et al. 2015). Finally, it should be noted that emissions occurring at the pilot plant scale were expected to be smaller at a larger scale because of the improved gas transfer in larger water columns.

Table 9: N_2O emission factors.

		SBR single chamber	Mesh SBR	Mesh continuous
Parameter	Unit		Average (range)	
N_2O EF	[%]	4.3 (1.8–7.7)	3.7 (2.7–4.5)	1.8 (0. 8–3.3)
N_2O monitoring time	[d]	17.8	3.1	8.8
DO	mg L^{-1}	0.09 (0.00–0.40)	0.13 (0.00–1.04)	0.11 (0.00–0.59)
pH	-	7.38 (7.25–7.81)	7.36 (7.34–7.43)	7.32 (7.12–7.40)
Aeration	L h^{-1}	450 (98–615)	407 (334–490)	364 (295–501)

Table 10: Process parameters, performance, and effluent values.

		SBR single chamber	Mesh SBR	Mesh continuous
Parameter	Unit		Average (range)	
Ammonia removal rate	%	96 (86–99)	96 (95–97)	94 (89–97)
Nitrogen removal rate	%	76 (69–83)	71 (70–72)	69 (65–71)
Effluent NO_3-N	mg L^{-1}	246 (188–327)	286 (277–294)	315 (262–353)
Effluent NO_2-N	mg L^{-1}	3 (1–7)	1.6 (1.3–2.2)	4.3 (2.8–6.0)

Effluent NH_4-N	mg L^{-1}	56 (3–168)	51 (31–68)	84 (40–131)
Effluent TOC	mg L^{-1}	92 (49–144)	115	80 (49–111)
TOC removal	%	67 (52–77)	62	71 (66–77)
Effluent Ks	mmol L^{-1}	17 (13–27)	17	36 (12–57)
Sludge age	D	36 (31–45)	20	24 (15–33)
Volumetric loading rate	kg N m- 3 d^{-1}	0.51 (0.17–0.52)	0.52 (0.45–0.59)	0.57 (0.52–0.69)
Reactor VSS	g VSS L^{-1}	4.6 (4.2–5.4)	4.2 (3.5–4.9)	4.2 (2.3–5.2)

The observations made in this study indicated that continuous operation is a key factor in reducing N_2O emissions. It is suspected that the factor most likely influencing this is the avoidance of prolonged unaerated periods which occur during the settling phase of the SBR. This is supported by the observation that the reactor configuration had only a minor effect on reducing N_2O emissions.

This is in line with observations reported in the literature: Castro-Barros et al. (2015) observed that the peak emission occurred during a transition from low to high aeration conditions, and also reasoned that a more continuous aeration would reduce overall emissions. Domingo-Félez et al. (2014) found that an increase in aeration frequency would decrease the EF. Observations made on a SHARON process led to the conclusion that EF could be reduced if anoxic phases were avoided (Mampaey et al. 2016). Pijuan et al. (2014) were able to measure an increased N_2O production rate during the settling phase.

Unfortunately, this reduction of N_2O comes at a certain price because there seems to be a minor trade-off between GHG emissions and NOB suppression. While the regular interchange between aerobic and anaerobic conditions is known to be beneficial for the suppression of NOB (Ma et al. 2015), such conditions favour N_2O formation (Tsutsui et al. 2013). These observations are well in line with the results of the current study, where the single chamber SBR showed slightly superior nitrogen removal efficiency but higher N_2O EF. Therefore, it can be concluded that superior selection mechanisms to suppress NOB such as granular selection by hydro-cyclones (Wett et al. 2010b) or screens become increasingly important to maintaining stable PNA systems with good removal efficiency while maintaining low N_2O emissions. Mesh reactors are a promising approach to achieve a relatively low tech continuous PNA system, which was shown by the prolonged operation of a mesh reactor (Fuchs et al. 2017) and the first pilot plant system used in this study.

5 General summary and conclusions

The overall target of this wastewater treatment study was to study the limitations of the small-scale implementation of the ammonia (NH_4^+) nitrogen (N) removal technology PNA. Inside a PNA system, ANAMMOX bacteria and AOB perform a two-step process: first, AOB convert NH_4^+ to NO_2^- using O_2 supplied by aeration, and then ANAMMOX converts NO_2^- and the remaining NH_4^+ to nitrogen gas (N_2). The N_2 is released into the atmosphere and therefore removed from the wastewater in an energy-efficient manner.
Equal to all PNA systems, small-scale systems must establish selective means to retain the slowly growing ANAMMOX fraction of the biomass inside the bioreactor. For example, granular biomass is commonly retained during SBR operation by settling at the end of each treatment cycle. However, other methods such as meshes, sieves, or carrier material are other possible options to retain the biomass. Furthermore, they need to maintain process stability mainly by controlling the aeration in such a manner that the AOB and ANAMMOX fractions are kept in a narrow equilibrium, while NOB are suppressed. Aeration control can utilise the fact that AOB activity decreases the pH when air is supplied, while ANAMMOX activity (and influent) increases the pH and is inhibited if too much air is supplied. Furthermore, too much aeration can lead to system failure as too much AOB activity will lead to toxic levels of NO_2^-. Finally, PNA has the potential to emit problematic amounts of GHGs, which must be kept at a minimum.
Those targets were worked on in two phases. First, the lab-scale phase involved the implementation of a conventional single chamber lab-scale and a novel single mesh separated system, and the implementation and testing of monitoring tools. Then, in the second phase, the lessons learned from the lab-scale phase were implemented at the pilot scale. The pilot plant consisted of a single chamber system and a mesh separated system. During the start-up period, constant improvements to the reactor configuration and process control were made until stable operations were achieved. Different modifications of the pH-based control strategy were tested, such as pH-based feed and a robust aeration control algorithm to increase the tolerance against process disturbances affecting the pH-controlled aeration at a small scale. Once performances similar to industrial-scale plants were achieved, the GHG emissions of the systems were closely monitored, and the impact of switching from discontinuous SBR to continuous operation evaluated. Finally, the impact of different alkalinity concentrations was investigated at pilot and lab scales as this has been suspected of playing an essential role in the limitations of small-scale plants, especially with respect to pH-based process control.

5.1 Improving biomass retention

5.1.1 Lab scale

The investigation of methods for biomass retention that are suitable for small-scale implementations was shown to be most interlinked with the other targets of this study because it affected GHG emissions and process stability. It began using the established approach of a single chamber system operating in SBR mode (Subsection 4.1.1.1). Although the lab-scale single chamber system principally worked, several disadvantages became apparent such as decreased process stability.
By integrating a mesh into the reactor configuration, which separated the aerated from the nonaerated zone, it was intended to improve biomass retention and to create zones that favoured ANAMMOX and AOB activity. Initially, the configuration was investigated at lab

scale (Subsection 4.1.1.2), with fine meshes that imposed a strong barrier for the interchange of biomass. It quickly showed that a too fine mesh was prone to clogging due to biofilm formation, resulting in a larger diameter of the mesh where the biofilm became essential for generating distinct zones. Although sludge collected from the effluent had to be returned to the reactor, the lab-scale reactor showed the potential of the mesh reactor for continuous operation if the biomass separation could be improved at a larger scale.

5.1.2 Pilot scale

Upon finding a suitable mesh at lab scale, it was implemented at pilot scale. It was decided to cultivate a biofilm using an SBR mode operation until a stable biofilm was achieved. Although several modifications were tested, no permanent biofilm could be cultivated due to the higher shear forces present at larger scales. A piece of curtain fabric supported by a mosquito net finally allowed the generation of the desired biomass retention while permitting sufficient permeability. To prevent clogging of the mesh, the aerator was placed next to it. Furthermore, the agitator in the nonaerated zone was adjusted in such a way that a laminar layer was created in the top section of the unaerated section, allowing for biomass retention and sludge selection. Subsequently, a continuous operation was possible (Subsection 4.3.1.2).

5.2 Increase of process stability

5.2.1 pH-based process control

5.2.1.1 Lab scale

Controlling the aeration and thus the activity of AOB, which oxidise NH_4^+ to NO_2^-, and ANAMMOX activity, which consumes NO_2^- and NH_4^+ to form N_2, has been one of the major challenges for maintaining process stability. pH-based aeration control, such as that applied by the DEMON® process, have been successful at a large scale. It exploits the fact that pH drops when the aeration is turned on, and NO_2^- is produced by AOB and increases when it is turned off, which occurs when NH_4^+ and NO_2 are consumed by ANAMMOX to form N_2 and influent enters the system. This results in the commonly applied intermittent aeration of PNA systems, where a typical sawtooth pH signal can be observed. Furthermore, pH sensors are relatively cheap and reliable technology commonly applied in WWTPs. Together this motivated the application at a small scale.

The initial experiences with the lab-scale SBR reactor showed that a pH-based aeration controlled PNA SBR process such as the DEMON® process is possible but prone to disturbances not known at a larger scale (Subsection 4.1.1.1). Disturbances destabilise the pH response of the system, rendering pH-based aeration control useless at best but harmful at worst. For example, after each settling phase, an increase of pH was observed, basically inverting the response of the pH value to aeration. This means that the aeration does not turn off, as a drop in pH is necessary to do so; thus, too much air facilitates the AOB to potentially produce problematic NO_2^- levels, which could severely impact the overall process. A similar inversion of the pH response that lasted for several hours was observed after changing to a new batch of reject water or after a halt of operation (Figure 16).

The lab-scale mesh reactor was not subject to such problems due to its different operation mode and a different approach to controlling the aeration (Subsection 4.1.1.2). It was initially started with simple time-dependent aeration and continuous operation and showed a more stable behaviour than did the lab-scale SBR.

5.2.1.2 Pilot scale

It was suspected that the pH artefact would diminish at the pilot scale. The two pilot plant systems (single chamber SBR and mesh separated single chamber) used pH-based aeration control with aerated and nonaerated phases. In contrast to the lab-scale mesh system, the pilot-scale mesh system had to be operated in SBR mode similar to the single-chamber system to prevent biomass loss, a limitation which was circumvented later on.
Although the pH-dependent aeration was more stable at pilot-scale, it still was prone to disturbances—a problem that could be surpassed by integrating a time- and pH-dependent robust aeration control algorithm that would force a change to the state of the aeration, irrespective of the pH signal after a predefined passage of time. Using a timer when the pH was not suitable for pH based aeration control drastically improved the process stability and minimised manual intervention, as the process was kept up and running even when technical faults occurred, and the pH response inverted or the pH signal was too low to switch on aeration after a prolonged time. Thus, it quickly returned the system to its normal pH response, exhibiting a typical pH sawtooth pattern (Subsection 4.3.2.1). Therefore, it can be concluded that small-scale pH-controlled systems need to be able to detect when the pH signal is compromised. Furthermore, it was shown that suboptimal time- and pH-dependent aeration algorithms perform better under such conditions and may be used to re-establish a process status suitable for pH-controlled aeration.
The problem remained that adjusting the loading rate had to be done slowly and manually, slowing the attempts to increase the loading rate. Subsequent tests with pH-based PID algorithm, operating with much more inertia than the aeration logic, showed that in principle it is possible to achieve aeration control and feed adjustment with the pH signal (Subsection 4.3.2.1). Subsequent modifications to aeration control in the lab-scale mesh reactor completely removed the nonaerated phase. Effluent values indicated that the continuous aeration further simplified the process but slightly compromised NOB suppression (Subsection 4.1.1.2).

Because of these changes to the control algorithm, the process stability of the pilot plants had improved. Yet, it was not possible to obtain the desired loading rates comparable to industrial plants. Only by gradually increasing the HCO_3^- content was it possible to reach this target. This indicated that the feasibility of pH-controlled small-scale PNA processes, and the N removal performances that may be achieved, are affected by the amount of CO_2 stripping that occurs when the systems are aerated, thereby affecting the pH response to aeration, and the availability of carbonate to AOB. This also highlights the importance of mass transport for pH-controlled small-scale PNA processes, which could be shown by monitoring the effect of a stepwise variation of the influent NH_4-N to HCO_3^- ratio. The experiment showed that the reactor sensitivity to alkalinity reduction increased with decreasing oxygen transfer efficiency (Subsection 4.3.2.2).

5.2.1.3 Comparison of pilot and lab scales

To further investigate how scale affects pH-based aeration, the lab-scale single-chamber system was run with an aliquot of the pilot-scale single-chamber system, keeping the feed and

biomass concentration in proportion to the reactor volume, while applying the same control algorithm. By comparing both the pilot- and lab-scale systems, it was shown that scale and geometry changed the result of the pH-dependent aeration and resulted in different relative NOB activities (Subsection 4.3.2.2). This highlights that the pH set point used for controlling aeration are seldom comparable among different systems, especially at a small scale—which implies that small-scale industrial systems will require individual optimisation unless a sufficiently accurate model for this problem has been developed.

From the findings of this study, it can be concluded that the pH artefacts bothering the small-scale PNA implementations can be dealt with. It was shown that the pH signal could be used to have a self-adjusting reactor feed to improve the process stability when attempting to increase the reactor performance. Furthermore, it was shown that pH set points are affected by mass transfer, which is influenced by scale and geometry. Moreover, it was shown that process stability was increased by the continuous operation as it reduces the imbalances of the bicarbonate system.

5.2.2 Process monitoring

5.2.2.1 Lab scale and pilot scale

Due to its complex nature, PNA is thought to be prone to process disturbances. Relying solely on conventional process monitoring of influent and effluent values bears the risk of misinterpreting the wellbeing of the bacteria responsible for the PNA process, where ANAMMOX are generally considered to be more sensitive. Therefore, two different ANAMMOX monitoring methods were compared: the specific ANAMMOX activity, a test performed by supplying a well-defined medium and monitoring its turn-over, and the determination of the heme concentration, which represents a prosthetic group central to the ANAMMOX metabolism.

Both methods were applied during the pilot-plant start-up and during a prolonged batch test. The batch test showed that heme concentration and ANAMMOX activity exhibited different dynamics and that the heme concentration is the more suitable method for ANAMMOX monitoring purposes due to the variability of ANAMMOX activity (Section 4.2.3), which has been shown to be closely linked to the N removal rate of the system during pilot plant start-up (Subsection 4.3.1.1); thus, it offers little additional information, whereas heme quantification can be useful for monitoring the development of the ANAMMOX concentration of the system.

5.2.3 Additives in sludge dewatering

5.2.4 Lab scale

Motivated by the process imbalances encountered during the first trial run of the lab-scale single-chamber system when switching the process water source to one relatively rich in iron deposits, it was suspected that the commonly used sludge dewatering additives iron chloride and a polymer had a harmful effect on the ANAMMOX fraction, which is generally considered to be more vulnerable in literature. However, the batch test conducted to demonstrate this did not reveal any harmful effect (Section 4.2.1). In hindsight of the

alkalinity related problems observed during pilot-plant and lab-scale operation, the author suspects that, although stoichiometrically sufficient alkalinity was present, the impact of the iron chloride addition during sludge dewatering impacted the carbonate buffer system to such an extent that a stable PNA process was hindered. Therefore, caution should be applied when implementing small-scale PNA systems at WWTPs where sludge dewatering depends on the intense use of iron chloride. It is therefore recommended to optimise sludge dewatering to achieve NH_4-N to alkalinity ratios that are as high as possible (a molar ratio of 0.8 worked fine in this study) before considering small-scale PNA implementation.

5.3 Reduction of greenhouse gas emissions

5.3.1 Pilot scale

GHG emissions in the form of nitrous oxide (N_2O) may outweigh the efficiency gains from PNA plants. Thus, it was necessary to investigate N_2O emissions and evaluate the novel mesh reactor configuration in comparison with a conventional single-chamber reactor. Therefore, the pilot-scale single chamber and mesh reactors were monitored for 1 month at an N loading rate representative of a large-scale implementation, and with comparable removal rates. When both pilot-scale systems were operated in SBR mode, only a slight reduction was observed in the mesh system. This minor difference could either be caused by the differences in the community composition or the separation of the aerated and nonaerated zones, thereby reducing the stripping of anaerobically produced N_2O. Nevertheless, the largest saving was achieved when switching to continuous operation (Subsection 4.3.3.2).
Therefore, it was shown that reactor configurations allowing for continuous operation, such as mesh reactors, reduce N_2O emissions. In accordance with other findings in the literature, it can be assumed that this reduction most likely occurs due to avoiding prolonged anoxic phases. Furthermore, it can be argued that the absence of NOB suppression by prolonged anoxic phases increases the importance of NOB suppression by mechanical means, and thus is a key to maintaining PNA systems with a low N_2O emission factor. NGS data suggest that the difference of N_2O emissions could partly be explained by community composition (Subsection 4.3.3.1), but that the change to continuous operation is most crucial.

5.4 Overall conclusion and answer to the research questions

Overall, the abovementioned conclusions allow the research questions developed in this thesis to be answered:

> *What are the problems associated with small-scale implementations of PNA processes, and what can be done to circumvent them?*

It could be shown that small-scale systems are dependent on influent characteristics, which is problematic because influent characteristics of small-scale systems are likely to vary more in comparison to large-scale systems because sludge dewatering is often performed discontinuously. In addition, the increased tendency to strip influent alkalinity may hinder the stable operation of a small-scale PNA process, which leads to problems unknown at a large

scale. This also highlights that good practices in sludge dewatering should be enforced to reduce the impact of additives on the available influent alkalinity.

What are the conditions necessary for pH-dependent aeration control algorithms to function under small-scale conditions?

This study showed that aeration control by pH of small-scale systems is affected by pH artefacts, which are caused by the influent variability or halts of operation due to technical malfunctions. It is possible to cope with them using a relatively simple algorithm that switches to a time-dependent aeration control until a pH signal suitable for aeration control is regained.

What are the advantages of mesh-based reactor configurations for small-scale implementations?

The mesh separated reactor design is a simple mean to perform sludge retention and selection while continuously operating a PNA system, which increases the process stability of a small-scale PNA system.

What is the effect of a mesh separated reactor configuration and operation mode on N_2O emissions?

It was shown that the mesh-based reactor configuration itself did not reduce the N_2O emissions, but it allowed the continuous operation of a PNA system, which reduced emissions.

Are ANAMMOX activity and heme concentration suitable methods for detecting process disturbances and do they offer more information than regular monitoring of influent and effluent values?

The application of both monitoring methods showed that they allow disturbances to be detected. However, little additional information is gained in relation to the effort required compared with just monitoring influent and effluent values.

5.5 Outlook

For the future development of small-scale PNA plants, the author envisions the following directions for future research:

- A systematic investigation of how geometry, scale, OTE, and pH set point affect the stripping dynamics of PNA plants, to identify limits of feasibility regarding alkalinity limitation during the design process; for example, the depth of the pH probe is suspected to be crucial. Ultimately, this should allow PNA alkalinity limitations to be identified during the design process and small-scale tests.
- It should be investigated how stripping in continuously operated PNA plants affects NOB suppression, because they are kinetically favoured by the decrease of alkalinity caused by stripping in relation to the AOB, and if simple means such as the mesh reactor can assure long-term stability (> 1 year) of the system.

- Controller development should consider whether the pH pattern, aeration volume, and influent volume could be used to reset the pH set point or be used to apply a fuzzy controller to achieve similar but more flexible behaviour.
- The first successful attempts of the continuously aerated lab-scale mesh reactor should be investigated at a larger scale while collecting more data on the prolonged operation of a mesh separated system.

6 Literature / References

Ali M, Rathnayake RMLD, Zhang L, et al (2016) Source identification of nitrous oxide emission pathways from a single-stage nitritation-anammox granular reactor. Water Res 102:147–157. doi: 10.1016/j.watres.2016.06.034

Bagchi S, Biswas R, Nandy T (2010) Alkalinity and dissolved oxygen as controlling parameters for ammonia removal through partial nitritation and ANAMMOX in a single-stage bioreactor. J Ind Microbiol Biotechnol 37:871–876. doi: 10.1007/s10295-010-0744-3

Bai Y, Wang D (2006) Fundamentals of Fuzzy Logic Control — Fuzzy Sets, Fuzzy Rules and Defuzzifications. In: Advanced Fuzzy Logic Technologies in Industrial Applications. Springer, London, pp 17–36

Boiocchi R, Mauricio-Iglesias M, Vangsgaard AK, et al (2015) Aeration control by monitoring the microbiological activity using fuzzy logic diagnosis and control. Application to a complete autotrophic nitrogen removal reactor. J Process Control 30:22–33. doi: 10.1016/j.jprocont.2014.10.011

Bousek J, Schöpp T, Schwaiger B, et al (2018) Behaviour of doxycycline, oxytetracycline, tetracycline and flumequine during manure up-cycling for fertilizer production. J Environ Manage 223:545–553. doi: 10.1016/j.jenvman.2018.06.067

Broda E (1977) Two kinds of lithotrophs missing in nature. Z Für Allg Mikrobiol 17:491–493. doi: 10.1002/jobm.19770170611

Brotto A, Li H, Dumit M, et al (2015) Characterization and mitigation of nitrous oxide (N2O) emissions from partial and full-nitrification BNR processes based on post-anoxic aeration control. Biotechnol Bioeng 112:. doi: 10.1002/bit.25635

Carvajal-Arroyo JM, Sun W, Sierra-Alvarez R, Field JA (2013) Inhibition of anaerobic ammonium oxidizing (anammox) enrichment cultures by substrates, metabolites and common wastewater constituents. Chemosphere 91:22–27. doi: 10.1016/j.chemosphere.2012.11.025

Castro-Barros CM, Daelman MRJ, Mampaey KE, et al (2015) Effect of aeration regime on N2O emission from partial nitritation-anammox in a full-scale granular sludge reactor. Water Res 68:793–803. doi: 10.1016/j.watres.2014.10.056

Chen H, Yu J-J, Jia X-Y, Jin R-C (2014) Enhancement of anammox performance by Cu(II), Ni(II) and Fe(III) supplementation. Chemosphere 117:610–616. doi: 10.1016/j.chemosphere.2014.09.047

Chen T-T, Zheng P, Shen L-D (2012) Growth and metabolism characteristics of anaerobic ammonium-oxidizing bacteria aggregates. Appl Microbiol Biotechnol 97:5575–5583. doi: 10.1007/s00253-012-4346-z

Chuang H-P, Ohashi A, Imachi H, et al (2007) Effective partial nitrification to nitrite by down-flow hanging sponge reactor under limited oxygen condition. Water Res 41:295–302. doi: 10.1016/j.watres.2006.10.019

Dapena-Mora A, Fernández I, Campos JL, et al (2007) Evaluation of activity and inhibition effects on Anammox process by batch tests based on the nitrogen gas production. Enzyme Microb Technol 40:859–865. doi: 10.1016/j.enzmictec.2006.06.018

Dapena-Mora A, Vázquez-Padín JR, Campos JL, et al (2010) Monitoring the stability of an Anammox reactor under high salinity conditions. Biochem Eng J 51:167–171. doi: 10.1016/j.bej.2010.06.014

Daverey A, Chen Y-C, Sung S, Lin J-G (2014) Effect of zinc on anammox activity and performance of simultaneous partial nitrification, anammox and denitrification (SNAD) process. Bioresour Technol 165:105–110. doi: 10.1016/j.biortech.2014.04.034

De Prá MC, Kunz A, Bortoli M, et al (2016) Kinetic models for nitrogen inhibition in ANAMMOX and nitrification process on deammonification system at room temperature. Bioresour Technol 202:33–41. doi: 10.1016/j.biortech.2015.11.048

Domingo-Félez C, Mutlu AG, Jensen MM, Smets BF (2014) Aeration Strategies To Mitigate Nitrous Oxide Emissions from Single-Stage Nitritation/Anammox Reactors. Environ Sci Technol 48:8679–8687. doi: 10.1021/es501819n

Dongen U van, Jetten MSM, Loosdrecht MCM van (2001) The SHARON®-Anammox® process for treatment of ammonium rich wastewater. Water Sci Technol 44:153–160

Dosta J, Fernández I, Vázquez-Padín JR, et al (2008) Short- and long-term effects of temperature on the Anammox process. J Hazard Mater 154:688–693. doi: 10.1016/j.jhazmat.2007.10.082

Erdim E, Yücesoy Özkan Z, Kurt H, Alpaslan Kocamemi B (2019) Overcoming challenges in mainstream Anammox applications: Utilization of nanoscale zero valent iron (nZVI). Sci Total Environ 651:3023–3033. doi: 10.1016/j.scitotenv.2018.09.140

Fernández I, Dosta J, Fajardo C, et al (2012) Short- and long-term effects of ammonium and nitrite on the Anammox process. J Environ Manage 95:S170–S174. doi: 10.1016/j.jenvman.2010.10.044

Ferousi C, Lindhoud S, Baymann F, et al (2017) Iron assimilation and utilization in anaerobic ammonium oxidizing bacteria. Curr Opin Chem Biol 37:129–136. doi: 10.1016/j.cbpa.2017.03.009

Fuchs W, Bierbaumer D, Schöpp T, et al (2017) New hybrid reactor concept incorporating a filter mesh for nitritation-anammox treatment of sludge return liquid. Water Sci Technol wst2017264. doi: 10.2166/wst.2017.264

Füreder K, Reichel M, Schaar H, Svardal K (2014) Faulung auf kleinen Kläranlagen. Wiener Mitteilungen. Band 230:279–304

Gonzalez-Estrella J, Li G, Neely SE, et al (2017) Elemental copper nanoparticle toxicity to anaerobic ammonium oxidation and the influence of ethylene diamine-tetra acetic acid (EDTA) on copper toxicity. Chemosphere 184:730–737. doi: 10.1016/j.chemosphere.2017.06.054

Gruber-Brunhumer MR, Montgomery LFR, Nussbaumer M, et al (2019) Effects of partial maize silage substitution with microalgae on viscosity and biogas yields in continuous AD trials. J Biotechnol 295:80–89. doi: 10.1016/j.jbiotec.2019.02.004

Han M, Vlaeminck SE, Al-Omari A, et al (2016a) Uncoupling the solids retention times of flocs and granules in mainstream deammonification: A screen as effective out-selection tool for nitrite oxidizing bacteria. Bioresour Technol 221:195–204. doi: 10.1016/j.biortech.2016.08.115

Han M, Vlaeminck SE, Al-Omari A, et al (2016b) Uncoupling the solids retention times of flocs and granules in mainstream deammonification: A screen as effective out-selection tool for nitrite oxidizing bacteria. Bioresour Technol 221:195–204. doi: 10.1016/j.biortech.2016.08.115

Hao X, Heijnen JJ, Van Loosdrecht MCM (2002) Model-based evaluation of temperature and inflow variations on a partial nitrification–ANAMMOX biofilm process. Water Res 36:4839–4849. doi: 10.1016/S0043-1354(02)00219-1

Hauck M, Maalcke-Luesken FA, Jetten MSM, Huijbregts MAJ (2016) Removing nitrogen from wastewater with side stream anammox: What are the trade-offs between environmental impacts? Resour Conserv Recycl 107:212–219. doi: 10.1016/j.resconrec.2015.11.019

Hippen A, Helmer C, Kunst S, et al (2001) Six years' practical experience with aerobic/anoxic deammonification in biofilm systems. Water Sci Technol 44:39–48

Hwang B-H, Hwang K-Y, Choi E-S, et al (2000) Enhanced nitrite build-up in proportion to increasing alklinity/NH4+ ratio of influent in biofilm reactor. Biotechnol Lett 22:1287–1290. doi: 10.1023/A:1005645317410

Jaroszynski LW, Cicek N, Sparling R, Oleszkiewicz JA (2011) Importance of the operating pH in maintaining the stability of anoxic ammonium oxidation (anammox) activity in moving bed biofilm reactors. Bioresour Technol 102:7051–7056. doi: 10.1016/j.biortech.2011.04.069

Jaroszynski LW, Oleszkiewicz JA (2011) Autotrophic ammonium removal from reject water: partial nitrification and anammox in one-reactor versus two-reactor systems. Environ Technol 32:289–294. doi: 10.1080/09593330.2010.497500

Jin R-C, Xing B-S, Ni W-M (2013) Optimization of partial nitritation in a continuous flow internal loop airlift reactor. Bioresour Technol 147:516–524. doi: 10.1016/j.biortech.2013.08.077

Jin R-C, Yang G-F, Yu J-J, Zheng P (2012) The inhibition of the Anammox process: A review. Chem Eng J 197:67–79. doi: 10.1016/j.cej.2012.05.014

Kampschreur MJ, Temmink H, Kleerebezem R, et al (2009) Nitrous oxide emission during wastewater treatment. Water Res 43:4093–4103. doi: 10.1016/j.watres.2009.03.001

Kartal B, Keltjens JT (2016) Anammox Biochemistry: a Tale of Heme c Proteins. Trends Biochem Sci 41:998–1011. doi: 10.1016/j.tibs.2016.08.015

Kartal B, Kuypers MMM, Lavik G, et al (2007) Anammox bacteria disguised as denitrifiers: nitrate reduction to dinitrogen gas via nitrite and ammonium. Environ Microbiol 9:635–642. doi: 10.1111/j.1462-2920.2006.01183.x

Klaus S, Baumler R, Rutherford B, et al (2017) Startup of a Partial Nitritation-Anammox MBBR and the Implementation of pH-Based Aeration Control. Water Environ Res 89:500–508. doi: 10.2175/106143017X14902968254476

Lackner S, Gilbert EM, Vlaeminck SE, et al (2014) Full-scale partial nitritation/anammox experiences – An application survey. Water Res 55:292–303. doi: 10.1016/j.watres.2014.02.032

Liu S, Horn H (2012) Effects of Fe(II) and Fe(III) on the single-stage deammonification process treating high-strength reject water from sludge dewatering. Bioresour Technol 114:12–19. doi: 10.1016/j.biortech.2011.11.125

Loderer C, Wörle A, Fuchs W (2012) Influence of Different Mesh Filter Module Configurations on Effluent Quality and Long-Term Filtration Performance. Environ Sci Technol 46:3844–3850. doi: 10.1021/es204636s

Lotti T, Kleerebezem R, Hu Z, et al (2015) Pilot-scale evaluation of anammox-based mainstream nitrogen removal from municipal wastewater. Environ Technol 36:1167–1177. doi: 10.1080/09593330.2014.982722

Lotti T, Kleerebezem R, Lubello C, van Loosdrecht MCM (2014) Physiological and kinetic characterization of a suspended cell anammox culture. Water Res 60:1–14. doi: 10.1016/j.watres.2014.04.017

Lv Y, Ju K, Sun T, et al (2016) Effect of the dissolved oxygen concentration on the N2O emission from an autotrophic partial nitritation reactor treating high-ammonium wastewater. Int Biodeterior Biodegrad 114:209–215. doi: 10.1016/j.ibiod.2016.01.022

Ma B, Bao P, Wei Y, et al (2015) Suppressing Nitrite-oxidizing Bacteria Growth to Achieve Nitrogen Removal from Domestic Wastewater via Anammox Using Intermittent Aeration with Low Dissolved Oxygen. Sci Rep 5:13048. doi: 10.1038/srep13048

Ma H, Zhang Y, Xue Y, et al (2019) Relationship of heme c, nitrogen loading capacity and temperature in anammox reactor. Sci Total Environ 659:568–577. doi: 10.1016/j.scitotenv.2018.12.377

Ma Y, Domingo-Félez C, Smets BF (2017) Nitrous oxide Production in Membrane-aerated Nitrifying Biofilms: Experimentation and Modelling. In: Frontiers International Conference on Wastewater Treatment (FICWTM2017)

Mampaey KE, De Kreuk MK, van Dongen UGJM, et al (2016) Identifying N2O formation and emissions from a full-scale partial nitritation reactor. Water Res 88:575–585. doi: 10.1016/j.watres.2015.10.047

Montgomery LFR, -->Schoepp T, Fuchs W, Bochmann G (2016) Design, calibration and validation of a large lab-scale system for measuring viscosity in fermenting substrate from agricultural anaerobic digesters. Biochem Eng J 115:72–79. doi: 10.1016/j.bej.2016.08.009

Morrison GR (1965) Fluorometric Microdetermination of Heme Protein. Anal Chem 37:1124–1126. doi: 10.1021/ac60228a014

Mulder A, van de Graaf AA, Robertson LA, Kuenen JG (1995) Anaerobic ammonium oxidation discovered in a denitrifying fluidized bed reactor. FEMS Microbiol Ecol 16:177–183. doi: 10.1016/0168-6496(94)00081-7

Okabe S, Oshiki M, Takahashi Y, Satoh H (2011) N2O emission from a partial nitrification–anammox process and identification of a key biological process of N2O emission from anammox granules. Water Res 45:6461–6470. doi: 10.1016/j.watres.2011.09.040

Paredes D, Kuschk P, Mbwette TSA, et al (2007) New Aspects of Microbial Nitrogen Transformations in the Context of Wastewater Treatment – A Review. Eng Life Sci 7:13–25. doi: 10.1002/elsc.200620170

Pereira AD, Cabezas A, Etchebehere C, et al (2017) Microbial communities in anammox reactors: a review. Environ Technol Rev 6:74–93. doi: 10.1080/21622515.2017.1304457

Pijuan M, Torà J, Rodríguez-Caballero A, et al (2014) Effect of process parameters and operational mode on nitrous oxide emissions from a nitritation reactor treating reject wastewater. Water Res 49:23–33. doi: 10.1016/j.watres.2013.11.009

Sabine Marie P, Pümpel T, Markt R, et al (2015) Comparative evaluation of multiple methods to quantify and characterise granular anammox biomass. Water Res 68:194–205. doi: 10.1016/j.watres.2014.10.005

Sassa S (1976) Sequential induction of heme pathway enzymes during erythroid differentiation of mouse Friend leukemia virus-infected cells. J Exp Med 143:305–315. doi: 10.1084/jem.143.2.305

Schitzenhofer K (2016) DEVELOPMENT AND IMPLEMENTATION OF A MONITORING SYSTEM FOR ANAMMOX BIOMASS-Master thesis, University of Natural Resources and Life Sciences, Vienna(BOKU)

Schoepp T, Bousek J, Beqaj A, et al (2018) Nitrous oxide emissions of a mesh separated single stage deammonification reactor. Water Sci Technol 78:2239–2246. doi: 10.2166/wst.2018.500

Siegrist H, Salzgeber D, Eugster J, Joss A (2008) Anammox brings WWTP closer to energy autarky due to increased biogas production and reduced aeration energy for N-removal. Water Sci Technol 57:383–388. doi: 10.2166/wst.2008.048

Sinclair PR, Gorman N, Jacobs JM (2001) Measurement of Hem Concentration. In: Current Protocols in Toxicology. John Wiley & Sons, Inc.

Strous M, Gerven EV, Kuenen JG, Jetten M (1997) Effects of aerobic and microaerobic conditions on anaerobic ammonium-oxidizing (anammox) sludge. Appl Environ Microbiol 63:2446–2448

Strous M, Heijnen JJ, Kuenen JG, Jetten MSM (1998) The sequencing batch reactor as a powerful tool for the study of slowly growing anaerobic ammonium-oxidizing microorganisms. Appl Microbiol Biotechnol 50:589–596. doi: 10.1007/s002530051340

Strous M, Kuenen JG, Jetten MSM (1999) Key Physiology of Anaerobic Ammonium Oxidation. Appl Environ Microbiol 65:3248–3250

Strous M, Pelletier E, Mangenot S, et al (2006) Deciphering the evolution and metabolism of an anammox bacterium from a community genome. Nature 440:790–794. doi: 10.1038/nature04647

Thibodeau C, Monette F, Glaus M (2014) Comparison of development scenarios of a black water source-separation sanitation system using life cycle assessment and environmental life cycle costing. Resour Conserv Recycl 92:38–54. doi: 10.1016/j.resconrec.2014.08.004

Third KA, Sliekers O, Kuenen JG, Jetten MSM (2001) The CANON System (Completely Autotrophic Nitrogen-removal Over Nitrite) under Ammonium Limitation: Interaction and Competition between Three Groups of Bacteria. Syst Appl Microbiol 24:

Tokutomi T, Shibayama C, Soda S, Ike M (2010) A novel control method for nitritation: The domination of ammonia-oxidizing bacteria by high concentrations of inorganic carbon in an airlift-fluidized bed reactor. Water Res 44:4195–4203. doi: 10.1016/j.watres.2010.05.021

Trigo C, Campos JL, Garrido JM, Méndez R (2006) Start-up of the Anammox process in a membrane bioreactor. J Biotechnol 126:475–487. doi: 10.1016/j.jbiotec.2006.05.008

Tsutsui H, Fujiwara T, Matsukawa K, Funamizu N (2013) Nitrous oxide emission mechanisms during intermittently aerated composting of cattle manure. Bioresour Technol 141:205–211. doi: 10.1016/j.biortech.2013.02.071

Van de Graaf AA, De Bruijn P (1996) Autotrophic growth of anaerobic ammonium-oxidizing micro-organisms in a fluidized bed reactor. Microbiology (UK). Microbiol 1428 2187-2196 1996 142:. doi: 10.1099/13500872-142-8-2187

van der Star WRL, Abma WR, Blommers D, et al (2007) Startup of reactors for anoxic ammonium oxidation: Experiences from the first full-scale anammox reactor in Rotterdam. Water Res 41:4149–4163. doi: 10.1016/j.watres.2007.03.044

Wang Y, Fang H, Zhou D, et al (2016) Characterization of nitrous oxide and nitric oxide emissions from a full-scale biological aerated filter for secondary nitrification. Chem Eng J 299:304–313. doi: 10.1016/j.cej.2016.04.050

Ward NL, Challacombe JF, Janssen PH, et al (2009) Three Genomes from the Phylum Acidobacteria Provide Insight into the Lifestyles of These Microorganisms in Soils. Appl Environ Microbiol 75:2046–2056. doi: 10.1128/AEM.02294-08

Weissenbacher N, de Clippeleir H, Hell M, Wett B (2012) Lachgasemissionen bei der Behandlung von Prozesswässern im Deammonifikationsverfahren -Translation: Nitrous oxide emissions of treating reject water with the deammonification process. Österr Wasser- Abfallwirtsch 64:247–252

Weissenbacher N, Fuchs W, Schoepp T, Wett B (2017) Behandlung von Prozesswasser aus der Schlammbehandlung von mittels Deammonifikation-Translation: Treatment of reject water from sludge dewatering via deammonification. Bundesministerium für Land- und Forstwirtschaft, Umwelt und Wasserwirtschaft (BMLFUW)

Wett B (2006) Solved upscaling problems for implementing deammonification of rejection water. Water Sci Technol 53:121–128. doi: 10.2166/wst.2006.413

Wett B (2007) Development and implementation of a robust deammonification process. Water Sci Technol J Int Assoc Water Pollut Res 56:81–8. doi: 10.2166/wst.2007.611

Wett B, Hell M, Nyhuis G, et al (2010a) Syntrophy of aerobic and anaerobic ammonia oxidisers. Water Sci Technol 61:1915. doi: 10.2166/wst.2010.969

Wett B, Murthy S, Takács I, et al (2007) Key Parameters for Control of DEMON Deammonification Process. Water Pract 1:1–11. doi: 10.2175/193317707X257017

Wett B, Nyhuis G, Takács I, Murthy S (2010b) Development of Enhanced Deammonification Selector. Proc Water Environ Fed 2010:5917–5926. doi: 10.2175/193864710798194139

Wett B, Omari A, Podmirseg SM, et al (2013) Going for mainstream deammonification from bench to full scale for maximized resource efficiency. Water Sci Technol 68:283–289. doi: 10.2166/wst.2013.150

Wett B, Rauch W (2003) The role of inorganic carbon limitation in biological nitrogen removal of extremely ammonia concentrated wastewater. Water Res 37:1100–1110. doi: 10.1016/S0043-1354(02)00440-2

Xu J-J, Cheng Y-F, Xu L-Z-J, et al (2019) The revolution of performance, sludge characteristics and microbial community of anammox biogranules under long-term NiO NPs exposure. Sci Total Environ 649:440–447. doi: 10.1016/j.scitotenv.2018.08.386

Yan Y, Wang Y, Wang W, et al (2019) Comparison of short-term dosing ferrous ion and nanoscale zero-valent iron for rapid recovery of anammox activity from dissolved oxygen inhibition. Water Res 153:284–294. doi: 10.1016/j.watres.2019.01.029

Zekker I, Rikmann E, Tenno T, et al (2012) Achieving nitritation and anammox enrichment in a single moving-bed biofilm reactor treating reject water. Environ Technol 33:703–710. doi: 10.1080/09593330.2011.588962

Zhang Q-Q, Chen H, Liu J-H, et al (2014) The robustness of ANAMMOX process under the transient oxytetracycline (OTC) shock. Bioresour Technol 153:39–46. doi: 10.1016/j.biortech.2013.11.053

Zhang X, Chen Z, Zhou Y, et al (2019) Impacts of the heavy metals Cu (II), Zn (II) and Fe (II) on an Anammox system treating synthetic wastewater in low ammonia nitrogen and low temperature: Fe (II) makes a difference. Sci Total Environ 648:798–804. doi: 10.1016/j.scitotenv.2018.08.206

7 Tables

8 Figures

10 Appendix

Table 11: NGS results at genus level

Phylum	Class	Order	Family	Genus	Aerated mesh [%]	Nonaerated mesh [%]	Single chamber [%]
Acidobacteria	Acidobacteria	Subgroup 4	DS^{-1}00	Other	0.7	1.4	0.7
Acidobacteria	Acidobacteria	Subgroup 4	Unknown Family	Blastocatella	25.6	23.6	4.1
Acidobacteria	Acidobacteria	Subgroup 6	Other	Other	1	2.2	2.1
Chlorobi	Chlorobia	Chlorobiales	SJA-28	Culture clone SRAO 63	3	2.2	0.4
Chloroflexi	Other	Other	Other	Other	2.9	2.1	13.2
Chloroflexi	Anaerolineae	Anaerolineales	Anaerolineaceae	Other	1.5	1.8	0.7
Chloroflexi	Ardenticatenia	Other	Other	Other	0.5	0.7	1
Chloroflexi	Caldilineae	Caldilineales	Caldilineaceae	Other	1.8	1	3.2
Latescibacteria	Other	Other	Other	Other	0.8	1.1	0.2
Nitrospirae	Nitrospira	Nitrospirales	Nitrospiraceae	Nitrospira	1.1	0.7	0.8
Omnitrophica	NPL-UPA2	Other	Other	Other	1.4	1.8	2.5
Parcubacteria	Other	Other	Other	Other	0.3	0.6	1.6
Planctomycetes	Other	Other	Other	Other	3	2.8	1.6
Planctomycetes	OM190	Other	Other	Other	3.6	7	3.4
Planctomycetes	Phycisphaerae	CCM11a	Other	Other	0.1	0.4	3.3
Planctomycetes	Pla4 lineage	Other	Other	Other	0.8	1.2	0.5
Planctomycetes	Planctomycetacia	Brocadiales	Brocadiaceae	Candidatus Brocadia	4.3	12.4	5.6
Planctomycetes	Planctomycetacia	Planctomycetales	Planctomycetaceae	Other	4.4	1.9	4.5
Planctomycetes	Planctomycetacia	Planctomycetales	Planctomycetaceae	Pirellula	0.7	0.5	1.2
Planctomycetes	Planctomycetacia	Planctomycetales	Planctomycetaceae	Rhodopirellula	0.5	0.2	1.3
Proteobacteria	Betaproteobacteria	Nitrosomonadales	Nitrosomonadaceae	Nitrosomonas	1.9	0.8	1.3
Proteobacteria	Betaproteobacteria	Rhodocyclales	Rhodocyclaceae	Denitratisoma	3.2	4.3	2.8
SHA^{-1}09	Other	Other	Other	Other	2.1	0.9	0.6
Verrucomicrobia	OPB35 soil group	Other	Other	Other	6.2	7.4	5.1
Verrucomicrobia	Spartobacteria	Chthoniobacterales	DA101 soil group	Other	0.4	0.2	1.7
Verrucomicrobia	Spartobacteria	Chthoniobacterales	FukuN18 freshwater group	Other	4.3	3.6	0.2
Verrucomicrobia	Spartobacteria	Chthoniobacterales	LD29	Other	13.6	4.7	24.2

* If all results were < 0.1 they were removed.

Table 12: Summary of batch test data, based on group average (SD given in parentheses), relative differences are given in relation to blank

	Treatment			Treatment mean (SD)							Relative difference to blank		
	NO_2-N	$FeCl_3$	poly	NO_2-N	NH_4-N	NO_3-N	Heme	AA	Removal*	VSS	heme	AA	rem.
Cycle	[mg L^{-1}]	[mg L^{-1}]	[mg L^{-1}]	[mg L^{-1}]	[mg L^{-1}]	[mg L^{-1}]	[mg L^{-1}]	[mg L^{-1} d^{-1}]	[-]	[mg L^{-1}]	[%]	[%]	[%]
Start	420	0	0				18 (± 0)	616 (± 102)		0.5 (± 0)		0	
	630	0	0				18 (± 0)	521 (± 40)		0.5 (± 0)		-15	
	420	6	0				18 (± 0)	556 (± 379)		0.5 (± 0)		-10	
	630	6	0				18 (± 0)	372 (± 112)		0.5 (± 0)		-40	
	420	0	300				18 (± 0)	688 (± 107)		0.5 (± 0)		12	
	630	0	300				18 (± 0)	334 (± 111)		0.5 (± 0)		-46	
	420	6	300				18 (± 0)	523 (± 50)		0.5 (± 0)		-15	
	630	6	300				18 (± 0)	598 (± 69)		0.5 (± 0)		-3	
1	420	0	0	0 (± 0.3)	51 (± 7.3)	13 (± 0.2)	15.46 (± 4.11)	549 (± 107)	0.72 (± 0.03)		0	0	0
	630	0	0	0 (± 0)	44 (± 3.1)	9 (± 0.1)	13.72 (± 1.12)	650 (± 80)	0.8 (± 0.01)		-11	18	11
	420	6	0	0 (± 0.2)	55 (± 2.2)	12 (± 6.8)	13.72 (± 0.99)	546 (± 72)	0.7 (± 0.04)		-11	-1	-2
	630	6	0	0 (± 0)	39 (± 3.9)	11 (± 3.6)	13.17 (± 2.92)	779 (± 91)	0.81 (± 0.01)		-15	42	13
	420	0	300	1 (± 0.6)	6 (± 1.2)	25 (± 7)	15.41 (± 1.6)	335 (± 201)	0.86 (± 0.03)		0	-39	20
	630	0	300	0 (± 0)	44 (± 2.3)	4 (± 3.8)	17.15 (± 3.33)	521 (± 101)	0.82 (± 0.01)		11	-5	14
	420	6	300	0 (± 0)	45 (± 7.9)	4 (± 4.4)	16.83 (± 1.5)	936 (± 137)	0.79 (± 0.03)		9	71	9
	630	6	300	0 (± 0.1)	45 (± 3.9)	4 (± 4.7)	22.64 (± 6.66)	777 (± 397)	0.81 (± 0.02)		46	42	13
2	420	0	0	0 (± 0.2)	158 (± 14.2)	14 (± 13.9)	6.48 (± 0.58)	248 (± 235)	0.53 (± 0.08)		0	0	0
	630	0	0	0 (± 0.5)	76 (± 15.9)	0 (± 0)		497 (± 491)	0.91 (± 0.05)			101	73
	420	6	0	0 (± 0)	185 (± 36.8)	4 (± 6.3)	9.73 (± 2.15)	292 (± 251)	0.46 (± 0.22)		50	18	-12
	630	6	0	0 (± 0)	85 (± 1.5)	0 (± 0)	11.34 (± 1.72)	763 (± 146)	0.87 (± 0.01)		75	208	65
	420	0	300	0 (± 0.1)	94 (± 11)	16 (± 26.8)	8.49 (± 1.93)	467 (± 104)	0.66 (± 0.14)		31	89	25
	630	0	300	3 (± 0.1)	80 (± 3.8)	8 (± 13.1)	12 (± 4.92)	423 (± 28)	0.84 (± 0.06)		85	71	59
	420	6	300	0 (± 0)	214 (± 37.3)	4 (± 7.8)	11.16 (± 1.72)	78 (± 136)	0.25 (± 0.13)		72	-68	-53
	630	6	300	0 (± 0.3)	97 (± 2.5)	9 (± 11.2)	11.27 (± 3.74)	600 (± 170)	0.78 (± 0.04)		74	142	49
3	420	0	0	1 (± 2.4)	105 (± 23)	32 (± 12.6)	8.09 (± 1.66)	778 (± 358)	1.15 (± 0.14)	0.18 (± 0.02)	0	0	0
	630	0	0	0 (± 0.6)	85 (± 9.3)	36 (± 16.5)	9.6 (± 2.49)	483 (± 203)	0.83 (± 0.07)	0.17 (± 0.01)	19	-38	-28
	420	6	0	1 (± 1.2)	127 (± 8.8)	24 (± 11.4)	8.16 (± 1.75)	847 (± 324)	1.17 (± 0.22)	0.38 (± 0.08)	1	9	2
	630	6	0	0 (± 0)	93 (± 8)	20 (± 2.8)	10.7 (± 1.48)	304 (± 294)	0.9 (± 0.02)	0.19 (± 0.06)	32	-61	-22
	420	0	300	0 (± 0)	66 (± 11.8)	42 (± 6.5)	7.98 (± 1.64)	547 (± 194)	1.01 (± 0.13)	0.33 (± 0.03)	-1	-30	-12
	630	0	300	20 (± 34.4)	114 (± 11.1)	41 (± 6.6)	4.19 (± 0.59)	262 (± 453)	0.67 (± 0.13)	0.19 (± 0.06)	-48	-66	-41
	420	6	300	0 (± 0)	120 (± 2.7)	7 (± 6.3)	8.6 (± 1.76)	879 (± 771)	1.41 (± 0.16)	0.39 (± 0.07)	6	13	23
	630	6	300	0 (± 0.5)	110 (± 3.2)	24 (± 3.1)	4.65 (± 0.75)	383 (± 209)	0.89 (± 0.05)	0.14 (± 0.03)	-43	-51	-22

*The removal rate may be > 1 as it is calculated as N removed per cycle over N add per cycle, and N from previous cycles may contribute to the consumption of N.

Table 13: Summary of pooled data grouped by treatment

Treatment means by group

Treatment	Cycle	Level	Heme [mg L^{-1}]	AA [mg L^{-1} d^{-1}]	Removal [-]
NO_2-N	Start	420	18 (± 0)	596 (± 187)	
		630	18 (± 0)	456 (± 135)	
	1	420	15.4 (± 2.3)	591 (± 255)	0.77 (± 0.07)
		630	16.7 (± 5.2)	682 (± 214)	0.81 (± 0.01)
	2	420	9 (± 2.3)	271 (± 218)	0.47 (± 0.2)
		630	11.3 (± 3.3)	571 (± 266)	0.85 (± 0.06)
	3	420	8.2 (± 1.5)	763 (± 419)	1.18 (± 0.21)
		630	7.3 (± 3.3)	358 (± 276)	0.82 (± 0.12)
FeCl3	Start	0	18 (± 0)	540 (± 160)	
		6	18 (± 0)	512 (± 194)	
	1	0	15.4 (± 2.7)	514 (± 163)	0.8 (± 0.06)
		6	16.6 (± 5.1)	759 (± 236)	0.78 (± 0.05)
	2	0	9.2 (± 3.6)	409 (± 257)	0.73 (± 0.17)
		6	10.9 (± 2.2)	433 (± 318)	0.59 (± 0.28)
	3	0	7.5 (± 2.6)	517 (± 335)	0.91 (± 0.21)
		6	8 (± 2.6)	604 (± 475)	1.09 (± 0.25)
Poly	Start	0	18 (± 0)	516 (± 199)	
		300	18 (± 0)	536 (± 155)	
	1	0	14 (± 2.4)	631 (± 125)	0.76 (± 0.05)
		300	18 (± 4.4)	642 (± 316)	0.82 (± 0.03)
	2	0	9.4 (± 2.9)	450 (± 338)	0.69 (± 0.23)
		300	10.7 (± 3.2)	392 (± 226)	0.63 (± 0.26)
	3	0	9.1 (± 2)	603 (± 344)	1.01 (± 0.2)
		300	6.4 (± 2.3)	518 (± 468)	0.99 (± 0.3)

Table 14: MANOVA results for each cycle

Treatment	Cycle I (after 4 days) Pillai, (p-value)	Cycle II (after 8 days) Pillai, (p-value)	Cycle III (12 days) Pillai, (p-value)
NO_2-N	0.43 (0.015)**	0.73 (0.001)***	0.76 (0.001)***
$FeCl_3$	0.35 (0.046)**	0.47 (0.011)**	0.37 (0.037)**
Polymer	0.64 (0.001)***	0.16 (0.386)	0.34 (0.052)*
Observations:	24	23	24

Results are given as Pillai's trace, p-value of F estimate in brackets, and the level of significance is indicated by ***p < 0.001, **p < 0.05, * p < 0.1

Table 15: Post-hoc regression results

DV	Treatment	Cycle I (after 4 days)	Adj. R^2	Cycle II (after 8 days)	Adj. R^2	Cycle III (12 days)	Adj. R^2
AA	Intercept	282.266 (± 223.378) 0.221		$^{-3}$11.397 (± 273.007) 0.268		1571.548 (± 395.57) 0.001	
	NO_2-N	0.43 (± 0.402) 0.298		1.427 (± 0.491) 0.009**		$^{-1}$.927 (± 0.712) 0.014**	
	$FeCl_3$	40.943 (± 14.072) 0.009**		4.092 (± 17.198) 0.814		14.371 (± 24.919) 0.571	
	Polymer	0.039 (± 0.281) 0.891	0.22	-0.193 (± 0.344) 0.582	0.20	-0.283 (± 0.498) 0.576	0.18
Heme	Intercept	10.154 (± 3.874) 0.016		3.047 (± 3.02) 0.326		11.154 (± 2.352) 0.001	
	NO_2-N	0.006 (± 0.007) 0.38		0.011 (± 0.006) 0.07*		-0.004 (± 0.004) 0.314	
	$FeCl_3$	0.192 (± 0.244) 0.44		0.264 (± 0.194) 0.19		0.094 (± 0.148) 0.534	
	Polymer	0.013 (± 0.005) 0.013**	0.20	0.004 (± 0.004) 0.282	0.16	-0.009 (± 0.003) 0.005	0.26
Removal	Intercept	0.661 (± 0.042) 0.001		-0.175 (± 0.14) 0.228		1.824 (± 0.158) 0.001	
	NO_2-N	0.001 (±0.001) 0.014**		0.002 (±0.001) 0.001***		-0.002 (±0.001) 0.001***	
	$FeCl_3$	-0.003 (± 0.003) 0.211		-0.024 (± 0.009) 0.013**		0.03 (± 0.01) 0.008**	
	Polymer	0.001 (±0.001) 0.001**	0.48	0.001 (±0.001) 0.283	0.71	0.001 (±0.001) 0.819	0.66

For each cycle the coefficient is followed by the SD in brackets followed by the p-value; the level of significance is indicated by ***p < 0.001, **p < 0.05, * p < 0.1, only treatments that were significant in prior MANOVA were considered.

11 Curriculum vitae

Education

- 2015–2020 Ph.D. Focused on Environmental Biotechnology and Sanitary Engineering (BOKU)
- 2011–2015 M.Sc. Material and Energetic Exploitation of Renewable Raw Materials (NAWARO), (BOKU/TUM)
- 2008–2011 B.Sc. Environmental and Bioresource Management (BOKU)

Experience

- 2018 to present. Vogelbusch Biopharma GmbH, Vienna
  Process engineer
- 2015–2018. Institute of Sanitary Engineering and Water Pollution Control (BOKU), Vienna
  Research assistant
- 2013–2015. Department for Agrobiotechnology - Institute for Environmental Biotechnology (BOKU), Tulln
  Student assistant
- 2010. Imperial College, OPAL Programme, London
  Research internship

12 List of Publications

All publishing activities performed during the period of the PhD project are listed as follows:

Norbert Weissenbacher, Thomas Schöpp, Bernhard Wett und Werner Fuchs Behandlung von Prozesswässern aus der Schlammbehandlung mittels Deammonifikation für kleine bis mittlere kommunale Kläranlagen
Published in Wiener Mitteilungen (2017) Band 246

Gruber-Brunhumer, M. R., L. F. R. Montgomery, M. Nussbaumer, T. Schoepp, E. Zohar, M. Muccio, I. Ludwig, G. Bochmann, W. Fuchs, and B. Drosg. "Effects of Partial Maize Silage Substitution with Microalgae on Viscosity and Biogas Yields in Continuous AD Trials." *Journal of Biotechnology* 295 (April 10, 2019): 80–89. https://doi.org/10.1016/j.jbiotec.2019.02.004.

Weissenbacher, N., Schoepp, T., Bousek J., Fuchs, W. (2017): Performance of a continuous-flow single stage deammonification system with mesh separated compartments. [International IWA conference on sustainable solutions for small water and wastewater treatment systems (S2Small2017), Nantes, France, 22–26 October 2017] In: IWA (Eds.), Proceedings of the international IWA conference on sustainable solutions for small water and wastewater treatment systems (S2Small2017), 22–26 October 2017, Nantes, France, pp.385-387

Bousek, J., T. Schöpp, B. Schwaiger, C. Lesueur, W. Fuchs, and N. Weissenbacher. "Behaviour of Doxycycline, Oxytetracycline, Tetracycline and Flumequine during Manure up-Cycling for Fertilizer Production." *Journal of Environmental Management* 223 (October 1, 2018): 545–53. https://doi.org/10.1016/j.jenvman.2018.06.067.

Montgomery, LFR; Schopp, T; Fuchs, W; Bochmann, G, Design, calibration and validation of a large lab-scale system for measuring viscosity in fermenting substrate from agricultural anaerobic digesters. Published in *BIOCHEM ENG J.* 2016; 115: 72-79.

W. Fuchs*, D. Bierbaumer, T. Schöpp, N. Weissenbacher, J. Bousek, New hybrid reactor concept incorporating a filter mesh for nitritation-ANAMMOX treatment of sludge return liquid. Published in *Water Science and Technology* 2017.

Schoepp, T., J. Bousek, A. Beqaj, C. Fiedler, B. Wett, W. Fuchs, T. Ertl, and N. Weissenbacher. "Nitrous Oxide Emissions of a Mesh Separated Single Stage Deammonification Reactor." *Water Science and Technology* 78, no. 11 (December 28, 2018): 2239–46. https://doi.org/10.2166/wst.2018.500.

Weissenbacher, Norbert, Werner Fuchs, Thomas Schoepp, and Bernhard Wett. "Behandlung von Prozesswasser aus der Schlammbehandlung mittels Deammonifikation." Bundesministerium für Land- und Forstwirtschaft, Umwelt und Wasserwirtschaft (BMLFUW), December 21, 2017.